

UC Davis

UC Davis Electronic Theses and Dissertations

Title

Characterization of Acipenserid Herpesvirus 2 and its Effects on the Immune System of the Host

Permalink

<https://escholarship.org/uc/item/7vq8q8s0>

Author

Quijano Carde, Eva Marie

Publication Date

2023

Peer reviewed|Thesis/dissertation

Characterization of Acipenserid Herpesvirus 2 and its Effects on the Immune System of the Host

By

EVA MARIE QUIJANO CARDÉ
DISSERTATION

Submitted in partial satisfaction of the requirements for the degree of

DOCTOR OF PHILOSOPHY

in

Microbiology

in the

OFFICE OF GRADUATE STUDIES

of the

UNIVERSITY OF CALIFORNIA

DAVIS

Approved:

Esteban Soto, Chair

Titus Brown

Matt Griffin

Yoshihiro Izumiya

Committee in Charge

2023

TABLE OF CONTENTS

DEDICATION	iv
ACKNOWLEDGEMENTS	v
PREFACE.....	viii
LIST OF FIGURES.....	ix
LIST OF TABLES.....	xii
DISSERTATION ABSTRACT	xiii
<i>CHAPTER 1: A Review of Latency in the Alloherpesviridae Family.....</i>	<i>1</i>
Early evidence of latency.....	2
Asymptomatic carriers as sources of infection.....	5
Cell populations that support latent infections	6
Transcriptional profile during latency.....	8
Conclusion.....	11
References	11
<i>CHAPTER 2: Acipenserid Herpesvirus 2 Genome and Partial Validation of a qPCR for</i>	
<i>Detection in White Sturgeon (<i>Acipenser transmontanus</i>).....</i>	<i>15</i>
Abstract.....	15
Introduction	16
Materials and methods.....	17
Results.....	32
Discussion	55
References	62

<i>CHAPTER 3: Effects of Acipenserid Herpesvirus 2 on the Outcome of a <i>Streptococcus iniae</i> Co-</i>	
<i>Infection in White Sturgeon (<i>Acipenser transmontanus</i>)</i>	68
Abstract.....	68
Introduction	69
Materials and methods.....	73
Results.....	84
Discussion	93
References	106
<i>CHAPTER 4: Transcriptomic Analysis of White Sturgeon (<i>Acipenser transmontanus</i>) Skin Cells</i>	
<i>during Acipenserid Herpesvirus 2 Infection <i>in vitro</i></i>	111
Abstract.....	111
Introduction	112
Materials and methods.....	113
Results.....	116
Discussion	132
References	139
DISSERTATION CONCLUSION.....	145

DEDICATION

I dedicate this work to my sister, Natalia.

I was less than one year old when she came into my life. Like most children growing up with a sister, I took her for granted during our early years. It wasn't until I was in my mid-twenties that I started to understand what she meant to me. Natalia has been my most eager supporter and cheerleader. She has been there through every academic challenge, every heartbreak, every personal and professional breakthrough, and through every win as well as every loss...we cried and laughed together even though sometimes we were literally thousands of miles apart. Natalia is the reason I was able to pursue a lot of my clinical externships, with her never-ending generosity and willingness to help however she could. She always volunteered to join me on a journey – we drove together from Pennsylvania to Texas, and from Florida to California (Pedrito came on this trip too!) – and she was always willing to discuss pro and con lists for any shift in my plans. Her well-earned wisdom regarding graduate school life kept me grounded during my own PhD training years and wanting to be a role model for her kept me motivated during hard times.

Natalia, you are my biggest inspiration in life. I aim to be as kind, forgiving, and loving as you are, and to be as good a hostess as you one day. Thank you for seeing all of me – truly seeing me – and loving me unconditionally despite my wounded parts. You are my best friend and I hope this work makes you proud. Te amo, hermanita.

ACKNOWLEDGMENTS

While my time in graduate school was only 3.5 years long, it feels like this PhD has been in the making since 2009 when I was a bright-eyed undergraduate student starting to fall in love with the intriguing world of scientific research. That was 14 years ago, so there are numerous people to thank for making this work possible. And while I don't have the room in this document to name every single person involved in my journey, know that I deeply appreciate everyone who has crossed paths with me during this time.

I want to start by thanking my co-authors and collaborators who worked tirelessly with me to collect samples, analyze data, and write manuscripts. Your contributions made my work stronger and your gentle way of providing feedback has influenced much of the way I mentor others today. I also want to thank the Comparative Medical Science Training Program at the University of California – Davis (NIH T-32 OD011147EMQC) and the United States Department of Agriculture National Institute of Food and Agriculture (Animal Health project CACALV-AH-410) for financially supporting my research and my development as a researcher. Particularly, I want to thank Dr. Sara Thomasy, the co-director of the Comparative Medical Science Training Program, for her never-ending supply of encouragement and support. Thank you for all the conversations about the future and for always being willing to recommend me for opportunities that would propel my professional growth. Three other people who always made time for me when I needed feedback or guidance were my committee members: Dr. Matt Griffin, Dr. Yoshihiro Izumiya, and Dr. C. Titus Brown. I hope we can continue to work together in the future!

When it comes to mentors, I have been outstandingly fortunate. I want to thank all the mentors I have had throughout the years: from my time as an undergraduate student at the University of Puerto Rico – Mayagüez, including the mentors I met through summers of research

opportunities, to my time as a veterinary student at Cornell University. Thank you so very much for believing in me and getting me started. Because of all of you, I had the chance to experience various fields and find my true passion in research. I also want to thank the members of the Aquatic Animal Health Laboratory at the University of California – Davis. I cannot imagine a more supportive and collaborative group of peers. To Susan Yun, our laboratory manager, thank you for teaching me everything I know regarding virus culture in fish cell lines. You are authentically kind and profoundly knowledgeable, and I am so lucky I got to learn from you. I wish to thank the Center for Aquatic Biology and Aquaculture, particularly Linda Deanovic and Matt Stone, for the outstanding help with housing and care of the fish that we used in these experiments. And I want to take a moment to express appreciation for all the sturgeon who gave up their lives so we could learn more about this disease process. I value their sacrifice and I hope this information will lead to a better life for their kind in the future. Finally, I do not think I have enough words to accurately reflect what the mentorship of Dr. Esteban Soto has meant to me. You are extraordinary and I truly cannot imagine a better fit than you to guide me through this journey. I have not met anyone more dedicated than you to their work, who also prioritizes family and health, and makes the time to get to know his students on a personal level to understand how best to guide them. I am truly fortunate to have learned from you about science and life, and your support of women and minorities in science made me feel like I belonged. You never waste an opportunity to open doors for us or tell us how proud you are of our success. All in all, you are an amazing role model, gracias por todo.

On a personal note, I would like to express my most sincere gratitude to all my family members and friends who have cheered me on along the way. A special mention to Dr. Hali Jungers and Dr. Taylor Heckman, my chronic illness sisters, thanks for being such an incredible source of inspiration and strength every day. When my health was at its worst, you made me feel

normal and strong, and made me believe I could overcome anything! To Dr. Rachel Pollard, Dr. Erica Lachenauer, and Dr. Monika Mostowy, thank you for your long-lasting friendship beyond our veterinary school years. I didn't know what I would have done without you then, and I am so lucky to have you all now. I can't wait to see where our careers and family lives will take us. To all my dear friends who are strong female leaders in this field, taking space and making room for others like us, you inspire me to push forward and make me feel hopeful about the future. To my dance community and all the friends I have made through dancing with Ruedamento, I am eternally grateful for the weekly dance practices, the paddleboard sessions, the camping trips, the dinner parties, and the festival trips we have taken together. When my life was at its darkest, you were my light...and you have no idea the impact you have made in my life. In particular, to my partner Juan Gallardo. Dance brought us together, but I fell in love with your kindness, honesty, and compassion. Thank you for embracing my never-ending supply of energy and my very busy life. I can't wait to share this next step in my life with you. To my parents, Evelyn Cardé y Victor Quijano, gracias por todos los sacrificios a través de los años y por el apoyo en todas mis aventuras académicas. Gracias por estar ahí siempre para celebrar mis triunfos y por enseñarme el valor de la educación y la importancia de la disciplina. And to my siblings, Natalia y Pedro Quijano, me quedo corta de palabras. Son mi más grande tesoro y le doy mil gracias a la vida por recorrer esta existencia con ustedes. Son mi más grande fuente de inspiración y mis ejemplos a seguir: gracias por las horas incontables de compression y apoyo durante toda la vida. Los amo con todo mi ser. Finally, I want to make a special mention of my late pets Osito and Phlox. Thank you for being with me through some of the roughest times of my life, loving me selfishly, teaching me strength, trust, and gratitude, and keeping me company through really lonely periods. I miss you beyond compare and I am grateful for the time we had together.

PREFACE

The chapters comprising this dissertation are works in various stages of the publication process. All chapters have been modified to fulfill formatting requirements.

Chapter 1 is being adapted for a literature review under the title “A Review of Latency in the *Alloherpesviridae* Family” with coauthor Dr. Esteban Soto.

Chapter 2 is a full reprint of the work accepted for publication: Quijano Cardé, E.M., Anenson, K., Waldbieser, G., Brown, C.T., Griffin, M., Henderson, E.E., Yun, S., & Soto, E. (2023). Acipenserid Herpesvirus 2 Genome and Partial Validation of a qPCR for Detection in White Sturgeon (*Acipenser transmontanus*). *Diseases of Aquatic Organisms*.

Chapter 3 is a full reprint of the work in review for publication at *Frontiers in Aquaculture*: Quijano Cardé, E.M., Anenson, K., Yun, S., Heckman, T.I., Jungers, H.T., Henderson, E.E., Purcell, S.L., Mark Fast, M.F., & Soto, E. Effects of Acipenserid Herpesvirus 2 on the Outcome of a *Streptococcus iniae* Co-Infection in White Sturgeon (*Acipenser transmontanus*).

Chapter 4 is being adapted for submission for publication: Quijano Cardé, E.M. & Soto, E. Transcriptomic Analysis of White Sturgeon (*Acipenser transmontanus*) Skin Cells during Acipenserid Herpesvirus 2 Infection *in vitro*

LIST OF FIGURES

Chapter 2

- Figure 2.1: Genome similarity matrix.....31
- Figure 2.2: Phylogenetic unrooted tree of selected members of the *Alloherpesviridae* family33
- Figure 2.3: Acipenserid Herpesvirus 2 (AciHV-2) genome map37
- Figure 2.4: Terminase (ter1) sequence comparison between Acipenserid herpesvirus 2 (AciHV-2, UCD3-30 isolate) and Acipenserid Herpesvirus 1 (AciHV-1).....51
- Figure 2.5: Acipenserid Herpesvirus 2 (AciHV-2) challenge.....52
- Figure 2.6: Acipenserid Herpesvirus 2 (AciHV-2) quantitative polymerase chain reaction (qPCR) standard curve.....53
- Figure 2.7: Internal positive control assay54
- Figure 2.8: Degenerate primer test for Acipenserid Herpesvirus 2 (AciHV-2) in white sturgeon (*Acipenser transmontanus*).....55
- Figure 2.9: Spleen performance during Acipenserid Herpesvirus 2 (AciHV-2) quantitative polymerase chain reaction.....60

Chapter 3

- Graphical abstract: Effects of a recent Acipenserid Herpesvirus 2 infection on a *Streptococcus iniae* challenge in white sturgeon (*Acipenser transmontanus*).....69
- Figure 3.1: Large-scale challenge timeline75
- Figure 3.2: Clinical signs in white sturgeon during Acipenserid Herpesvirus 2 (AciHV-2) challenge.....84

- Figure 3.3: Acipenserid Herpesvirus 2 (AciHV-2) challenge during pilot challenge
.....85
- Figure 3.4. Acipenserid Herpesvirus 2 (AciHV-2) challenge during large-scale challenge
.....87
- Figure 3.5: Clinical signs in white sturgeon during Acipenserid Herpesvirus 2 (AciHV-2)
and *Streptococcus iniae* co-infection challenge88
- Figure 3.6: Acipenserid Herpesvirus 2 (AciHV-2) and *Streptococcus iniae* (*S. iniae*) co-
infection pilot challenge89
- Figure 3.7: Acipenserid Herpesvirus 2 (AciHV-2) and *Streptococcus iniae* (*S. iniae*) co-
infection large-scale challenge91
- Figure 3.8: Histopathologic evaluation of tissues from mortalities of the co-infection
challenge.....92
- Figure 3.9: Representative microscopic findings and the corresponding scoring of the
described epithelial lesions during co-infection challenge94
- Figure 3.10: Histopathologic findings during co-infection challenge95
- Figure 3.11: Gene expression at 15 days post co-infection challenge.....96
- Figure 3.12: Gene expression at 28 days post co-infection challenge.....97
- Figure 3.13: Detection of serum anti-*S. iniae* IgM in survivors of co-infection challenge
.....98
- Figure 3.14: Detection of serum serotransferrin in survivors of co-infection challenge
.....99
- Figure 3.15: Pilot challenge Acipenserid Herpesvirus 2 (AciHV-2) positivity distribution
.....101

Chapter 4

- Figure 4.1: Filtering and normalization of host counts.....118
- Figure 4.2: Filtering and normalization of viral counts120
- Figure 4.3: Hierarchical clustering of samples121
- Figure 4.4: Principal component analysis122
- Figure 4.5: Volcano plot123
- Figure 4.6: Heat map.....124
- Figure 4.7: Scatter plot of gene ontology terms of the biological process domain for upregulated transcripts125
- Figure 4.8: Scatter plot of gene ontology terms of the biological process domain for downregulated transcripts.....126
- Figure 4.9: Scatter plot of gene ontology terms of the molecular function domain for upregulated transcripts132
- Figure 4.10: Scatter plot of gene ontology terms of the molecular function domain for downregulated transcripts.....134
- Figure 4.11: Scatter plot of gene ontology terms of the cellular component domain for upregulated transcripts135
- Figure 4.12: Scatter plot of gene ontology terms of the cellular component domain for downregulated transcripts.....136
- Figure 4.13: Transcriptional profile of Acipenserid Herpesvirus 2 *in vitro*.....137

LIST OF TABLES

Chapter 2

- Table 2.1: GenBank accession information for genomes utilized in comparison experiments using sourmash19
- Table 2.2: GenBank accession information for genomes utilized in core genes comparison experiments.....22
- Table 2.3: Acipenserid Herpesvirus 2 genome description30
- Table 2.4: Genetic relationship of Acipenserid Herpesvirus 2 isolates at the nucleotide level.....32
- Table 2.5: Nucleotide similarity of the 12 core Alloherpesvirus genes between various members of the family *Alloherpesviridae*, including the newly sequenced Acipenserid Herpesvirus 2 (AciHV-2) isolates and the published AciHV-2 partial sequence (GenBank: FJ815289).....34
- Table 2.6: Acipenserid Herpesvirus 2 open reading frames (ORFs) characterization using Blast38

Chapter 3

- Table 3.1: Primers used in gene expression assay80

Chapter 4

- Table 4.1: RNA sequencing read statistics117
- Table 4.2: Differentially expressed transcripts with gene ontology terms associated with immunity127
- Table 4.3: DNA polymerase and transcriptase viral transcript locations when mapped to the viral genome.....133

ABSTRACT

Acipenserid Herpesvirus 2 (AciHV-2) is a double-stranded DNA virus in the family *Alloherpesviridae* that causes morbidity and mortality in white sturgeon (*Acipenser transmontanus*). As the primary source of caviar and sturgeon meat in the United States, losses of subadult white sturgeon due to AciHV-2 result in significant economic losses to the aquaculture industry and subsequently impact the communities that rely on this important agricultural practice. Despite the evidence that other members of the *Alloherpesviridae* family have shown latency capabilities and the current understanding that herpesviruses can impact the host's immunocompetency long term, little is known about AciHV-2 and its interactions with the immune system of the white sturgeon. The work presented in this dissertation aims to further characterize AciHV-2 and provide insight into its impact on the immune system of the white sturgeon. The whole genome of AciHV-2 was assembled and described, and an initial prediction of immune-related host homologs was performed. A diagnostic quantitative polymerase chain reaction assay was developed for the detection of the terminase gene in skin tissue of white sturgeon. This assay had a 100% relative accuracy for the detection of AciHV-2 during an active outbreak when compared to viral culture. Co-infection challenges with *Streptococcus iniae* in a latency/persistent-infection model were performed and revealed that fish exposed to AciHV-2 experienced increased mortality during subsequent *S. iniae* outbreaks in a bacterial dose-dependent manner. In addition, the co-infected group was unable to mount strong humoral immunity, had decreased transcription of tumor necrosis factor alpha, and had decreased serotransferrin 2 protein levels. Finally, differential transcript analysis of the host in response to AciHV-2 *in vitro* at 10 days post-infection suggests that several immune-related pathways are regulated in a manner that may benefit viral

infection. The contributions of this thesis work serve as a foundation for further host-microbe interaction studies as it pertains to AciHV-2 and the white sturgeon, and provide evidence of the need to consider the full history of the hatchery when designing preventative medicine strategies.

CHAPTER 1. A Review of Latency in the *Alloherpesvirus* Family

The *Herpesvirales* order is a large group of double-stranded DNA viruses, consisting of three families segregated based on host specificity. The *Herpesviridae* family affects mammals, birds, and reptiles, the *Alloherpesviridae* family infects fish and amphibians, and the *Malacoherpesviridae* family includes viruses of mollusks.¹ One characteristic that has differentiated the *Herpesvirales* order from most other groups of viruses is the ability to establish latency.

Latency is defined as a reversible, non-productive state achieved at the level of individual cells², which means that at any given time, a subpopulation of latently infected cells may undergo reactivation, resulting in the production of new viral progeny.³ This makes latency dynamic and challenging to study. However, latency is a biologically significant characteristic, given that it has allowed herpesviruses to be incredibly successful within their respective hosts. In addition, it has been demonstrated that herpesviruses are capable of impacting hosts' immune responses against heterologous infections during periods of latency.⁴

Research on herpesvirus latency has been predominantly centered on mammalian herpesviruses, particularly those that affect humans, where the various strategies employed by these herpesviruses to establish and maintain latency have been extensively documented. This review will focus on the hallmarks of latency known from mammalian systems in the context of the *Alloherpesviridae* family. The most well-studied virus from the *Alloherpesviridae* family in terms of latency is Cyprinid Herpesvirus 3 (CyHV-3). However, it is essential to investigate numerous other herpesviruses in this family, as they hold significant importance for the aquaculture, aquarium, and pet fish industries.

1.1 Early evidence of latency

Supportive evidence for latency among members of the *Alloherpesviridae* family has been reported since the early 1980s.⁵ Some of the earliest reports focus on Ictalurid Herpesvirus 1 (IcHV-1), also known as Channel Catfish Virus or CCV. These studies documented the presence of infectious virions or viral DNA in channel catfish (*Ictalurus punctatus*) that were considered “asymptomatic carriers.” The detection of infectious virions had been achieved by the co-cultivation of leukocytes from healthy individuals with channel catfish ovary (CCO) cells, observing the CCO cells for cytopathic effects. Although multiple passages were sometimes required, the authors successfully isolated IcHV-1 from 45% of asymptomatic individuals in a population with no previous history of IcHV-1 infection. Additionally, the study detected anti-CCV antibodies.⁶ These results supported that the virus was present in a dormant state within the leukocytes, but had the capacity to reactivate and cause cytopathic effect (CPE) in permissible cells. While this fits the definition of latency in terms of the lack of clinical signs in an infected individual, this study did not address the transcriptional profile of the latent virus and did not further characterize the specific cell type harboring the latent virus. In a subsequent study, the same population, as well as an additional group of channel catfish that had survived an IcHV-1 outbreak four years earlier, were evaluated for the presence of viral DNA in various tissues using nucleic acid probing. The results revealed the presence of IcHV-1 DNA in the livers of 100% of the asymptomatic population and in 79% of the catfish that had previously survived an IcHV-1 outbreak.⁷ In addition, diverse banding patterns in this second group suggested potential changes to the IcHV-1 within the cell. This study highlighted the long-term persistence of IcHV-1 DNA in survivors from a previous outbreak and provided early evidence that the DNA in these cells may be modified (by methylation for example) to support a latent state. Building on these findings, later

work determined that IcHV-1 DNA structure in leukocytes from suspected latently infected channel catfish was circular, consistent with an episome,⁸ evincing the idea that IcHV-1 DNA in the latent state may control the transcription of viral antigens via structural changes or reversible modifications.

In the 1990s, another member of the family, Cyprinid Herpesvirus 1 (CyHV-1), also known as Herpesvirus Cyprini or CHV, was reported to cause mass mortality in young naïve common and koi carp (*Cyprinus carpio*) and papillomas in carp that survived the acute infection. These outbreaks are typically self-limiting but will recur in most cases.⁹ In these instances, latency was suspected due to the resemblance to human herpesviruses, which cause intermittent skin lesions, such as Herpes Simplex Virus 1 (HSV-1). While viral proteins can be detected in koi tissues during the initial infection, as well as in the papillomas themselves during subsequent events, no viral proteins were detected and no virus could be isolated in culture during periods between flare-ups. Nonetheless, CyHV-1 DNA can be detected in a variety of tissues throughout all periods.¹⁰ These studies provided supportive evidence for a non-productive infection in koi cells consistent with a latent state, as indicated by the presence of CyHV-1 DNA and the absence of infectious virion or viral antigen detection. Furthermore, it was discovered that temperature plays a role in the seasonality of recurring tumors, which is thought to be attributed to the effects of lower temperatures on the physiology and immune status of poikilotherms, such as fish.¹¹ Researchers have used higher temperatures to trigger the regression of the papillomas and the induction of the non-productive state of CyHV-1.¹⁰ Moreover, given the detection of viral DNA in the cranial nerve ganglia and spinal cord, it is thought that latent CyHV-1 may be harbored in the peripheral nervous tissue.¹⁰

Similar to CyHV-1, Cyprinid Herpesvirus 3 (CyHV-3), also known as Koi Herpesvirus or KHV, is another alloherpesvirus that affects carp. The detection of CyHV-3 DNA in gills, kidney, and brain 64 days post-outbreak provided evidence of a possible latent state.¹² This was supported by subsequent studies that confirmed the presence of CyHV-3 DNA in leukocytes of asymptomatic fish, in concurrence with the absence of infectious virus and mRNA in gill mucus and feces.¹³ Research on CyHV-3 also highlighted the role of temperature in the pathogenesis of the disease, showing somewhat complementary findings to CyHV-1. Low (13°C) or high (28°C) temperatures led to an asymptomatic infection of CyHV-3 in carp, while temperate conditions (23°C) resulted in disease.¹² In light of these findings, it is thought that temperature influences not only the fish immune response, which keeps the virus in a latent state during warmer periods, but also the pathogenicity of the virus, which may be suppressed at cold temperatures. For example, CyHV-3 displays a narrow temperature range in which it can cause disease. These findings emphasize the delicate balance between temperatures that induce immunosuppression in the fish and temperatures that are permissible for the virus to become active.

In the early 2000s, studies used dexamethasone to immunosuppress the fish and reactivate herpesviruses. This approach was applied to IchHV-1, wherein reactivation of the virus following immunosuppression was confirmed directly by culturing the virus⁶, or assumed by measuring increased anti-IchHV-1 antibody.¹⁴ This approach produced similar results when the shedding of Anguillid Herpesvirus 1 (AngHV-1), also known as Herpesvirus anguillae or HVA, was induced following immune suppression in farmed European eels (*Anguilla anguilla*). In this study, a seemingly healthy population of eels underwent dexamethasone treatment and was compared to a negative control group. The population had tested negative for AngHV-1 prior to the study but had detectable anti-HVA antibodies. Eels treated with dexamethasone started shedding AngHV-1 from

various tissues as early as two days after treatment, continuing for up to 14 days. While non-dexamethasone treated eels also shed the virus, it occurred much less frequently. Neither group displayed clinical signs during the study. Taken together, these works demonstrate that *Alloherpesviridae* family behaves similar to the rest of the *Herpesvirales* order in terms of latency and reactivation.

1.2 Asymptomatic carriers as sources of infection

Early research on latency within the *Alloherpesviridae* family was primarily motivated by the question of whether asymptomatic carriers posed a risk to uninfected fish. This was particularly relevant given the practice of exposing carp to CyHV-3 at elevated temperatures, which prevented mortality while also immunizing them against future CyHV-3 exposures.¹⁶ In one study, authors exposed carp to CyHV-3 at 23°C for 4 days, then decreased the temperature to 12°C. After 125 days, the temperature was raised to 20°C and naïve fish were introduced into the system. Results showed that 100% of the naïve carp and 57% of the originally infected carp died when the temperature was permissible for CyHV-3¹⁷, indicating that CyHV-3 can persist long-term and asymptomatic carriers can pose a threat to naïve populations, even when initial virus exposures did not cause significant disease.

Subsequent studies aimed to determine whether the stress induced by netting or temporary confinement could trigger the reactivation of CyHV-3 in asymptomatic carriers, potentially endangering uninfected fish. In one study, researchers successfully reactivated CyHV-3 in fish 81 days after the initial infection when fish were subjected to two brief netting episodes and held out of water for 30 seconds each. Levels of CyHV-3 DNA in gill swabs increased from two to four days post-netting, followed by a gradual decrease until it was no longer detectable 10 days post-

netting.¹⁸ This is consistent with reports of other herpesviruses that can be reactivated when the host is stressed¹⁹

Similar to CyHV-3, Cyprinid Herpesvirus 2 (CyHV-2) causes mass mortality in members of the cyprinid family including goldfish (*Carassius auratus*), crucian carp (*Carassius carassius*), and Gibel carp (*Carassius auratus gibelio*). In one study, goldfish from a farm with a prior history of CyHV-2 infection appeared to be in good health at 15°C. However, when the temperature was raised to 25°C, mortality occurred ranging between 46-57%, with CyHV-2 detected by tissue culture and PCR. Subsequently, introducing naive goldfish into the same tanks as the infected fish resulted in 100% mortality among these cohabiting populations, demonstrating the capacity for CyHV-2 to be transferred horizontally.²⁰

Some herpesviruses have also demonstrated vertical transmission, where the virus is transmitted to the offspring either during pregnancy or birth. This has been extensively discussed for HSV-1 due to the potentially fatal effects of neonatal herpes in humans, for which *in utero* transmission, peripartum transmission, and postpartum infection have been reported.²⁷ Similar evidence is present for the vertical transmission of IcHV-1 from asymptomatic broodstock. In one study, two channel catfish broodfish positive for IcHV-1 were successfully mated. The fertilized eggs were monitored and kept in isolated conditions, yet the offspring tested positive for IcHV-1 upon hatching.²⁸

1.3 Cell populations that support latent infections

Herpesviruses are capable of infecting multiple cell types, and frequently the cell type that harbors the initial productive infection differs from the cell type where the virus establishes latency.³ For example, in the *Herpesviridae* family, the human alphaherpesviruses, namely HSV-

1, Herpes Simplex Virus 2 (HSV-2), and Varicella-Zoster Virus (VZV), primarily infect the epithelial cells of the oropharyngeal and genital tract mucosa. However, these viruses establish latency in sensory neurons.²¹ On the other hand, the human gammaherpesviruses Epstein-Barr Virus (EBV) and Kaposi's Sarcoma-associated Herpesvirus (KSHV) are epitheliotropic in terms of their primary productive infection, but establish latency in B cells.²²

When the *Alloherpesviridae* family was initially suspected of achieving latency, it was unclear which cell types were capable of supporting latency in fish. Based on the characteristics of mammalian viruses, it was believed the ability to establish latency varied depending on the specific virus. At the time, knowledge regarding alloherpesviruses was primarily limited to IchV-1, which was suspected to remain latent in leukocytes given the production of CPE in CCO cells co-cultured with leukocytes originating from potentially latently infected fish. Building on these findings, subsequent studies revealed the presence of CyHV-3 DNA in leukocytes and other tissues in asymptomatic fish.^{17,23,24} Working under the assumption that leukocytes are the site of latency and that the detection in tissues was due to circulating leukocytes, one study assessed multiple populations of peripheral leukocytes to narrow down which cell type within this group was supporting the latent CyHV-3. Findings indicated that CyHV-3 DNA was 20-fold more abundant in IgM+ B cells than in IgM- cells²⁵, suggesting IgM+ B cells are a preferential site of latency but may not be the only site. Building on these findings, tests have been developed to identify asymptomatic carrier koi fish, where DNA is extracted from leukocytes and used in recombinase polymerase amplification (RPA). This test has been shown to be more rapid, sensitive, and less costly than quantitative polymerase chain reaction (qPCR) for the detection of CyHV-3 DNA in latently infected leukocytes²⁶, although further optimization and validation are needed before this diagnostic test can be applied in the field.

Lastly, an *in vitro* model was characterized for the study of latent CyHV-3 using a cell line derived from carp caudal fin tissue (CCF-K104). This cell line was instrumental in studying latency and CyHV-3 reactivation via controlled temperature variations. Notably, productive viral replication and the presence of CPE consistently occurred at temperatures ranging from 25-30°C, while viral replication was inhibited at temperatures of 15°C or 35°C, evinced by the absence of observable CPE. However, when cells incubated at 15°C or 35°C were returned to 25°C, productive infection resumed and CPE was observed.²⁹ In addition, the study revealed a distinct head-to-tail conformation of the CyHV-3 genome, marked by a 12-nucleotide insertion, a 120-nucleotide deletion, and three nucleotide substitutions when the temperature was increased to 35°C. This circularization of the herpesvirus genome aligns with existing reports on other members of the *Herpesvirales* order, which exhibit similar circularization during various phases of their life cycles.^{30,31}

1.4 Transcriptional profile during latency

One of the hallmarks of latency as it is currently defined is a transcriptional downregulation of most genes along with the expression of a specific set of transcripts.^{3,21} This has been relatively well characterized in HSV-1 and KSHV, with the expression of the latency-associated transcripts (LATs) or latency-associated genes.^{32,33} Studies have demonstrated that IcHV-1 has a tightly regulated gene expression program with expression of immediate-early, early, and, late genes, consistent with other members of the order *Herpesvirales*.³⁴ A subsequent study investigated whether IcHV-1 transcripts could be detected in channel catfish during the latent period. In this study, transcription of IcHV-1 genes (open reading frames (ORFs) 1-14) was indeed limited to the

lytic cycle and there was no evidence of mRNA corresponding to these ORFs during the latent period.³⁵ While this supported previous reports regarding the lytic cycle transcriptome landscape, it does not indicate the absence of latency-specific transcripts for ICHV-1, since the study focused on select transcripts and expression of all sections of the genome was not assessed. The investigation of non-coding RNAs was challenging at the time of these studies, largely because RNA sequencing technology was not optimized until the mid-2000s.

Similarly, studies on the transcriptional landscape of CyHV-3 revealed that all annotated ORFs of CyHV-3 are transcribed *in vitro* during active infection at the permissible temperature of 22°C and can be temporally classified, similar to other herpesviruses.³⁶ Nonetheless, when the temperature was increased to a non-permissible temperature (30°C), only 58% of the annotated ORFs were transcribed in the days following infection. In fact, most ORF transcripts were no longer detected after eight days post-infection. The exception were ORFs 114 and 115 (previously classified as late genes and coding membrane proteins), which were detected up to 18 days post-infection. In addition, no replication of the viral genome is detected.³⁷

Building on these findings, the transcription of several replication-related genes (ORF 79 and ORF 81) and multiple persistence-related genes (ORF 32, ORF 38, and ORF 114) was assessed in wild, CyHV-3 seropositive carp collected at different times of the year, corresponding to various temperature ranges. Transcripts for replication-related genes were only observed during the spring, when water temperatures were between 15-25°C, in only 19% of seropositive fish tested. These fish also had high levels of CyHV-3 linear DNA in the brain tissue. While transcripts for persistence-related genes were detected in fish collected during spring, these transcripts were also detected in fish collected during the summer, when water temperatures exceeded 25°C, as well as early spring when water temperatures were below 15°C, and no replication-related gene transcripts

or linear CyHV-3 DNA was detected in these fish.³⁸ This is consistent with previous findings, indicating CyHV-3 genome replication occurs only at permissible temperatures. The presence of these persistence-related gene transcripts is thus not exclusive to the period of latency, but the fact that they are continuously transcribed in the absence of viral replication or capsid assembly suggests a role in the establishment or maintenance of latency. The seasonality of replication also supports the strategy of survival of herpesviruses, where the balance between latency and replication ensures progeny and protects against immune clearance.

In contrast, a different study assessing various ORFs in latently infected koi found that ORF6 was expressed in B cells in a spliced form.²⁵ It was unclear how long these fish had been infected with CyHV-3 and therefore it is difficult to compare to the study above³⁷ that assessed CyHV-3 expression *in vitro* 18 days after temperature shift. Regardless, ORF6 seems to be an important study candidate due to homology at the amino acid level to the EBNA-3B domain, which is found in a family of EBV antigens that are only expressed in human B cells during latent EBV infections.²⁵ In addition, due to its abundance in B cells latently infected with CyHV-3, ORF6 can be used to enrich KHV-infected leukocytes via a nanoflare probe.³⁹ In fact, with this technique and subsequent RNAseq, researchers determined that ORF6 was the major transcript expressed in IgM+ B cells latently infected with CyHV-3 and the only one consistently identified, with a latent infection rate of approximately 1-2 leukocytes out of every 1000, which is a larger population than that described for other herpesviruses such as EBV.³⁹

In addition to transcripts for ORFs, herpesviruses may also generate non-coding RNAs (ncRNAs) that are critical for the establishment and maintenance of latency. These ncRNAs are thought to be involved in the regulation of metabolic processes, apoptosis, gene expression, and host microRNA mimicry.⁴⁰ For CyHV-3, the presence of at least two precursor micro-RNAs have

been reported, namely CyHV3-mir-1 and CyHV3-mir-2 (with six additional predicted ones: CyHV3-mir-3-8).⁴¹ Similarly, CyHV-2 transcribes up to 17 ncRNAs, of which CyHV2-mir-C12 is capable of downregulating caspase 8 expression and thus is considered a suppressor of apoptosis.⁴² In light of these findings, additional studies are needed to elucidate the role of these ncRNAs in latency for these members of the *Alloherpesviridae* family.

1.5 Conclusions

The capacity to achieve latency has made herpesviruses immensely successful in their co-evolutionary journey alongside their respective hosts.³ The family *Alloherpesviridae* is no exception, with several members demonstrating long-term dynamic infections with particular transcriptional profiles based on supporting cell type, water temperature, stress environment, and immunosuppression status of the host. Interactions between latent herpesvirus and the host immune system can lead to modulation of the host's ability to fight heterologous infections.⁴³ Understanding the precise molecular and cellular mechanisms underlying latency in alloherpesviruses will allow better predictability of disease prognosis when dealing with co-infections in aquaculture.

References

1. Davison AJ, Eberle R, Ehlers B, Hayward GS, McGeoch DJ, Minson AC, et al. The order Herpesvirales. *Arch Virol.* 2009 Jan;154(1):171–7.
2. Siliciano RF, Greene WC. HIV Latency. *Cold Spring Harb Perspect Med.* 2011 Sep 1;1(1):a007096–a007096.
3. Cohen JI. Herpesvirus latency. *J Clin Invest.* 2020 May 4;130(7):3361–9.
4. White DW, Suzanne Beard R, Barton ES. Immune modulation during latent herpesvirus infection. *Immunol Rev.* 2012 Jan;245(1):189–208.

5. Hanson L, Dishon A, Kotler M. Herpesviruses that Infect Fish. *Viruses*. 2011 Nov 8;3(11):2160–91.
6. Bowser PR, Munson AD, Jarboe HH, Francis-Floyd R, Waterstrat PR. Isolation of channele catfish virus from channel catfish, *Ictalurus punctatus* (Rafinesque), broodstock. *J Fish Dis*. 1985;8:557–61.
7. Wise JA, Bowser PR, Boyle JA. Detection of channel catfish virus in asymptomatic adult channel catfish, *Ictalurus punctatus* (Rafinesque)*. *J Fish Dis*. 1985 Nov;8(6):485–93.
8. Gray WL, Williams RJ, Jordan RL, Griffin BR. Detection of channel catfish virus DNA in latently infected catfish. *J Gen Virol*. 1999 Jul 1;80(7):1817–22.
9. Sano T, Morita N, Shima N, Akimoto M. Herpesvirus cyprini: lethality and oncogenicity. *J Fish Dis*. 1991 Sep;14(5):533–43.
10. Sano N, Moriwake M, Hondo R, Sano T. Herpesvirus cyprini: a search for viral genome in infected fish by in situ hybridization. *J Fish Dis*. 1993 Sep;16(5):495–9.
11. Abram Q, Dixon B, Katzenback B. Impacts of Low Temperature on the Teleost Immune System. *Biology*. 2017 Nov 22;6(4):39.
12. Gilad O, Yun S, Zagmutt-Vergara F, Leutenegger C, Bercovier H, Hedrick R. Concentrations of a Koi herpesvirus (KHV) in tissues of experimentally-infected *Cyprinus carpio* koi as assessed by real-time TaqMan PCR. *Dis Aquat Organ*. 2004;60:179–87.
13. Eide KE, Miller-Morgan T, Heidel JR, Kent ML, Bildfell RJ, LaPatra S, et al. Investigation of Koi Herpesvirus Latency in Koi. *J Virol*. 2011 May 15;85(10):4954–62.
14. Arnizaut A, Hanson L. Antibody response of channel catfish after channel catfish virus infection and following dexamethasone treatment. *Dis Aquat Organ*. 2011 Jul 12;95(3):189–201.
15. Van Nieuwstadt A, Dijkstra S, Haenen O. Persistence of herpesvirus of eel *Herpesvirus anguillae* in farmed European eel *Anguilla anguilla*. *Dis Aquat Organ*. 2001;45:103–7.
16. Ronen A, Perelberg A, Abramowitz J, Hutoran M, Tinman S, Bejerano I, et al. Efficient vaccine against the virus causing a lethal disease in cultured *Cyprinus carpio*. *Vaccine*. 2003 Dec;21(32):4677–84.
17. St-Hilaire S, Beevers N, Way K, Le Deuff R, Martin P, Joiner C. Reactivation of koi herpesvirus infections in common carp *Cyprinus carpio*. *Dis Aquat Organ*. 2005;67:15–23.
18. Bergmann SM, Kempter J. Detection of koi herpesvirus (KHV) after re-activation in persistently infected common carp (*Cyprinus carpio* L.) using non-lethal sampling methods. *Bull Eur Fish Pathol*. 2011;31(3):92.

19. Hasanah NT, Hidayat W. Stress as Trigger Factor of HSV-1 Reactivation Causing Recurrent Intraoral Herpes Mimicking HAEM: A Case Report. *Int Med Case Rep J*. 2022 Dec;Volume 15:699–706.
20. Wang F, Xu Y, Zhou Y, Ding C, Duan H. Isolation and characterization of a Cyprinid herpesvirus strain YZ01 from apparently healthy goldfish after rising water temperature [Internet]. *Microbiology*; 2021 Jul [cited 2023 Oct 2]. Available from: <http://biorxiv.org/lookup/doi/10.1101/2021.07.05.451087>
21. Nicoll MP, Proença JT, Efsthathiou S. The molecular basis of herpes simplex virus latency. *FEMS Microbiol Rev*. 2012 May;36(3):684–705.
22. Chiu YF, Sugden B. Epstein-Barr Virus: The Path from Latent to Productive Infection. *Annu Rev Virol*. 2016 Sep 29;3(1):359–72.
23. Eide K, Miller-Morgan T, Heidel J, Bildfell R, Jin L. Results of total DNA measurement in koi tissue by Koi Herpes Virus real-time PCR. *J Virol Methods*. 2011 Mar;172(1–2):81–4.
24. Zheng S, Wang Q, Bergmann SM, Li Y, Zeng W, Wang Y, et al. Investigation of latent infections caused by cyprinid herpesvirus 3 in koi (*Cyprinus carpio*) in southern China. *J Vet Diagn Invest*. 2017 May;29(3):366–9.
25. Reed AN, Izume S, Dolan BP, LaPatra S, Kent M, Dong J, et al. Identification of B Cells as a Major Site for Cyprinid Herpesvirus 3 Latency. *J Virol*. 2014 Aug 15;88(16):9297–309.
26. Prescott MA, Reed AN, Jin L, Pастey MK. Rapid Detection of Cyprinid Herpesvirus 3 in Latently Infected Koi by Recombinase Polymerase Amplification. *J Aquat Anim Health*. 2016 Sep;28(3):173–80.
27. Bhatta AK, Keyal U, Liu Y, Gellen E. Vertical transmission of herpes simplex virus: an update. *JDDG J Dtsch Dermatol Ges*. 2018 Jun;16(6):685–92.
28. Wise JA, Harrell SF, Busch RL, Boyle JA. Vertical transmission of channel catfish virus. *Am J Vet Res*. 49(9):1506–9.
29. Imajoh M, Fujioka H, Furusawa K, Tamura K, Yamasaki K, Kurihara S, et al. Establishment of a new cell line susceptible to Cyprinid herpesvirus 3 (CyHV-3) and possible latency of CyHV-3 by temperature shift in the cells. *J Fish Dis*. 2015 Jun;38(6):507–14.
30. Nixon DE, McVoy MA. Terminally Repeated Sequences on a Herpesvirus Genome Are Deleted following Circularization but Are Reconstituted by Duplication during Cleavage and Packaging of Concatemeric DNA. *J Virol*. 2002 Feb 15;76(4):2009–13.
31. Strang BL, Stow ND. Circularization of the Herpes Simplex Virus Type 1 Genome upon Lytic Infection. *J Virol*. 2005 Oct;79(19):12487–94.

32. Zhang Y, Xin Q, Zhang JY, Wang YY, Cheng JT, Cai WQ, et al. Transcriptional Regulation of Latency-Associated Transcripts (LATs) of Herpes Simplex Viruses. *J Cancer*. 2020;11(11):3387–99.
33. Fakhari FD, Dittmer DP. Charting Latency Transcripts in Kaposi's Sarcoma-Associated Herpesvirus by Whole-Genome Real-Time Quantitative PCR. *J Virol*. 2002 Jun 15;76(12):6213–23.
34. Huang S, Hanson LA. Temporal Gene Regulation of the Channel Catfish Virus (Ictalurid Herpesvirus 1). *J Virol*. 1998 Mar;72(3):1910–7.
35. Stingley RL, Griffin BR, Gray WL. Channel catfish virus gene expression in experimentally infected channel catfish, *Ictalurus punctatus* (Rafinesque). *J Fish Dis*. 2003 Aug;26(8):487–93.
36. Ilouze M, Dishon A, Kotler M. Coordinated and sequential transcription of the cyprinid herpesvirus-3 annotated genes. *Virus Res*. 2012 Oct;169(1):98–106.
37. Ilouze M, Dishon A, Kotler M. Down-regulation of the cyprinid herpesvirus-3 annotated genes in cultured cells maintained at restrictive high temperature. *Virus Res*. 2012 Oct;169(1):289–95.
38. Uchii K, Minamoto T, Honjo MN, Kawabata Z. Seasonal reactivation enables *Cyprinid herpesvirus 3* to persist in a wild host population. *FEMS Microbiol Ecol*. 2014 Feb;87(2):536–42.
39. Reed AN, Putman T, Sullivan C, Jin L. Application of a nanoflare probe specific to a latency associated transcript for isolation of KHV latently infected cells. *Virus Res*. 2015 Oct;208:129–35.
40. Hancock MH, Skalsky RL. Roles of Non-coding RNAs During Herpesvirus Infection. In: Tripp RA, Tompkins SM, editors. *Roles of Host Gene and Non-coding RNA Expression in Virus Infection* [Internet]. Cham: Springer International Publishing; 2017 [cited 2023 Oct 2]. p. 243–80. (Current Topics in Microbiology and Immunology; vol. 419). Available from: http://link.springer.com/10.1007/82_2017_31
41. Donohoe OH, Henshilwood K, Way K, Hakimjavadi R, Stone DM, Walls D. Identification and Characterization of Cyprinid Herpesvirus-3 (CyHV-3) Encoded MicroRNAs. Pfeffer S, editor. *PLOS ONE*. 2015 Apr 30;10(4):e0125434.
42. Thangaraj RS, Nithianantham SR, Dharmaratnam A, Kumar R, Pradhan PK, Thangalazhy Gopakumar S, et al. Cyprinid herpesvirus-2 (CyHV-2): a comprehensive review. *Rev Aquac*. 2021 Mar;13(2):796–821.
43. Sheth PM, Sunderji S, Shin LYY, Rebbapragada A, Huibner S, Kimani J, et al. Coinfection with Herpes Simplex Virus Type 2 Is Associated with Reduced HIV-Specific T Cell Responses and Systemic Immune Activation. *J Infect Dis*. 2008 May 15;197(10):1394–401.

CHAPTER 2. Acipenserid Herpesvirus 2 Genome and Partial Validation of a qPCR for Detection in White Sturgeon (*Acipenser transmontanus*)

Abstract

White sturgeon (*Acipenser transmontanus*) is the primary species used for caviar and sturgeon meat production in the USA. An important pathogen of white sturgeon is Acipenserid herpesvirus 2 (AciHV-2). In this study, four archived isolates from temporally discrete natural outbreaks spanning the past 30 years were sequenced via Illumina and Oxford Nanopore Technologies platforms. Assemblies of approximately 134 Kb were obtained for each isolate, and the putative ATPase subunit of the terminase gene was selected as a potential quantitative PCR (qPCR) target based on sequence conservation among AciHV-2 and low sequence homology with other important viral pathogens. The qPCR was repeatable and reproducible, with a linear dynamic range covering 5 orders of magnitude, an efficiency of approximately 96%, an R^2 of 0.9872 and an analytical sensitivity of 10^3 copies per reaction after 35 cycles. There was no cross-reaction with other known viruses or closely related sturgeon species, and no inhibition by sturgeon DNA. Clinical accuracy was assessed from white sturgeon juveniles exposed to AciHV-2 by immersion. Viral culture (gold standard) and qPCR were in complete agreement for both cell culture negative and cell culture positive samples, indicating this assay has 100% relative accuracy compared to cell culture during an active outbreak. The availability of a whole genome sequence for AciHV-2 and a highly specific and sensitive qPCR assay for detection of AciHV-2 in white sturgeon lays a foundation for further studies on host-pathogen interactions while providing a specific and rapid test for AciHV-2 in captive and wild populations.

1. Introduction

The white sturgeon (*Acipenser transmontanus*) is an anadromous fish native to the Pacific Coast of North America¹ and a vital component of the aquaculture industry in California and surrounding western states. It is the primary species used for production of globally recognized high-quality caviar and sturgeon meat in the United States², generating over 200 million dollars in annual revenue.³ White sturgeon aquaculture provides not only substantial revenue for producers and employment opportunities for the agriculture sector of the Pacific Northwest, but it is also critical to conservation efforts by offering a sustainable alternative to wild-caught fish. The latter is particularly important due to the white sturgeon's vulnerability to habitat loss driven by climate dynamics and human activity.¹ A significant factor impacting the success of aquaculture operations and conservation efforts is information regarding established and emergent infectious diseases and their effects on wild and cultured fish populations.

Acipenserid Herpesvirus 2 (AciHV-2), previously known as White Sturgeon Herpesvirus 2 (WSHV-2), is a large double-stranded DNA virus in the family *Alloherpesviridae* reported to cause skin ulceration, lethargy, inappetence, and erratic swimming. Mortality rates approaching 10% in adult white sturgeon and up to 50% mortality in juveniles have been reported from natural outbreaks.^{4,5} While this virus has been isolated from various tissues throughout the years, including ovarian fluid of adult fish⁶, little is known regarding AciHV-2 diversity and pathogenesis. One limitation to further studies involving AciHV-2 is the lack of a publicly available complete genome sequence.⁷ In addition, the only diagnostic methods available for the detection of AciHV-2 are viral culture or amplification of the viral DNA polymerase gene using degenerate primers in an end-point PCR assay.^{8,9} Cell culture is the gold standard for viral detection, but it is both time-consuming and labor-intensive. The use of degenerate primers provides faster results but has the

disadvantage of 1) not being specific for the detection of AciHV-2, requiring subsequent sequencing to identify the amplified target, and 2) inability to accurately quantify viral load. In addition, these degenerate primers were not validated using white sturgeon-derived DNA¹⁰ and cross-reactivity with white sturgeon tissues has been suspected.

Given these current limitations, this study aimed to 1) determine the complete genome of AciHV-2 using four isolates from previous outbreaks in the western United States, and 2) design and validate a quantitative polymerase chain reaction (qPCR) assay for the diagnosis of AciHV-2 in white sturgeon fin tissue. These two accomplishments will lay a foundation and provide tools for future studies characterizing viral pathogenesis and assessing host-pathogen interactions at the genetic and molecular levels.

2. Materials and Methods

2.1 Viral DNA sample generation

White sturgeon skin (WSSK-1) cells^{11,12} were grown from stock and maintained in “Minimum essential media” (MEM; Corning Inc, Corning, NY) supplemented with 7.5% Fetal Bovine Serum (FBS; Genesee, El Cajón, CA), L-glutamine (Gibco, Grand Island, NY), and penicillin/streptomycin (Gibco, Grand Island, NY) at 20°C.

Seeding of WSSK-1 cells in T75 flasks was done at approximately 90% confluency in MEM supplemented with 2% FBS, L-glutamine, and penicillin/streptomycin. After 24 hours, four archived Acipenserid Herpesvirus 2 (AciHV-2) isolates (Identifiers: UCD3-30⁶, OCR¹³, SR-WSHV^{7,11}, and R20-11), isolated from natural outbreaks in 1991 (California), 1997 (Oregon), 1999 (Idaho), and 2020 (California) respectively, were propagated individually from stocks in WSSK-1 cells.

Ten days post-inoculation, infected cell cultures were collected and centrifuged at 1900 g for 10 min. For each isolate, genomic DNA (gDNA) was isolated from a 200 μ L aliquot of the supernatant using the DNeasy Blood & Tissue kit (QIAGEN, Hilden, Germany) and gDNA eluted in 100 μ L of elution buffer (EB; QIAGEN, Hilden, Germany). Quality and quantity of gDNA was assessed spectrophotometrically (Nanodrop; ThermoFisher Scientific, Waltham, MA). Due to low yields (<20 ng μ L⁻¹) whole genome amplification of viral DNA was performed using the RepliG mini kit (QIAGEN, Hilden, Germany). In addition to the four AciHV-2 isolates, gDNA was also isolated from the following archived virus stocks: White Sturgeon Iridovirus (isolate identifiers: F89-62, F93-39, F12-24, and F00-19), Missouri River Sturgeon Iridovirus (isolate identifier: R06-30), Lake Sturgeon Herpesvirus (isolate identifier: 200413-11TC)¹⁴, Salmonid Herpesvirus 3 (isolate identifiers: d49-E1-7-fin-tis and 170921-1-skin-hom)¹⁵, Acipenserid Herpesvirus 1 (isolate identifier: F90-33)¹⁶, Rana Catesbiana Virus (isolates identifiers: F98-16, and F93-45), and Frog Virus 3 (isolate identifier: R09-50).

2.2 Whole-genome sequencing and assembly

Samples with at least 500 ng of total DNA and a 260/280 ratio of absorbance between 1.8-2.0 were sent for Illumina sequencing at GENEWIZ (Azenta Lifesciences, Chelmsford, MA) and Oxford Nanopore Sequencing at the Thad Cochran National Warmwater Aquaculture Center in Stoneville, MS. For the Illumina data, reads of 150 bp were generated using the Illumina HiSeq 4000. Long sequencing reads were produced on a GridION platform (Oxford Nanopore Technologies, Oxford, UK; ONT) using the ligation sequencing kit (LSK109) with the Native Barcoding Expansion pack (EXP-NBD104) and v9.4.1 flow cells.

Illumina reads were uploaded to the University of California’s High-Performance Computing Farm Cluster. The command-line tool sourmash¹⁷ and Python library termplotlib were used to confirm the presence of a viral genome via k-mer exploration. Subsampling was performed to obtain approximately 250x coverage based on an estimated viral genome size of 160 kb to facilitate downstream processing while preserving appropriate sequencing coverage for correct genome assembly.¹⁸ Assembly was then performed using MEGAHIT¹⁹ with a min count value set to 3, and results were evaluated for quality with QUASt²⁰. Based on quality assessment, contigs with low abundance suspected to be contamination from the WSSK-1 cells used for propagation were removed using Khmer²¹. The script used in this study is available upon request.

Long reads (ONT) were filtered by quality and a minimum length of 1000 bp using NanoPack²² to obtain approximately 90x coverage. A single large contig for each isolate was assembled with Canu²³. Filtered raw reads were aligned to assembled contigs using Minimap2²⁴ and one round of base correction was performed using Medaka (Oxford Nanopore Technologies, Oxford, UK). Illumina reads were then aligned to ONT-assembled contigs using Minimap2 and base correction was performed using Pilon²⁵.

Table 2.1 | GenBank accession information for genomes utilized in comparison experiments using sourmash.

Organism	GenBank Accession Number	Family
Anguillid Herpesvirus 1 (AngHV-1)	GCA_000886195.1	<i>Alloherpesviridae</i>
Cyprinid Herpesvirus 1 (CyHV-1)	GCA_000903355.1	<i>Alloherpesviridae</i>
Cyprinid Herpesvirus 2 (CyHV-2)	GCA_000900815.1	<i>Alloherpesviridae</i>
Cyprinid Herpesvirus 3 (CyHV-3)	GCA_000871465.1	<i>Alloherpesviridae</i>

Ictalurid Herpesvirus 1 (IcHV-1)	GCA_000839325.1	<i>Alloherpesviridae</i>
Ictalurid Herpesvirus 2 (IcHV-2)	GCA_008792765.1	<i>Alloherpesviridae</i>
Ranid Herpesvirus 1 (RaHV-1)	GCA_000869925.1	<i>Alloherpesviridae</i>
Ranid Herpesvirus 2 (RaHV-2)	GCA_000869245.1	<i>Alloherpesviridae</i>
Ranid Herpesvirus 3 (RaHV-3)	GCA_002158775.1	<i>Alloherpesviridae</i>
Salmonid Herpesvirus 1 (SalHV-1) [†]	GCA_002814575.1	<i>Alloherpesviridae</i>
Salmonid Herpesvirus 2 (SalHV-2) [†]	GCA_002814595.1	<i>Alloherpesviridae</i>
Salmonid Herpesvirus 3 (SalHV-3) [†]	GCA_003181315.1	<i>Alloherpesviridae</i>
Chenolid Herpesvirus 5 (ChHV-5) [†]	GCA_008792165.1	<i>Herpesviridae</i> (alphaherpesvirus)
Gallid Herpesvirus 2 (GaHV-2)	GCA_000846265.1	<i>Herpesviridae</i> (alphaherpesvirus)
Herpes Simplex Virus 1 (HSV-1)	GCA_000859985.2	<i>Herpesviridae</i> (alphaherpesvirus)
Herpes Simplex Virus 2 (HSV-2)	GCA_000858385.2	<i>Herpesviridae</i> (alphaherpesvirus)
Psittacid Herpesvirus 1 (PsHV-1)	GCA_000840765.1	<i>Herpesviridae</i> (alphaherpesvirus)
Varicella-Zoster Virus (VZV)	GCA_000858285.1	<i>Herpesviridae</i> (alphaherpesvirus)
Cytomegalovirus (CMV)	GCA_000845245.1	<i>Herpesviridae</i> (betaherpesvirus)
Elephantid Betaherpesvirus 1 (EIHV-1)	GCA_000905835.1	<i>Herpesviridae</i> (betaherpesvirus)

Human Betaherpesvirus 7 (HHV-7)	GCA_000848125.1	<i>Herpesviridae</i> (betaherpesvirus)
Murid herpesvirus 1 (MHV-1)	GCA_008792765.1	<i>Herpesviridae</i> (betaherpesvirus)
Alcelaphine Herpesvirus (AIHV-1)	GCA_000838825.1	<i>Herpesviridae</i> (gammaherpesvirus)
Epstein-Barr Virus (EBV)	GCA_002402265.1	<i>Herpesviridae</i> (gammaherpesvirus)
Equid Gammaherpesvirus 2 (EHV-2)	GCA_000843985.2	<i>Herpesviridae</i> (gammaherpesvirus)
Kaposi's Sarcoma-associated Herpesvirus (HHV-8)	GCA_000838265.1	<i>Herpesviridae</i> (gammaherpesvirus)
Abalone Herpesvirus (AbHV-1)	GCA_000900375.1	<i>Malacoherpesviridae</i>
Ostreid Herpesvirus 1 (OsHV-1)	GCA_000846065.1	<i>Malacoherpesviridae</i>

† = Partial genome

Manual inspection and corrections of the whole genome assemblies were performed in Geneious Prime (version 2022.0.2). In summary, both Illumina and ONT reads were mapped to the contigs derived from the long reads, revealing a region with deeper coverage (suspected assembly error due to circularization of the herpesvirus during replication, which has been described for other herpesviruses²⁶). Illumina and ONT contigs of the OCR isolate were aligned to the Ictalurid herpesvirus 1 genome²⁷ (GenBank assembly accession: GCA_000839325.1) using Minimap2 to help elucidate the correct beginning and end of the linear DNA, which was confirmed by finding the location where many of the ONT reads abruptly ended. Illumina and ONT reads were aligned to the OCR preliminary genome separately using Minimap2 to manually correct individual base errors and long repeats respectively. Once the OCR isolate genome was finalized,

it was used as a reference to correct the beginning and end of the linear DNA of the remaining three isolates. Illumina and ONT reads were aligned to the preliminary genomes separately using Minimap2 to manually correct individual base errors and long repeats respectively. Annotation was performed with Prokka^{28,29}, using the kingdom setting “Viruses”. Predicted open reading frames (ORFs) were investigated using blastx (BLAST; National Center for Biotechnology Information, Bethesda, MD) and the NCBI Conserved Domains Database.

Table 2.2 | GenBank accession information for genomes utilized in core genes comparison experiments.

Organism	Isolate	GenBank Accession Number
Acipenserid Herpesvirus 2	UCD3-30	OQ626810
Acipenserid Herpesvirus 2	OCR	OQ626811
Acipenserid Herpesvirus 2	SR-WSHV	OQ626812
Acipenserid Herpesvirus 2	R20-11	OQ626813
Acipenserid Herpesvirus 2	SR-WSHV	FJ815289.2
Acipenserid herpesvirus 1	California	OK275729.1 OK275734.1 OK275725.1 OK275730.1 OK275731.1 OK275732.1 OK275728.1 OK275733,1 OK275723.1

		OK275727.1 OK275726.1 OK275724.1
Lake Sturgeon Herpesvirus	Wolf River	OK485036.1
Sterlet Herpesvirus	Gen_M01	VTUV01000924.1
Silurid Herpesvirus 1	KRB14001	MH048901.1
Ictalurid Herpesvirus 1	Auburn1	M75136.2
Cyprinid Herpesvirus 1	NG-J1	JQ815363.1
Cyprinid Herpesvirus 2	ST-J1	JQ815364.1
Cyprinid Herpesvirus 3	KHV-U	DQ657948.1
Anguillid Herpesvirus 1	500138	FJ940765.3
Ranid Herpesvirus 2	Rafferty	DQ665652.1
Ranid Herpesvirus 3	FO1_2015	KX832224.1

Comparison of the obtained AciHV-2 genomes to other published herpesvirus genomes (Table 2.1) at the amino acid level was performed using sourmash¹⁷. In addition, a comparison of the 12 core genes between various members of the *Alloherpesviridae* family, including the AciHV-2 isolates presented here, and the published AciHV-2 partial sequence⁷ (Table 2.2) was performed at the nucleotide level via Multiple Alignment using Fast Fourier Transform (MAFFT) in Geneious Prime. Finally, the terminase coding sequence of the previously mentioned isolates (Table 2.2) was used to generate a maximum likelihood tree using the General Time-Reversible model with a discrete gamma distribution and assuming that a certain fraction of sites is evolutionarily invariable (GTR+G+I). Both the model selection and tree generation were performed in MEGAX³⁰ (version

10.2.6). The confidence levels were calculated from 1000 bootstrap trees³¹ and phylogenetic tree visualization was generated using the web tool iTol³² (version 6.7.1).

2.3 Development of qPCR and generation of positive controls

Obtained ORFs from the Prokka annotation of all four isolates were compared using BLAST. ORFs sharing 99% identity in nucleotide base comparison were selected and aligned to the published partial AciHV-2 genome⁷ (GenBank assembly accession: GCA_002814515.1) to identify potential targets for qPCR development. One of the selected ORFs was identified as the putative ATPase subunit of the terminase gene, which was subsequently compared to the Acipenserid Herpesvirus 1 terminase gene sequence (GenBank accession number: OK275734.1³³) using MUSCLE³⁴ within Geneious Prime. Based on high homology among the four AciHV-2 isolates and divergence (47.43% identity) to AciHV-1, the ATPase subunit of the terminase gene was chosen as the target for qPCR development.

Using the putative ATPase subunit of terminase as the template, a set of primers and probe was designed using the IDT PrimerQuest Tool and checked for significant hairpin structures, heterodimers, and homodimers using the IDT OligoAnalyzer Tool. Design criteria were selected based on published recommendations for qPCR primers and probe design optimization.³⁵

A conventional PCR was performed using the following master mix components per 25 μ L reaction: 12.5 μ L of Dream Taq Green PCR Master Mix 2X (Thermo Fisher Scientific, Waltham, MA), 1 μ L of each 10 μ M primer for a 0.4 μ M final concentration (forward primer: 5' – TCACATTTCCCTCGCACATAACC – 3' and reverse primer: 5' – CACTTGAACCGTTGGTTGATTAC – 3'), and 4.5 μ L of Ambion DEPC-treated water (Thermo Fisher Scientific, Waltham, MA). Cycling conditions were selected based on published

recommendations for PCR optimization,³⁶ with the final protocol consisting of: 1) an initial denaturation of 2 minutes at 95°C, 2) 35 cycles of 15 seconds of denaturation at 95°C followed by 30 seconds of annealing at 50°C followed by 45 seconds of extension at 68°C, and 3) a final extension of 5 min at 68°C. DNA samples generated for whole-genome sequencing were diluted to 50 ng μL^{-1} using Ambion DEPC-treated water. Each 25 μL reaction then contained 19 μL of master mix and 6 μL of DNA sample or 6 μL Ambion DEPC-treated water (negative control) in duplicate. Amplicons were passed through a 1% agarose (Fisher bioagents, Fair Lawn, NJ) gel stained with SYBR Safe DNA Gel Stain (Thermo Fisher Scientific, Waltham, MA) and visualized under UV light. The presence of the expected bands after 1 hour of electrophoresis was confirmed by comparisons to concurrently run molecular weight standards (GeneRuler 1 kb Plus DNA Ladder; Thermo Fisher Scientific, Waltham, MA). The PCR products were purified using the QIAquick PCR Purification kit (QIAGEN, Hilden, Germany) to be used in the generation of the qPCR standard curve. The quality and quantity of the purified DNA was assessed spectrophotometrically (Nanodrop).

2.4 Analytical specificity *in silico*

The obtained ORF for the putative terminase ATPase subunit and the theoretical PCR product were compared to both the white sturgeon (*Acipenser transmontanus*) genome (GenBank assembly accession: GCA_020113195.1) and the sterlet sturgeon genome³⁷ (*Acipenser ruthenus*, GenBank assembly accession: GCA_010645085.1) using BLAST. Off-target priming was assessed *in silico* using the NCBI Primer Blast tool. The PCR product was also used in BLAST for any significant matches.

2.5 Fish

White sturgeon fry (n = 1000; average weight = 1 g) were obtained from a commercial producer and acclimated to a 980-liter circular holding tank for four months. Fish were maintained in a flow-through system supplied with well water (18 – 20°C) with supplemental aeration. Fish were fed daily a combination of ground and 1 mm salmon sink pellet feed (Skretting: a Nutreco company, Stavanger, Norway) equating to 4% of their body weight via an automatic feeder. Water temperature was monitored daily and dissolved oxygen was measured weekly.

An arbitrary sample of 12 white sturgeon fry was selected for general health assessment, bacteriology, and viral culture. Briefly, fish were euthanized with 1000 mg l⁻¹ buffered tricaine methanesulfonate (MS-222, 1:1 sodium bicarbonate; Syndel USA, Ferndale, WA) and assessed grossly for any external lesions. Skin scrapes and gill clips were assessed microscopically for evidence of external parasites. Coelomic swabs were plated on tryptic soy agar supplemented with 5% sheep blood (Biological Media Service, University of California-Davis, CA) and incubated at 20°C for 7 days for bacterial assessment. Whole bodies were 1) pooled, 2) diluted 1:5 in MEM supplemented with 2% FBS, L-glutamine, and penicillin/streptomycin, 3) processed using a Stomacher 80 laboratory blender (Tekmar Company, Cincinnati, OH), 4) brought to a 1:25 final dilution in an antibiotic mixture (FBS, Gentamycin (10 mg mL⁻¹; Gemini Bio Products, West Sacramento, CA), Fungizone (amphotericin B 10 mg mL⁻¹; Sigma, St. Louis, MO) and HEPES (Mediatech Inc, Manassas, VA), 5) incubated overnight at 10°C, 6) and plated in duplicate onto WSSK-1 and White sturgeon spleen (WSS-2)³⁸ cells seeded 24 hours in advance at 90% confluency in 12-well plates with MEM supplemented with 2% FBS, L-glutamine, HEPES, and penicillin/streptomycin. No external parasites, pathogenic bacteria, or viruses were identified during this screening process. All protocols and procedures using these fish were ethically

reviewed and approved by the University of California Institutional Animal Care and Use Committee.

2.6 Infection challenge

White sturgeon fingerlings (n = 720; average weight = 12 g) were used for the challenge experiment. A subgroup of 360 fish were exposed to a 5.96×10^2 Median Tissue Culture Infectious Dose (TCID₅₀) mL⁻¹ bath³⁹ of AciHV-2 (isolate UCD3-30⁶, passage number 8) for 1 hour. The remaining 360 fish were exposed to the same volume of sterile MEM supplemented with 2% FBS, L-glutamine, and penicillin/streptomycin for 1 hour and served as negative controls. Fish were maintained at 17-19°C in 980-liter circular tanks, fed 1% of their body weight of 1 mm-salmon sink pellet feed once daily, and monitored closely. Mortality was recorded for 72 days and pectoral fin clips were collected from all dead fish (n = 180) to confirm AciHV-2 status and determine viral load via the newly developed qPCR. Once the first dead fish was confirmed to be AciHV-2 positive via qPCR, the contralateral pectoral fin of all subsequent mortalities (n=133) was collected for viral culture. In addition to observed mortalities in the exposed fish, two control fish died and were subsequently tested for the presence of AciHV-2.

All survivors were euthanized with 1000 mg µL⁻¹ buffered MS222 72 days after infection. Fin clips from 36 white sturgeon survivors from the AciHV-2 group were obtained to assess the ability of the qPCR to detect AciHV-2 after an outbreak. Twelve of those 36 survivors were arbitrarily selected for assessment of viral load by qPCR in various other tissues (posterior kidney, brain, heart, gills, snout, liver, and spleen). Both pectoral fins were clipped from 120 white sturgeon survivors from the negative control group. One fin clip was processed for detection of AciHV-2 via qPCR, while the other fin clip was used for viral culture. All samples to be used in molecular

assays were saved at -80°C until processing. Whole bodies (n = 6 negative control euthanized fish and n = 13 AciHV-2 fresh mortalities) were preserved in 10% neutral buffered formalin and submitted for histopathological analysis.

2.7 Viral culture from fish tissues

The relative accuracy of the qPCR for detecting AciHV-2 infection was compared to viral culture.¹² Briefly, WSSK-1 cells were plated on 12-well plates at 90% confluency in MEM supplemented with 2% FBS, L-glutamine, HEPES, and penicillin/streptomycin, and allowed to attach for 24 hours. Fins were individually diluted 1:25 in MEM supplemented with 2% FBS, L-glutamine, and penicillin/streptomycin and then subjected to three 1-minute rounds of Stomacher homogenization. Samples were incubated overnight at 10°C in an antibiotic mixture (1:1 ratio; described in section 2.5) and seeded in duplicate onto the WSSK-1 cells with MEM supplemented with 2% FBS, L-glutamine, HEPES, and penicillin/streptomycin. A negative control was included in each plate in duplicate, which comprised of sterile cell culture media. Cultures were monitored daily for one month and cytopathic effects were documented. These results were obtained prior to processing samples for qPCR, making the reader blind to the results of the qPCR for the same fish.

2.8 Generation of standard curve and use of qPCR for viral load quantification

The quantity of purified PCR product obtained for each AciHV-2 isolate (section 2.3) was estimated using the following formula⁴⁰:

$$\text{Copy number in copies}/\mu\text{L} = \frac{(\text{Avogadro's number})(\text{DNA concentration in } g \mu\text{L}^{-1})}{(\text{PCR product length})(\text{Average mass of 1 bp of dsDNA})}$$

Based on these copy number estimations, amplicons from each isolate were diluted 10-fold in Ambion DEPC-treated water, creating a dilution series ranging from 10^7 – 10^1 copies μL^{-1} . These dilution series were assessed by qPCR to generate standard curves for each isolate. Dilutions were run in triplicate, for a total of 4 biological replicates and 3 technical replicates for each biological replicate. Each dilution was then spiked with 250 ng of white sturgeon fin DNA from confirmed AciHV-2 negative fish and assessed similarly to compare PCR performance in the presence and absence of host DNA.

Genomic DNA from tissue samples was isolated using the DNeasy Blood & Tissue kit with the following modifications: tissues were incubated with ATL buffer and proteinase K at 56°C for 1 hour, samples were incubated with AL buffer at 56°C for 10 minutes, and DNA was eluted in 100 μL of AE buffer. Isolated DNA was stored at -80°C until analysis.

Quantitative PCR was performed using the QuantStudio3 qPCR system (Thermo Fisher Scientific, Waltham, MA) to evaluate viral load throughout the challenge experiment. The qPCR was performed in 12- μL reactions consisting of: 6 μL of TaqMan Environmental Master Mix 2.0 (Thermo Fisher Scientific, Waltham, MA), 0.58 μL of the primer/probe cocktail (20 μL of each 100 μM primer, 4 μL of the 100 μM probe, and 196 μL of Ambion DEPC-treated water), 0.46 μL of Ambion DEPC-treated water, and either 5 μL of template DNA ($50 \text{ ng } \mu\text{L}^{-1}$), 5 μL Ambion DEPC-treated water (negative control), or 5 μL of the 10^7 AciHV-2 μL^{-1} dilution made for the standard curve (positive control) in triplicate. The conditions followed are described in section 2.3 and a $\Delta R_n = 0.01$ was used.

PCR inhibition was tested using the TaqMan Exogenous Internal Positive Control (IPC) Reagents – VIC Probe Assay (Thermo Fisher Scientific, Waltham, MA) on the QuantStudio3 qPCR System. The DNA samples used (white sturgeon fin clip DNA from 8 fish previously

confirmed to be AciHV-2 negative) were diluted to 83.3 ng μL^{-1} using Ambion DEPC-treated water. Each 12 μL reaction then contained 9 μL of master mix and 3 μL of DNA sample, or 3 μL Ambion DEPC-treated water (negative control) in triplicate.

2.9 Assessment of conventional PCR using degenerate primers for white sturgeon tissues

End-point PCR using degenerate alloherpesvirus primers¹⁰ was performed in 25- μL reactions consisting of: 12.5 μL of Dream Taq Green PCR Master Mix 2X, 1 μL of each 10 μM primer¹⁰, 6 μL of template DNA (50 ng μL^{-1}), and 4.5 μL of Ambion DEPC-treated water. Analyzed samples consisted of gDNA from AciHV-2 negative fish (confirmed via qPCR and cell culture), AciHV-2 positive fish (confirmed via qPCR and cell culture), and AciHV-2 isolate UCD3-30. Reaction conditions followed previously published protocols.¹⁰

Table 2.3 | Acipenserid Herpesvirus 2 genome description.

Isolate	Length (bp)	Number of ORFs	Illumina raw / assembly depth of coverage (X genome coverage)	Nanopore raw / assembly depth of coverage (X genome coverage)	GC Content (%)
UCD3-30 (1991)	133,739	105	5918.1 / 269.2	449 / 86.9	40.6
OCR (1997)	133,981	103	6805.1 / 268.7	448 / 96.14	40.7
SR-WSHV (1999)	134,180	103	5589.6 / 268.3	447 / 97.64	40.7
R20-11 (2020)	134,203	104	6525 / 268.3	447 / 86.69	40.7

Amplicons and molecular weight standards (GeneRuler 100 bp DNA Ladder; Thermo Fisher Scientific, Waltham, MA) were passed by electrophoresis through a 1% agarose gel in the presence of SYBR Safe DNA Gel Stain. Amplicons were visualized by ultraviolet transillumination, excised, purified using the QIAquick Gel Extraction kit (QIAGEN, Hilden, Germany), and submitted to GENEWIZ for Sanger sequencing using the same primers used to generate the amplicons. Obtained sequences were aligned using MUSCLE³⁴ within Geneious Prime.

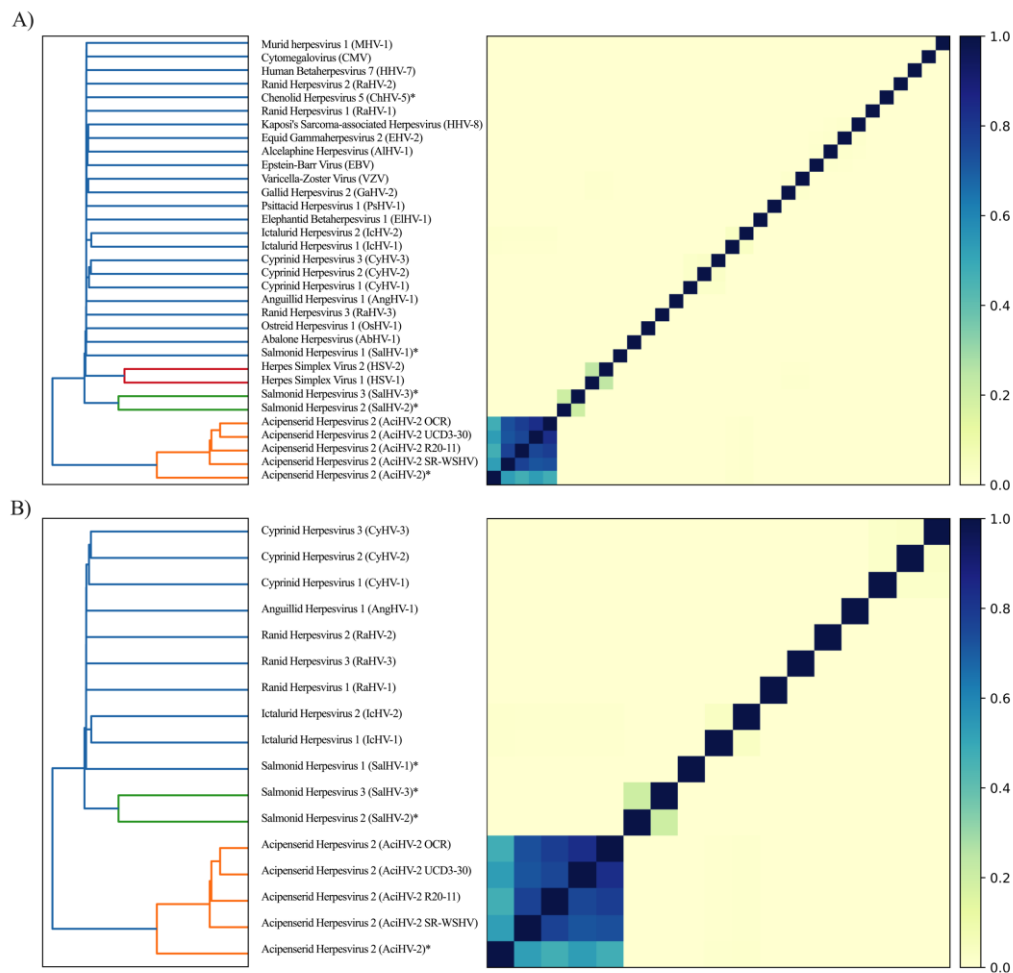


Figure 2.1 | Genome similarity matrix. Obtained Acipenserid Herpesvirus 2 (AciHV-2) amino acid sequences were compared to published herpesvirus amino acid sequences using sourmash. The AciHV-2 genomes cluster with the published AciHV-2 partial genome and separate from other herpesviruses. A) Comparison of representatives from various families of the order *Herpesvirales*. B) Comparison of representatives from various genera of the family *Alloherpesviridae*. The superscript asterisk indicates this is a partial genome.

2.10 Statistical data analysis

The normality of the standard curve and IPC data sets was tested using the Shapiro-Wilk test. A ratio two-tailed paired *t* test was used to compare mean cycle threshold (Ct or Cq) values per dilution between standard curves generated in the presence or absence of host DNA. A Mantel-Cox test was used to compare survival curves. An unpaired *t* test was performed to compare Cq values obtained in the IPC Assay. All analyses were performed using GraphPad Prism 9 (Version 9.3.0 (345), GraphPad Software LLC) at a significance level of ≤ 0.05 .

Table 2.4 | Genetic relationship of Acipenserid Herpesvirus 2 isolates at the nucleotide level.

Isolate	UCD3-30 (1991)	OCR (1997)	SR-WSHV (1999)	R20-11 (2020)
UCD3-30 (1991)	100	98.93	98.70	98.61
OCR (1997)	98.93	100	98.95	98.95
SR-WSHV (1999)	98.70	98.95	100	99.28
R20-11 (2020)	98.61	98.95	99.28	100

Cells show the percentage of bases that are identical between the two compared isolates defined by the column and row titles.

3. Results

3.1 AciHV-2 Whole Genome

The four archived Acipenserid Herpesvirus 2 (AciHV-2) isolates were sequenced to an average coverage depth of 6,209x (Illumina) and 447x (ONT) (Table 2.3), which was reduced to 268x and 92x genome coverage after subsampling (Table 2.3). The final assembled genomes for the AciHV-2 isolates (GenBank Accession Numbers OQ626810 (UCD3-30), OQ626811 (OCR), OQ626812 (SR-WSHV), OQ626813 (R20-11)) were approximately 134 kb (Table 2.3) with high levels of similarity to a published, partial AciHV-2 genome⁷, while discrete from other

alloherpesviruses (Figure 2.1 and Table 2.1). When assessing similarity among the AciHV-2 isolates, the older isolates (UCD3-30 and OCR from outbreaks in 1991 and 1997, respectively) cluster separate from the more recent isolates (SR-WSHV and R20-11 from the outbreaks in 1999

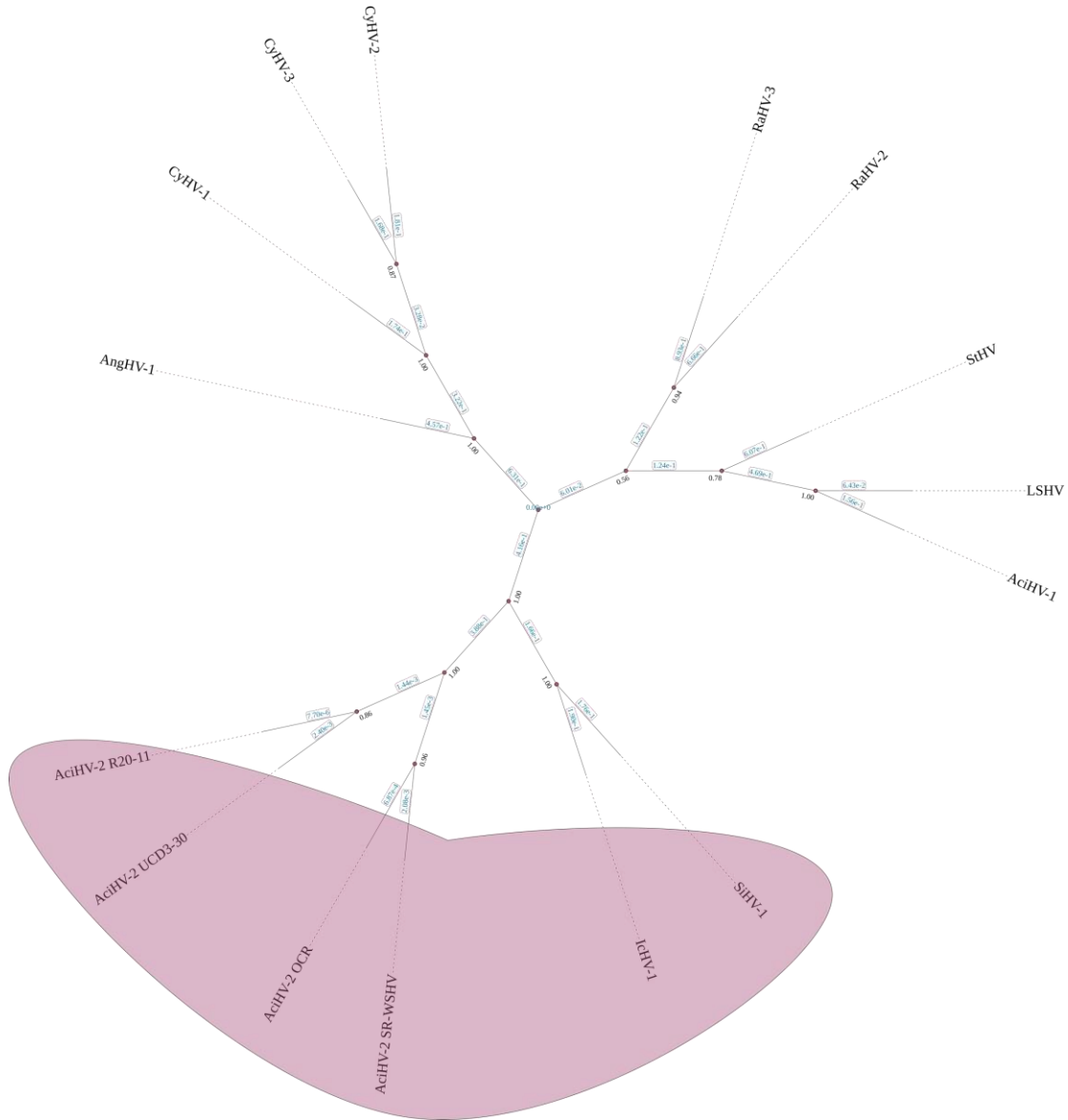


Figure 2.2 | Phylogenetic unrooted tree of selected members of the *Alloherpesviridae* family. The nucleotide coding sequences of the DNA packaging terminase for selected representatives of the *Alloherpesviridae* family were aligned and used to construct a maximum likelihood tree using the General Time-Reversible model with a discrete gamma distribution and assuming an evolutionarily invariable fraction of sites. The reported Acipenserid Herpesvirus 2 (AciHV-2) terminase sequences in this study cluster together with very little divergence and group with the other members of the genus *Ictalurivirus* (shaded in pink). Nodes are marked with a pink circle and labeled with the bootstrap value. Branch length is indicated in blue within a box on the corresponding branch. Complete name for each viral isolate along with the corresponding GenBank accession number can be found in Table 2.2.

and 2020, respectively) (Figure 2.1). Still, whole genome alignments indicate these four isolates share more than 98% identity (Table 2.4), with GC content of approximately 40%. (Table 2.3). Comparisons of the 12 core genes of the *Alloherpesviridae* family to the published partial AciHV-2 genome⁷ revealed high homology (>99%) for each core gene (Table 2.5). Phylogenetic analyses using the maximum likelihood model based on the complete coding sequence of the DNA packaging terminase, which had not been reported for AciHV-2 before, was consistent with previous studies^{8,14,33}. The four AciHV-2 isolates fall within the genus *Ictalurivirus*, along with Ictalurid herpesvirus 1 (IcHV-1) and Silurid herpesvirus 1 (SiHV-1) (Figure 2.2). In addition, there is apparent geographic separation, as isolates from California (UCD3-30 and R20-11) form their own branch separate from isolates from neighboring states (OCR and SR-WSHV) (Figure 2.2).

Table 2.5 | Nucleotide similarity of the 12 core Alloherpesvirus genes between various members of the family *Alloherpesviridae*, including the four newly sequenced Acipenserid herpesvirus 2 (AciHV-2) isolates, and the published AciHV-2 partial sequence (GenBank: FJ815289).

Virus Isolate GenBank Accession Number	pol	ter1	allo56	hel	pri	mcp	tri2	pro	allo37	allo64	allo60	allo54
AciHV2 UCD3-30	99.9	99.6	100	99.9	99.9	99.9	100	99.8	100	99.9	99.6	99.9
OQ626810												
AciHV2 OCR	99.7	99.7	99.9	100	99.9	99.4	100	99.7	99.7	99.9	99.5	99.8
OQ626811												

AciHV2 SR-WSHV ----- OQ626812	99.9	99.9	100	100	100	99.9	100	99.9	100	100	99.9	100
AciHV2 R20-11 ----- OQ626813	99.9	99.7	100	99.7	99.9	100	100	99.9	100	100	99.7	99.8
AciHV2 SR-WSHV ----- FJ815289.2	100	100	100	100	100	100	100	100	100	100	100	100
AciHV1 California ----- OK275729.1 OK275734.1 OK275725.1 OK275730.1 OK275731.1 OK275732.1 OK275728.1 OK275733.1 OK275723.1 OK275727.1 OK275726.1 OK275724.1	39	45.5	30.4	39.2	28.9	30.7	34.9	28.8	30.1	31.4	36.5	33.4
LSHV Wolf River ----- OK485036.1	37.7	45.1	30.1	38.6	28.9	30.1	35.1	27.7	29.7	29.9	35.8	31.7
StHV Gen_M01 -----	37.1	45.8	30.1	39.8	30.1	30.3	31.9	28.2	26.4	31.0	35.4	30.8

VTUV01000924.1												
SiHV1 KRB14001 ————— MH048901.1	56.9	61.1	51.2	52.7	45.2	43.5	51.4	39.6	46.5	48.8	47.8	48.2
IcHV1 Auburn1 ————— M75136.2	56.5	59.4	50.0	53.6	44.5	42.7	49.8	37.8	45.1	47.1	46.7	48.7
CyHV1 NG-J1 ————— JQ815363.1	31.5	38.2	25	31.2	23.4	29.7	27.4	24.1	26.7	28	26.6	25.0
CyHV2 ST-J1 ————— JQ815364.1	31.4	40.3	25.5	27.1	22.4	28.6	28.3	25.2	25.2	25.3	30.6	23.5
CyHV3 KHV-U ————— DQ657948.1	30.7	38.4	23.6	25.9	23.0	28.9	26	24.7	25.4	24.1	28.7	21.8
AngHV1 500138 ————— FJ940765.3	31.1	40.1	25.4	34.6	23.5	28.3	27.6	27.1	28	25.7	29.8	25.0
RaHV2 Rafferty ————— DQ665652.1	32.5	41.2	27.2	35.5	25.9	28.1	27.6	26.4	26.8	26.6	29.9	28.9
RaHV3	35	41.1	33.3	37.8	27.3	30.8	30.8	27.9	27.3	30.5	29.1	31.4

F01_2015																
KX832224.1																

Cells show the percentage of bases that are identical between the isolate defined by the row and the published partial sequence of Acipenserid herpesvirus 2 (FJ815289). Isolates are color-coded by current phylogenetic grouping (teal = AciHV-2 isolates presented in this manuscript; gray = unclassified; pink = *Ictalurivirus*; purple = *Cyprinivirus*; blue = *Batrachovirus*). Abbreviations are as follows: AciHV2 = Acipenserid Herpesvirus 2; AciHV1 = Acipenserid herpesvirus 1; LSHV = Lake Sturgeon Herpesvirus; StHV = Sterlet Herpesvirus; SiHV1 = Silurid herpesvirus 1; IcHV1 = Ictalurid Herpesvirus 1; CyHV1 = Cyprinid Herpesvirus 1; CyHV2 = Cyprinid Herpesvirus 2; CyHV3 = Cyprinid herpesvirus 3; AngHV1 = Anguillid Herpesvirus 1; RaHV2 = Ranid Herpesvirus 2; RaHV3 = Ranid Herpesvirus 3; pol = DNA polymerase catalytic subunit; ter1 = DNA packaging terminase subunit 1; allo56 = Alloherpesvirus protein 56; hel = helicase-primase helicase subunit; pri = helicase-primase primase subunit; mcp = major capsid protein; tri2 = capsid triplex protein 2; pro = capsid maturation protease; allo37 = Alloherpesvirus protein 37; allo64 = Alloherpesvirus protein 64; allo60 = Alloherpesvirus protein 60; allo54 = Alloherpesvirus protein 54.

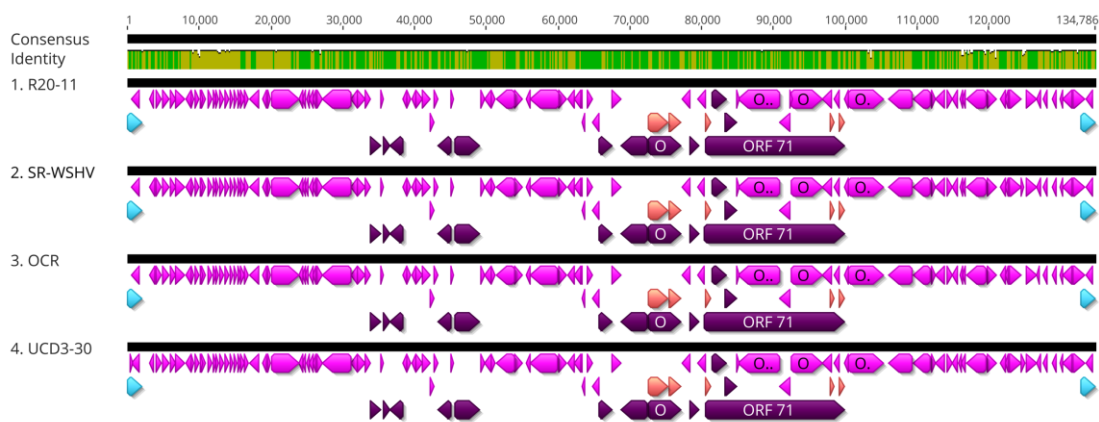


Figure 2.3 | Acipenserid Herpesvirus 2 (AciHV-2) genome map. Four isolates of AciHV-2 were sequenced and their whole genomes were assembled. The AciHV-2 genomes were aligned using MUSCLE within Geneious Prime. The black bars represent the genomes, with length enumerated at the top. Open Reading Frames (ORFs) are depicted in pink (or purple if designated as core genes), with exons of predicted spliced ORFs in red underneath the appropriate ORF. Terminal repeats are depicted in blue. All ORFs, terminal repeats, and exons are directional. The similarity map at the top indicates the mean pairwise identity over all base pairs in the column. Green indicates 100% identity and red indicates less than 30% identity, with yellow indicating $30\% \leq \text{identity} < 100\%$. This depiction was made using Geneious Prime.

Annotation with Prokka²⁸ revealed all four isolates share 101 ORFs, with an additional 1-4 unique ORFs that may be shared with one or more AciHV-2 isolates (Figure 2.3 and Table 2.3). Blast searches revealed several ORFs possess conserved domains consistent with other proteins in the Blast database (Table 2.6), however many of these predicted ORFs do not share significant

homology with any characterized proteins and remain hypothetical proteins of unknown function. Two ORFs (putative DNA polymerase and putative terminase) were spliced, consistent with other alloverpesviruses, with two and three predicted exons respectively (Figure 2.3). In addition, all four AciHV-2 isolates have direct long terminal repeats of 1,907 bp with very little variation among isolates (Figure 2.3). During manual inspection of the genome assembly, long reads generated from Nanopore sequencing were observed to extend from upstream flanking sequence through the terminal repeat into downstream flanking sequence, which was consistent with the circularization of the virus genome with only one copy of the terminal repeats.

Table 2.6 | Acipenserid Herpesvirus 2 open reading frames (ORFs) characterization using Blast.

ORFs	Conserved domain	Accession number	Interval	E value	Putative identity based on homology	E value
1	None detected	N/A	N/A	N/A	Hypothetical protein	N/A
1U	None detected	N/A	N/A	N/A	Hypothetical protein	N/A
2	None detected	N/A	N/A	N/A	Hypothetical protein	N/A
3	RING_Ubox superfamily	c117238	25-126	5.20×10^{-3}	Hypothetical protein	N/A
4	RING_Ubox superfamily (Incomplete conserved domain)	c117238	25-123	7.35×10^{-3}	Hypothetical protein	N/A
5	RING_Ubox superfamily (Incomplete conserved domain)	c117238	22-123	1.32×10^{-4}	Hypothetical protein	N/A
6	None detected	N/A	N/A	N/A	Hypothetical protein	N/A
7	None detected	N/A	N/A	N/A	Hypothetical protein (No significant match)	N/A

8	None detected	N/A	N/A	N/A	Hypothetical protein	N/A
9	None detected	N/A	N/A	N/A	Hypothetical protein	N/A
10	None detected	N/A	N/A	N/A	Hypothetical protein (No significant match)	N/A
11	None detected	N/A	N/A	N/A	Hypothetical protein (Just one match with <i>Salmonella enterica</i> - WP_206667793.1)	2×10^{-117}
12	None detected	N/A	N/A	N/A	Hypothetical protein	N/A
13	None detected	N/A	N/A	N/A	Hypothetical protein	N/A
14	None detected	N/A	N/A	N/A	Hypothetical protein	N/A
15	None detected	N/A	N/A	N/A	Hypothetical protein	N/A
16	None detected	N/A	N/A	N/A	Hypothetical protein (Just one match with <i>Salmonella enterica</i> - WP_147187508.1)	9×10^{-129}
17	None detected	N/A	N/A	N/A	Hypothetical protein	N/A
18	None detected	N/A	N/A	N/A	Hypothetical protein	N/A
19	None detected	N/A	N/A	N/A	Hypothetical protein (Just one match with <i>Salmonella enterica</i> - TXC12839.1)	4×10^{-41}
20	None detected	N/A	N/A	N/A	Hypothetical protein	N/A
21	None detected	N/A	N/A	N/A	Hypothetical protein (Just one match with <i>Salmonella enterica</i> - WP_147187529.1)	5×10^{-70}

22	PKc_like superfamily (incomplete catalytic domain of the serine/threonine kinases and similar kinases)	cd06629	538-1134	2.07x10 ⁻⁸	Protein kinase (Serine/threonine or mitogen-activated protein kinase)	N/A
23	None detected	N/A	N/A	N/A	Hypothetical protein (No significant match)	N/A
24	None detected	N/A	N/A	N/A	Hypothetical protein (Just one match with <i>Salmonella enterica</i> - WP_206667776.1)	3x10 ⁻⁶⁷
25	None detected	N/A	N/A	N/A	Hypothetical protein - suspected membrane protein	N/A
26	None detected	N/A	N/A	N/A	Hypothetical protein (No significant match)	N/A
27	None detected	N/A	N/A	N/A	Hypothetical protein (No significant match)	N/A
28	None detected	N/A	N/A	N/A	Hypothetical protein (No significant match)	N/A
29	None detected	N/A	N/A	N/A	Hypothetical protein (No significant match)	N/A
30	None detected	N/A	N/A	N/A	Hypothetical protein found in various members of the <i>Alloherpesviridae</i> family	N/A
31	None detected	N/A	N/A	N/A	Hypothetical protein (Just one match with <i>Salmonella enterica</i> - TXC12928.1)	9x10 ⁻³⁶

32	PRK03918 superfamily (ATPase) / PTZ00440 (Reticulocyte binding protein 2-like protein)	PRK03918 / PTZ00440	1516-3366 / 10-1983	$8.57 \times 10^{-17} / 2.69 \times 10^{-10}$	Hypothetical protein	N/A
33	None detected	N/A	N/A	N/A	Hypothetical protein found in various members of the <i>Alloherpesviridae</i> family	N/A
34	None detected	N/A	N/A	N/A	Hypothetical protein found in various members of the <i>Alloherpesviridae</i> family	N/A
35	PKc_like superfamily (incomplete catalytic domain of the serine/threonine kinases and similar kinases)	cl21453	157-585	4.79×10^{-16}	Protein kinase (Serine/threonine or mitogen-activated protein kinase)	N/A
36	None detected	N/A	N/A	N/A	Hypothetical protein - Putative helicase (one of the 12 core genes)	N/A
37	None detected	N/A	N/A	N/A	Hypothetical protein	N/A
38	PHA03260 superfamily - Capsid triplex subunit 2; provisional	cl15613	262-879	2.81×10^{-3}	Putative Capsid triplex subunit 2 (one of the 12 core genes)	N/A
39	PHA03369 superfamily - capsid maturation protease; provisional	PHA03369	13-1545	6.63×10^{-45}	Putative capsid maturation protease (one of the 12 core genes)	N/A

40	None detected	N/A	N/A	N/A	Hypothetical protein found in various members of the <i>Alloherpesviridae</i> family	N/A
41	None detected	N/A	N/A	N/A	Hypothetical protein found in various members of the <i>Alloherpesviridae</i> family	N/A
42	None detected	N/A	N/A	N/A	Hypothetical protein found in various members of the <i>Alloherpesviridae</i> family	N/A
43	None detected	N/A	N/A	N/A	Hypothetical protein found in various members of the <i>Alloherpesviridae</i> family	N/A
44	PHA03336 superfamily	c114542	4-900	1.47×10^{-86}	Hypothetical protein found in various members of the <i>Alloherpesviridae</i> family	N/A
45	None detected	N/A	N/A	N/A	Hypothetical protein found in various members of the <i>Alloherpesviridae</i> family	N/A
46	None detected	N/A	N/A	N/A	Hypothetical protein found in various members of the <i>Alloherpesviridae</i> family	N/A
47	None detected	N/A	N/A	N/A	Hypothetical protein found in various members of the	N/A

					<i>Alloherpesviridae</i> family – One of the 12 core genes: allo37	
48	None detected	N/A	N/A	N/A	Hypothetical protein found in various members of the <i>Alloherpesviridae</i> family	N/A
49	None detected	N/A	N/A	N/A	Putative major capsid protein (one of the 12 core genes)	N/A
50	None detected	N/A	N/A	N/A	Hypothetical protein found in various members of the <i>Alloherpesviridae</i> family	N/A
51	None detected	N/A	N/A	N/A	Hypothetical protein found in various members of the <i>Alloherpesviridae</i> family	N/A
52	None detected	N/A	N/A	N/A	Hypothetical protein	N/A
53	None detected	N/A	N/A	N/A	Hypothetical protein found in various members of the <i>Alloherpesviridae</i> family	N/A
54	None detected	N/A	N/A	N/A	Hypothetical protein found in various members of the <i>Alloherpesviridae</i> family	N/A
55	None detected	N/A	N/A	N/A	Hypothetical protein	N/A
56	PHA03332 superfamily - membrane	cl33726	310-702; 1843-3621	1.16×10^{-5} ; 2.39×10^{-69}	Putative Membrane Glycoprotein	N/A

	glycoprotein; provisional					
56	Glyco_hydro_18 superfamily - Glycosyl hydrolases family 18	cl38006	892-1494	9.32×10^{-10}	Putative Glycoside hydrolase	N/A
57	Peptidases_S8_S53 superfamily - peptidase domain in the S8 and S53 families	cl10459	70-741	1.20×10^{-22}	Putative Subtilisin-like proprotein convertase	N/A
58	None detected	N/A	N/A	N/A	Hypothetical protein found in various members of the <i>Alloherpesviridae</i> family	N/A
59	Trimeric_dUTPase superfamily - complete domain	cl00493	37-420	3.58×10^{-19}	Putative dUTP diphosphatase	N/A
60	None detected	N/A	N/A	N/A	Hypothetical protein (No significant match)	N/A
61	None detected	N/A	N/A	N/A	Hypothetical protein (No significant match)	N/A
62	None detected	N/A	N/A	N/A	Hypothetical protein found in various members of the <i>Alloherpesviridae</i> family	N/A
63	None detected	N/A	N/A	N/A	Hypothetical protein found in various members of the <i>Alloherpesviridae</i> family	N/A

64	None detected	N/A	N/A	N/A	Hypothetical protein found in various members of the <i>Alloherpesviridae</i> family – One of the 12 core genes: allo64	N/A
65	None detected	N/A	N/A	N/A	Hypothetical protein found in various members of the <i>Alloherpesviridae</i> family	N/A
66	None detected	N/A	N/A	N/A	Hypothetical protein found in various members of the <i>Alloherpesviridae</i> family – One of the 12 core genes: allo56	N/A
67	PHA03334 superfamily - putative DNA polymerase catalytic subunit; provisional	cl33727	70-2793; 2889-4616	0; 0	Putative DNA-dependent DNA Polymerase (one of the 12 core genes)	N/A
68	None detected	N/A	N/A	N/A	Hypothetical protein found in various members of the <i>Alloherpesviridae</i> family	N/A
69	None detected	N/A	N/A	N/A	Hypothetical protein found in various members of the <i>Alloherpesviridae</i> family – One of the 12 core genes: allo60	N/A

70	None detected	N/A	N/A	N/A	Hypothetical protein found in various members of the <i>Alloherpesviridae</i> family	N/A
71 - First Exon	PHA03333 superfamily - putative ATPase subunit of terminase (incomplete domain)	PHA03333 3	23-799	6.28x10 ⁻⁷⁸	Putative DNA packaging terminase subunit 1 - found in various members of the <i>Alloherpesviridae</i> family (one of the 12 core genes)	N/A
71 - Second Exon	PHA03333 superfamily - putative ATPase subunit of terminase (incomplete domain) / DNA_pack_C - probable DNA packaging protein (C-terminus)	pfam0249 9	1-549 / 211-519	3.43x10 ⁻⁵¹ / 5.59x10 ⁻⁵	Putative DNA packaging terminase - found in various members of the <i>Alloherpesviridae</i> family (one of the 12 core genes)	N/A
71 - Third Exon	PHA03333 superfamily - putative ATPase subunit of terminase (incomplete domain)	PHA03333 3	10-801	2.91x10 ⁻⁵²	Putative DNA packaging terminase subunit 1 - found in various members of the <i>Alloherpesviridae</i> family (one of the 12 core genes)	N/A
72	None detected	N/A	N/A	N/A	Hypothetical protein - Putative helicase-primase found in various members of the <i>Alloherpesviridae</i> family (one of the 12 core genes)	N/A

73	None detected	N/A	N/A	N/A	Hypothetical protein - Putative flap endonuclease 1 like protein (matched the flap endonuclease 1 protein of the spiny head croaker - <i>Collichthys lucidus</i>) – One of the 12 core genes: allo64	6×10^{-9}
74	None detected	N/A	N/A	N/A	Hypothetical protein (No significant match)	N/A
75	Smc superfamily (Chromosome segregation ATPase - cell cycle control, cell division, chromosome partitioning) / PRK03918 superfamily (DNA double-strand break repair ATPase)	COG119 6 / PRK0391 8	2794- 5010 / 3262- 4953	2.22×10^{-20} / 3.72×10^{-15}	Hypothetical protein found in various members of the <i>Alloherpesviridae</i> family	N/A
76	None detected	N/A	N/A	N/A	Hypothetical protein found in various members of the <i>Alloherpesviridae</i> family	N/A
76R	None detected	N/A	N/A	N/A	Hypothetical protein (Just one match with <i>Salmonella enterica</i> - WP_147187523.1)	N/A
77	None detected	N/A	N/A	N/A	Hypothetical protein found in various members of the <i>Alloherpesviridae</i> family	N/A

78	PHA03333 superfamily - putative ATPase subunit of terminase (incomplete domain)	PHA03333	1-228	6.56x10 ⁻¹⁵	Hypothetical protein - overlaps with the second exon of the putative terminase (ORF 71)	N/A
79	None detected	N/A	N/A	N/A	Hypothetical protein found in various members of the <i>Alloherpesviridae</i> family	N/A
80	None detected	N/A	N/A	N/A	Hypothetical protein (Just one match with <i>Salmonella enterica</i> - WP_147187551.1)	3x10 ⁻¹¹⁸
81	None detected	N/A	N/A	N/A	Hypothetical protein (No significant match)	N/A
82	PKc-like superfamily (Protein kinase, catalytic domain)	cl21453	1327-1947; 1681-2223	7.42x10 ⁻¹⁸ ; 2.35x10 ⁻⁸	Putative protein kinase	N/A
83	PKc-like superfamily (Protein kinase, catalytic domain)	cl21453	604-1170; 907-1434	1.39x10 ⁻¹⁰ ; 0	Putative protein kinase	N/A
84	None detected	N/A	N/A	N/A	Hypothetical protein (No significant match)	N/A
85	None detected	N/A	N/A	N/A	Hypothetical protein found in various members of the <i>Alloherpesviridae</i> family	N/A

86	None detected	N/A	N/A	N/A	Hypothetical protein found in various members of the <i>Alloherpesviridae</i> family	N/A
87	None detected	N/A	N/A	N/A	Hypothetical protein (No significant match)	N/A
88	None detected	N/A	N/A	N/A	Hypothetical protein	N/A
89	None detected	N/A	N/A	N/A	Hypothetical protein	N/A
89U	None detected	N/A	N/A	N/A	Hypothetical protein (No significant match)	N/A
89O	None detected	N/A	N/A	N/A	Hypothetical protein (No significant match)	N/A
90	None detected	N/A	N/A	N/A	Hypothetical protein found in various members of the <i>Alloherpesviridae</i> family	N/A
91	None detected	N/A	N/A	N/A	Hypothetical protein (No significant match)	N/A
92	None detected	N/A	N/A	N/A	Hypothetical protein (Just one match with <i>Salmonella enterica</i> - WP_206667779.1)	2×10^{-136}
93	None detected	N/A	N/A	N/A	Hypothetical protein (Just one match with <i>Salmonella enterica</i> - WP_147187539.1)	9×10^{-71}
94	None detected	N/A	N/A	N/A	Hypothetical protein found in various members of the <i>Alloherpesviridae</i> family	N/A

94U	None detected	N/A	N/A	N/A	Hypothetical protein	N/A
95	NK superfamily - Nucleoside/nucleotide kinase	cl17190	643-1188	3.99×10^{-13}	Hypothetical protein - putative thymidine kinase 2 - like protein	N/A
96	None detected	N/A	N/A	N/A	Hypothetical protein (No significant match)	N/A
97	None detected	N/A	N/A	N/A	Hypothetical protein (No significant match)	N/A
98	None detected	N/A	N/A	N/A	Hypothetical protein (Just one match with <i>Salmonella enterica</i> - TXC15802.1)	2×10^{-7}
99	None detected	N/A	N/A	N/A	Hypothetical protein (Just one match with <i>Salmonella enterica</i> - TXC15802.1)	1×10^{-95}
100	None detected	N/A	N/A	N/A	Hypothetical protein (Just one match with <i>Salmonella enterica</i> - WP_147187516.1)	0
101	TNFRSF14_tleost (tumor necrosis factor receptor superfamily member 14 - also known as herpes virus entry mediator)	cd13405	28-258	8.36×10^{-13}	Hypothetical protein (putative tumor necrosis factor receptor member 14 - like protein)	N/A
102	None detected	N/A	N/A	N/A	Hypothetical protein (Just one match with <i>Salmonella enterica</i> - WP_206667781.1)	0

3.2 Primer performance

The putative ATPase subunit of terminase was identified as the top candidate for primer design. Alignments of the AciHV-2 isolates with AciHV-1 revealed <50% identity at the terminase gene (Figure 2.4). Initial assessment of primer performance revealed the presence of a single 105 bp amplicon for all four AciHV-2 isolates.

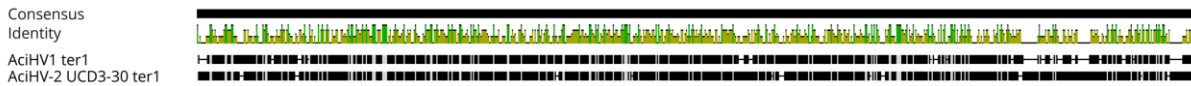


Figure 2.4 | Terminase (ter1) sequence comparison between Acipenserid Herpesvirus 2 (AciHV-2, UCD3-30 isolate) and Acipenserid herpesvirus 1 (AciHV-1). The ter1 open reading frame was identified as a good candidate for primer design. The sequence for ter1 in both AciHV-1 and AciHV-2 were aligned using MUSCLE within Geneious Prime. The black bars represent the genomes, which are labeled on the left column. The similarity map at the top indicates the mean pairwise identity over all base pairs in the column. Green indicates 100% identity and red indicates less than 30% identity, with yellow indicating $30\% \leq \text{identity} < 100\%$. This depiction was made using Geneious Prime.

Analytical specificity *in silico* of the primers using NCBI Primer Blast revealed no significant match to the white sturgeon (*Acipenser transmontanus*), sterlet sturgeon (*Acipenser ruthenus*), or to any other member of the *Alloherpesviridae* family. Moreover, the qPCR was tested against several representatives of the *Alloherpesviridae* family, revealing no observed amplification for all tested isolates (White Sturgeon Iridovirus, Missouri Sturgeon Iridovirus, Lake Sturgeon Herpesvirus, Salmonid Herpesvirus 3, Acipenserid Herpesvirus 1, Rana Catesbiana Virus, and Frog Virus 3).

3.3 AciHV-2 challenge, analytical sensitivity, and relative accuracy

Immersion of white sturgeon fingerlings with AciHV-2 resulted in significant ($p < 0.0001$) mortality (50.5%) compared to fish exposed to sterile cell culture media (Figure 2.5A). The overall

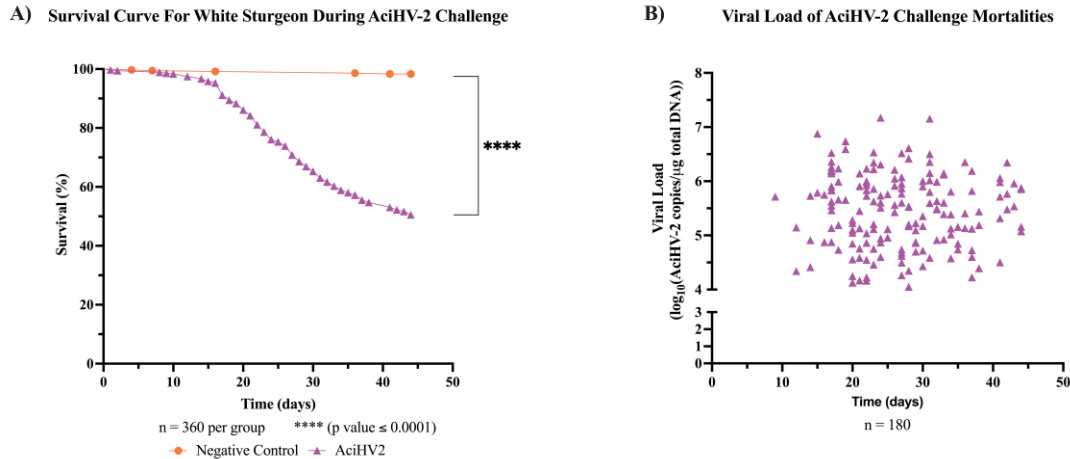


Figure 2.5 | Acipenserid Herpesvirus 2 (AciHV-2) challenge. An immersion challenge model was performed by exposing white sturgeon (*Acipenser transmontanus*) fingerlings to a 10^2 TCID₅₀ (median tissue culture infectious dose) per mL bath or a sterile cell culture media bath for 1 hour. Mortality was monitored for 44 days after immersion and mortalities tested for AciHV-2 via quantitative Polymerase Chain Reaction. A) The solid shapes represent the mean cumulative mortality at each day, with standard error of the mean plotted. The different experimental groups are color coded. The black stars indicate statistical significance when compared to the positive control with a $p \leq 0.0001$. A statistically significant reduction in cumulative mortality is seen in the AciHV-2 exposed group when compared with the negative control group. B) The solid dots represent the viral load of sampled mortalities per day. Both mortalities in the negative control group and seven mortalities in the AciHV-2 group had undetermined Cycle threshold (Ct or Cq) values and are not displayed in this graph.

mean viral load in mortalities was $\log_{10}(5.45 \text{ AciHV-2 copies per } \mu\text{g of total DNA})$, with the two mortalities in the negative control group testing negative for AciHV-2 (Figure 2.5B). All pectoral fin samples from survivors tested negative for AciHV-2 via qPCR. Of all the additional tissues tested from the survivors' subpopulation ($n = 12$), only one individual's snout sample tested positive for AciHV-2 via qPCR ($\log_{10}(5.01 \text{ AciHV-2 copies per } \mu\text{g of total DNA})$). Histopathology revealed no significant findings in the negative control group, while infected fish had severe epithelial changes, characterized by areas of erosion and ulceration of the skin or oral mucosa, often with secondary colonization by bacteria and/or oomycetes.

Reaction efficiency⁴¹ was 96% with an R^2 of 0.9872. Spiking with 250 ng of white sturgeon fin DNA revealed a decrease in efficiency to 90%, but no significant difference in the Cq values

obtained per dilution (Figure 2.6). Internal Positive Control (IPC) analysis revealed no significant inhibition by white sturgeon fin DNA (Figure 2.7). The limit of detection for this assay was 10^3 copies per reaction with a protocol of 35 cycles (Figure 2.6).

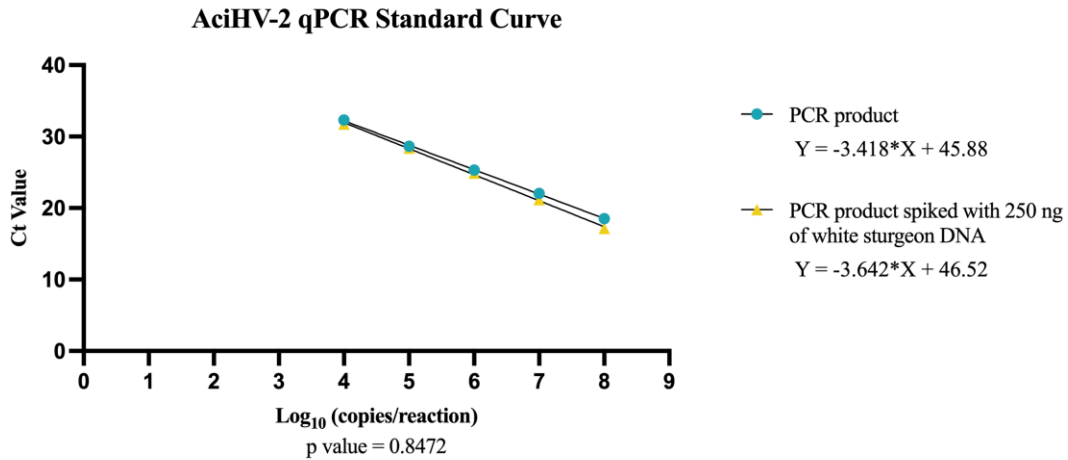


Figure 2.6 | Acipenserid Herpesvirus 2 (AciHV-2) quantitative polymerase chain reaction (qPCR) standard curve. A set of primers and a probe for the putative terminase ATPase subunit of AciHV-2 were designed and a standard curve was generated using PCR product from the same primers on a conventional PCR. A separate curve was generated by generating the same dilutions containing 250 ng of white sturgeon DNA. Curves are colored coded and the solid shapes are a result of four biological replicates, each with three technical replicates. The mean Cycle threshold (Ct or Cq) value and standard error of the mean is plotted. The PCR product curve had an $R^2 = 0.9872$, while the spiked curve had an $R^2 = 0.9844$. The curves reveal a reaction efficiency of 96% and 90% respectively, with no significant difference between the curves.

Diagnostic sensitivity (true positive rate) was assessed from fin clip samples obtained from fish that died following the immersion challenge. For this purpose, 133 fin samples were collected and they all tested positive by both qPCR (Figure 2.5B) and viral culture. Similarly, the true negative rate was assessed from the negative control group, where 120 fin samples from unexposed fish were both qPCR and cell culture negative.

3.4 Degenerate PCR assessment

Fish samples obtained from exposed and unexposed individuals, in addition to DNA from viral isolate (UCD3-30) were assessed using previously published degenerate alloherpesvirus primers¹⁰ to test the ability to detect AciHV-2 in tissues. All samples produced an amplicon at the expected 465 bp length for herpesvirus detection (Figure 2.8). Sequencing and alignments of these amplicons revealed products from uninfected white sturgeon shared 50% identity to the products from the AciHV-2 isolate. The region of priming was difficult to assess due to limitations of sequencing PCR products, however 22 of 28 bases on the 3' end of the reverse primer and 7 of 30

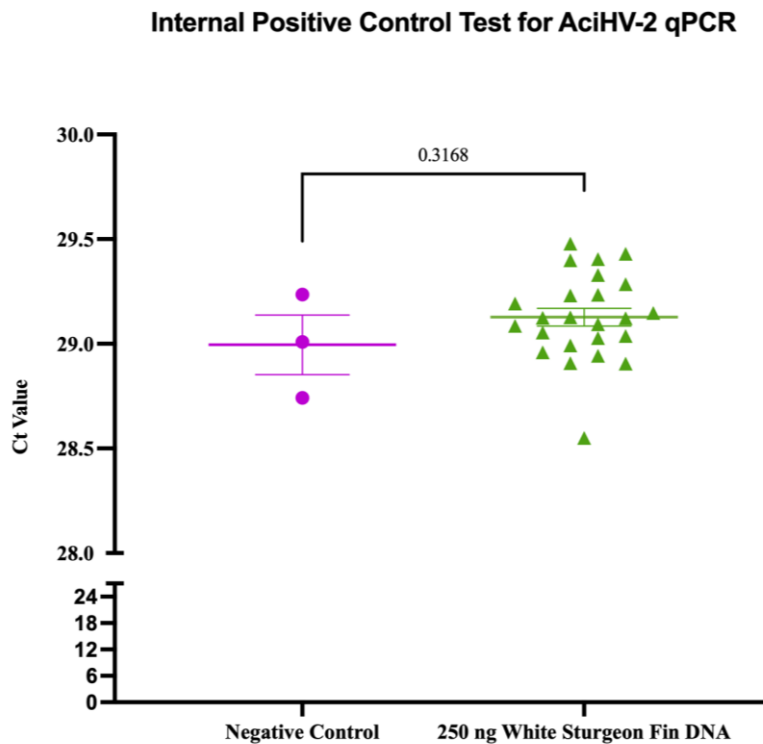


Figure 2.7 | Internal positive control assay. The TaqMan Exogenous Internal Positive Control (IPC) Reagents – VIC Probe Assay was used to assess inhibition of the PCR reaction. The experimental samples contained 83.3 ng of white sturgeon fin DNA per microliter (each in triplicate), while the negative control sample (in triplicate) received DEPC-treated sterile water. Results revealed there was no statistically significant difference in Cq values obtained between the negative control and the sample containing white sturgeon fin DNA.

bases on the 3' end of the forward primer were evaluated. Of those, 100% of the bases were identical between the uninfected sturgeon and the viral isolate.

4. Discussion

Acipenserid Herpesvirus 2 (AciHV-2) has been identified as a cause or contributor to various white sturgeon (*Acipenser transmontanus*) mortality events over the past thirty years^{6,7,42}. Despite

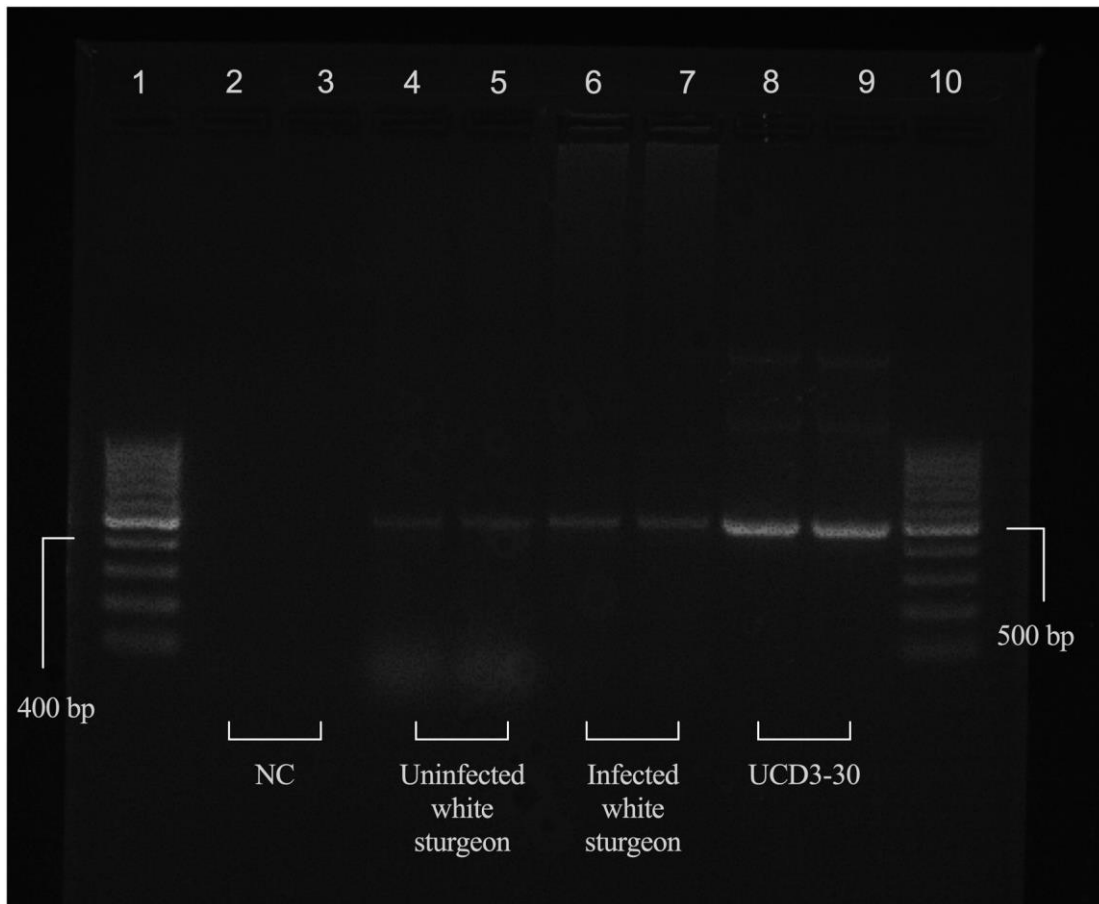


Figure 2.8 | Degenerate primer test for Acipenserid Herpesvirus 2 (AciHV-2) in white sturgeon (*Acipenser transmontanus*). Degenerate primers and its previously published conventional Polymerase Chain Reaction (PCR) protocol (Hanson et al 2006) were used to assess the ability of this assay to detect AciHV-2 in white sturgeon fin DNA samples (300 ng of total DNA loaded per well). Gel electrophoresis with subsequent exposure to ultraviolet light were used to visualize PCR products. Lanes 1 and 10 were loaded with the GeneRuler 100 bp DNA Ladder, with the relevant bands labeled. Lanes 2-9 were loaded with the PCR products indicated underneath. A single band near the expected 465 bp length was detected for all samples, except the negative control.

the potential impact on white sturgeon culture,⁴³ no studies have been done to characterize its virulence, investigate its capability to establish latency,^{44,45} or assess its role in co-infection scenarios.⁴² This was due, in part, to the lack of adequate sequence data for AciHV-2, which is needed to develop certain molecular tools.⁴⁶ Therefore, the first objective of this study was to sequence and assemble the whole genome of AciHV-2 using four isolates recovered from different natural outbreaks in the western United States.

Herein, AciHV-2 isolate genomes were sequenced using a hybridized approach employing both Illumina and Nanopore sequencing. While Illumina reads are generally more accurate with respect to individual base identification compared to Nanopore reads,⁴⁷ the short Illumina reads present a challenge to assemblers in long, repetitive regions, such as tandem repeats.⁴⁸ Moreover, as a member of the *Ictalurivirus*, it was expected that AciHV-2 would also circularize during replication in cell culture.⁴⁹ While more error-prone, long reads generated via ONT were able to span the junction that forms the circularized genome, facilitating determination of the correct ends of the linear genome.

The obtained AciHV-2 genomes are approximately 134 kb in length, consistent with other members of the *Ictaluriviridae* family, namely IchV-1 (Table 2.3).^{7,50} This includes an additional 32,226 bp of sequence upstream and the 36,471 bp of sequence downstream of the published partial genome of AciHV-2.⁷ The congruous region (66,037 bp) of this partial genome has high homology to the study isolates, with 99.7% of bases identical to isolates OCR and R20-11 isolates, and 99.9% identity to isolates SR-WSHV and UCD3-30 isolates. Analysis of the 12 core genes of the *Alloherpesviridae* family yields similar results (Table 2.5). Given the SR-WSHV isolate was originally used to generate the published partial genome, the differences in individual bases between the published partial genome and the sequence in this study are most likely a result of

utilizing different sequencing techniques, depth of coverage, and assemblers. Of the 46 predicted ORFs in the published partial genome, 43 were identified in this study with good agreement. The exceptions were ORF 48 and ORF 84 in the published partial genome, which was predicted to be a single ORF in this study, and ORF 87 in the published partial genome, which was not obtained from the annotation performed in this study. In addition, this study identified two ORFs not previously predicted in the published partial genome (ORF 76R and ORF 74) (Figure 2.3). This again may be a result of the annotation tool used, which has probably undergone modifications to its code in the past decade since the published partial genome was first described. The previously described 12 conserved ORFs among Alloherpesviruses^{7,14,33} were confirmed in this shared region as well, with identical putative identities based on Blast (Table 2.6). The hypothetical proteins included in this list of 12 conserved ORFs have different ORF numbers in this study: allo37 is ORF 47, allo54 is ORF 64, allo56 is ORF 66, allo60 is ORF 69, and allo64 is ORF 73. The last one, ORF 73, seemed to share some homology with a Flap Endonuclease-1 Protein in the spiny head croaker (*Collichthys lucidus*) (Table 2.6). The Flap endonuclease 1 is a protein involved in DNA repair and replication, and it has been described before as having viral homologs with similar function. More specifically, it has been shown that herpesviruses may encode Flap endonuclease 1 (FEN1) activators or homologs to promote successful replication. This has been described for example for Human Cytomegalovirus as a possible strategy to mitigate the difficult replication secondary to rich GC content (57.2%).⁵¹ It is possible that AciHV-2 has evolved mechanisms to guarantee replicative success that involve a FEN1-like protein. Interestingly, the potential functional capacity of FEN1 has been shown to depend heavily on modifications such as phosphorylation or acetylation,⁵¹ so further studies are needed to characterize ORF 73 and investigate its potential role in AciHV-2 infections.

Within the newly reported predicted ORFs in this study, an interesting finding is ORF 101. This ORF has the TNFRSF14_teleost conserved domain, present in Tumor Necrosis Factor Receptor Member 14-like proteins (Table 2.6). This superfamily of proteins, beyond being involved in viral entry to various cells⁵² (also known as Herpes Virus Entry Mediator), is also intertwined in the regulation of various host immune responses.⁵³ Due to its functionally diverse profile, this receptor is an attractive target for viral manipulation. In fact, herpesviruses have been shown to even encode soluble forms of TNFRSF14 members that inhibit cytotoxic and apoptotic responses of the host.⁵⁴ Recently, it was shown that Cyprinid herpesvirus 3 encodes two TNFR homologs capable of regulating apoptosis in host cells and leading to gene expression changes during infection.^{55,56} This is an outstanding candidate for further studies regarding immunomodulation of the white sturgeon during AciHV-2 infections.

In this study, five ORFs are predicted to be present in a subset of the isolates analyzed (ORF 1U in UCD3-30; ORF 76R in R20-11; ORF 89U in UCD3-30 and R20-11; ORF 89O in OCR; and ORF 94U in UCD3-30 and SR-WSHV (truncated)). These ORFs were named according to the closest shared ORF among all isolates and the earliest isolate that contains the ORF. The exception was ORF 96, which is present in all isolates, but the ORF in OCR is truncated. These predictions may represent unique genes in those isolates arising from mutations or loss of that particular ORF in the other isolates due to changes in the sequence leading to loss of starting codon or shift in the reading frame. Further analysis is warranted to assess their biological significance.

Terminal repeats are found in a variety of herpesviruses, including the representative of the genus ICHV-1.^{49,50} The precise function of terminal repeats is not well understood, but it is known that terminal repeats have been implicated in the process of cleaving DNA from concatemers for packaging.⁵⁷ The present study shows that AciHV-2 has direct long terminal repeats of 1907 bp in

length with very little variation among isolates (Figure 2.3). During the manual inspection of the assembly, it was observed that some Nanopore reads ended at the terminal repeat, but other Nanopore reads continued past the terminal repeat end into the unique sequence of the virus (Data not shown). This is supportive of two characteristics described for other herpesviruses, including IcHV-1⁴⁹: 1) the presence of a circular/concatemeric structure during replication, and 2) the presence of only one terminal repeat within that structure. The mechanism of duplicative cleavage, while not fully understood in herpesviruses, has been supported by other studies to describe the presence of one copy of the terminal repeat in these concatemeric herpesviral structures.⁵⁷ The circularization of the herpesviral genome by homologous recombination of the terminal repeats would also support the presence of this sequence detected in the sequencing reads. Further studies would be needed to assess the replication mechanism of AciHV-2 as it pertains to the terminal repeats involvement.

Finally, the second and third putative exons of the terminase are described, containing the complete conserved domain. The terminase gene plays an important role in virus genome packaging and is therefore under evolutionary pressure to remain conserved⁵⁸. Because this process is not present in eukaryotic cells, this makes the terminase gene not only an attractive target for drug development⁵⁹ but also for diagnostic test design.⁶⁰⁻⁶² This reasoning made this an ideal target to develop a diagnostic qPCR for AciHV-2, which was the second objective of the present study.

The diagnostic qPCR test developed and validated in this study, targeting the second exon of the terminase ORF, is highly sensitive and specific for the detection of AciHV-2 in white sturgeon fin DNA samples. The primers and probe set designed have a single target shared by all isolates assessed in this study (Data not shown) and there was no cross-reaction with other known available

viruses that affect white sturgeon and other closely related sturgeon species. In addition, this assay does not cross-react with white sturgeon fin DNA. This is in contrast to the available PCR assay using degenerate primers,¹⁰ which unfortunately cross-reacts with white sturgeon and lake sturgeon (Data not shown) genomic DNA. While the segments sequenced from the uninfected white sturgeon PCR product and the viral isolate PCR product differ significantly, they share enough similarity at the priming sites to lead to a false positive when utilizing the published protocol. It is possible that further processing of the sample before DNA extraction, such as

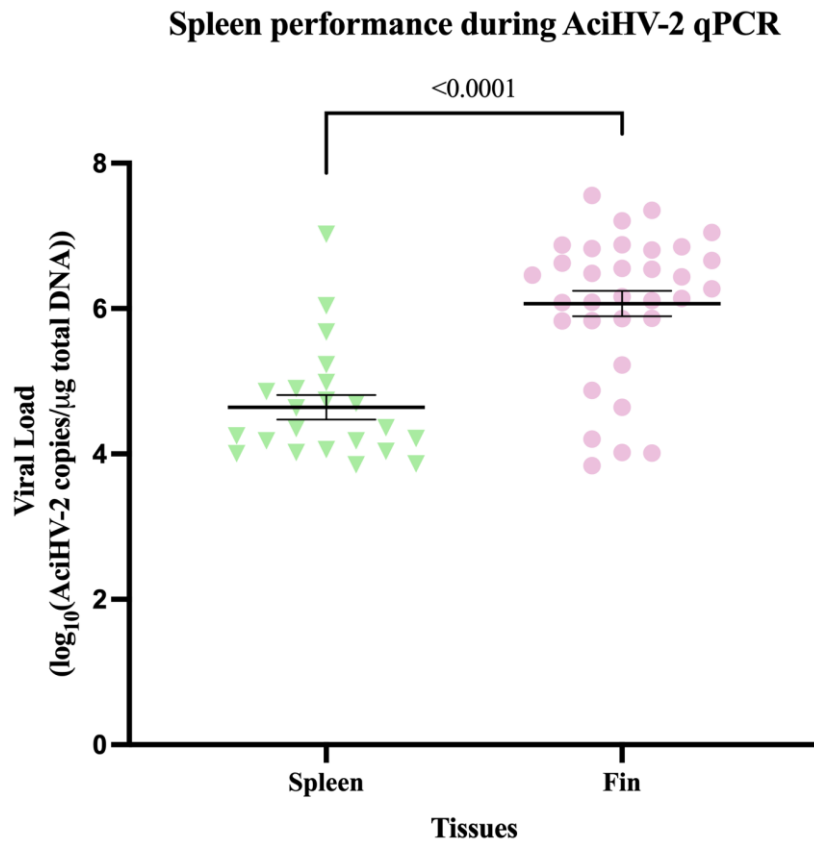


Figure 2.9 | Spleen performance during Acipenserid Herpesvirus 2 (AciHV-2) quantitative polymerase chain reaction (qPCR). An immersion challenge model was performed by exposing white sturgeon fingerlings to an AciHV-2 bath for 1 hour. Mortalities were tested for AciHV-2 via qPCR. The solid dots represent the mean viral load of sampled mortalities for each tissue type, with the standard error of the mean plotted. Results show a statistically significantly lower viral load in the spleen samples, with the spleen samples failing to detect positive individuals in 33.4% of the cases.

filtering through a 0.45 μm ,¹⁰ may reduce host DNA contamination enough to prevent these false positives, but that was not assessed in this study.

Validation of the qPCR assay was performed on infected fish from a laboratory challenge, where the overall mean viral load was $\log_{10}(5.45 \text{ AciHV-2 copies per } \mu\text{g of total DNA})$ (Figure 2.5B). This is not a trivial point because the viral copy number expected during a herpesviral outbreak is significantly higher than during a potential latent or chronic stage of the virus.⁶³ This fact is particularly important to emphasize given the limit of detection of this qPCR is 10^3 copies reaction⁻¹. The current study tested several survivors and did not detect the virus in all except one snout sample. While the potential for AciHV-2 to establish latency in the host has not been proven, there is evidence of this well-known characteristic in many other herpesviruses, including a member of the *Alloherpesviridae* family.⁴⁵ It is possible that increasing the cycle number from 35 to 40 in the protocol or increasing the amount of DNA per reaction would increase sensitivity. However, this was not evaluated given the current protocol was in 100% agreement with cell culture results. Furthermore, the assay performed less efficiently in the presence of 250 ng of host DNA. While this quantity did not result in a statistically significant change in the C_q value per dilution, the addition of more DNA, and potentially more inhibitors,⁶⁴ to the reaction may diminish PCR performance. Finally, an increase in cycle number may increase the detection of non-specific amplification.⁶⁵

As it is suggested by the one survivor with detectable virus levels, AciHV-2 is an epitheliotropic virus that has previously been shown to produce larger viral loads in the operculum and pectoral fin of white sturgeon.⁶ This inherent behavior of the virus combined with the ease of performing fin clips in diseased animals as a non-terminal sampling method was the reasoning behind utilizing the fin DNA in the validation of this assay. Nonetheless, the authors also used a

subset of individuals for which the spleens were tested as well (n = 33, only qPCR performed with no diagnostic validation). The spleen samples consistently showed lower viral loads, as expected, and failed to identify 33.4% of positive individuals (Figure 2.9). This supports the fin as a superior target for AciHV-2 diagnosis.

In summary, the results of this study contribute significantly to the ability to diagnose AciHV-2 in white sturgeon and the potential to develop further molecular tools to study the pathogenesis of AciHV-2. This study revealed the whole genome of AciHV-2 and performed the initial characterization of the ORFs predicted, and described a qPCR assay that is highly sensitive and specific for the identification and quantification of AciHV-2 from white sturgeon fin samples during an active outbreak.

References

1. Kelly J. White Sturgeon [Internet]. California Department of Fish and Wildlife. [cited 2022 Jan 20]. Available from: <https://wildlife.ca.gov/Conservation/Fishes/Sturgeon/White-Sturgeon>
2. Ethier V. Farmed Sturgeon [Internet]. Monterey Bay Aquarium Seafood Watch; 2014 [cited 2022 Jan 20]. Available from: <https://seafood.ocean.org/wp-content/uploads/2016/10/Sturgeon-Farmed-US.pdf>
3. Carocci F, Lagrange C, Levavasseur V, Yakimushkin A. Sturgeons (Acipenseriformes) [Internet]. Food and Agriculture Organization of the United Nations. Available from: <https://www.fao.org/3/Y5261E/y5261e06.htm>
4. Lepa A, Siwicki AK. Fish herpesvirus diseases: a short review of current knowledge. *Acta Vet Brno*. 2012;81(4):383–9.
5. Goodwin A. Herpesviruses in Fish. Southern Regional Aquaculture Center; 2012.
6. Watson L, Yun S, Groff J, Hedrick R. Characteristics and pathogenicity of a novel herpesvirus isolated from adult and subadult white sturgeon *Acipenser transmontanus*. *Dis Aquat Organ*. 1995;22:199–210.

7. Doszpoly A, Somogyi V, LaPatra SE, Benkő M. Partial genome characterization of acipenserid herpesvirus 2: taxonomical proposal for the demarcation of three subfamilies in Alloherpesviridae. *Arch Virol*. 2011 Dec;156(12):2291–6.
8. Kurobe T, Kelley GO, Waltzek TB, Hedrick RP. Revised Phylogenetic Relationships among Herpesviruses Isolated from Sturgeons. *J Aquat Anim Health*. 2008 Jun;20(2):96–102.
9. Waltzek T, Kelley G, Alfaro M, Kurobe T, Davison A, Hedrick R. Phylogenetic relationships in the family Alloherpesviridae. *Dis Aquat Organ*. 2009 Apr 27;84:179–94.
10. Hanson LA, Rudis MR, Vasquez-Lee M, Montgomery RD. A broadly applicable method to characterize large DNA viruses and adenoviruses based on the DNA polymerase gene. *Virol J*. 2006 Dec;3(1):28.
11. Doszpoly A, Kovács ER, Bovo G, LaPatra SE, Harrach B, Benkő M. Molecular confirmation of a new herpesvirus from catfish (*Ameiurus melas*) by testing the performance of a novel PCR method, designed to target the DNA polymerase gene of alloherpesviruses. *Arch Virol*. 2008 Nov;153(11):2123–7.
12. LaPatra SE. Section I: Diagnostic Procedures for Finfish and Shellfish Pathogens. In: *Fish Health Section Blue Book* [Internet]. 2020 Edition. AFS Fish Health Section; 2020. Available from: <https://units.fisheries.org/fhs/fish-health-section-blue-book-2020/>
13. LaPatra SE, Parker BL, Groff JM, Engelking HM, Kaufman J, Munn RJ. Epidemiology of Viral Infections in White Sturgeon from the Pacific Northwest. In: *Proceedings of the Forty-Ninth Pacific Northwest Fish Culture Conference*. Boise, Idaho: Idaho Department of Fish and Game; 1998. p. 27–31.
14. Johnston AE, Shavalier MA, Scribner KT, Soto E, Griffin MJ, Waldbieser GC, et al. First Isolation of a Herpesvirus (Family Alloherpesviridae) from Great Lakes Lake Sturgeon (*Acipenser fulvescens*). *Animals*. 2022 Nov 22;12(23):3230.
15. Faisal M, Loch TP, Shavalier M, VanDeuren MG, Standish I, Winters A, et al. Resurgence of Salmonid Herpesvirus-3 Infection (Epizootic Epitheliotropic Disease) in Hatchery-Propagated Lake Trout in Michigan. *J Aquat Anim Health*. 2019 Mar;31(1):31–45.
16. Hedrick R, McDowell T, Groff J, Yun S, Wingfield W. Isolation of an epitheliotropic herpesvirus from white sturgeon *Acipenser transmontanus*. *Dis Aquat Organ*. 1991;11:49–56.
17. Titus Brown C, Irber L. sourmash: a library for MinHash sketching of DNA. *J Open Source Softw*. 2016 Sep 14;1(5):27.
18. Eklom R, Wolf JBW. A field guide to whole-genome sequencing, assembly and annotation. *Evol Appl*. 2014 Nov;7(9):1026–42.

19. Li D, Luo R, Liu CM, Leung CM, Ting HF, Sadakane K, et al. MEGAHIT v1.0: A fast and scalable metagenome assembler driven by advanced methodologies and community practices. *Methods*. 2016 Jun;102:3–11.
20. Gurevich A, Saveliev V, Vyahhi N, Tesler G. QUAST: quality assessment tool for genome assemblies. *Bioinformatics*. 2013 Apr 15;29(8):1072–5.
21. Crusoe MR, Alameldin HF, Awad S, Boucher E, Caldwell A, Cartwright R, et al. The khmer software package: enabling efficient nucleotide sequence analysis. *F1000Research*. 2015 Sep 25;4:900.
22. De Coster W, D’Hert S, Schultz DT, Cruts M, Van Broeckhoven C. NanoPack: visualizing and processing long-read sequencing data. Berger B, editor. *Bioinformatics*. 2018 Aug 1;34(15):2666–9.
23. Koren S, Walenz BP, Berlin K, Miller JR, Bergman NH, Phillippy AM. Canu: scalable and accurate long-read assembly via adaptive k-mer weighting and repeat separation. *Genome Res*. 2017 Mar 15;36.
24. Li H. Minimap2: pairwise alignment for nucleotide sequences. Birol I, editor. *Bioinformatics*. 2018 Sep 15;34(18):3094–100.
25. Walker BJ, Abeel T, Shea T, Priest M, Abouelliel A, Sakthikumar S, et al. Pilon: An Integrated Tool for Comprehensive Microbial Variant Detection and Genome Assembly Improvement. Wang J, editor. *PLoS ONE*. 2014 Nov 19;9(11):e112963.
26. Strang BL, Stow ND. Circularization of the Herpes Simplex Virus Type 1 Genome upon Lytic Infection. *J Virol*. 2005 Oct;79(19):12487–94.
27. Davison AJ. Channel catfish virus: A new type of herpesvirus. *Virology*. 1992 Jan;186(1):9–14.
28. Seemann T. Prokka: rapid prokaryotic genome annotation. *Bioinformatics*. 2014 Jul 15;30(14):2068–9.
29. Gonzalez-Tortuero E, Krishnamurthi R, Allison H, Goodhead I, James C. Comparative analysis of gene prediction tools for genome annotation [Internet]. *bioRxiv*; 2021 [cited 2023 Jan 12]. Available from: <https://www.biorxiv.org/content/10.1101/2021.12.11.472104v1>
30. Kumar S, Stecher G, Li M, Knyaz C, Tamura K. MEGA X: Molecular Evolutionary Genetics Analysis across Computing Platforms. Battistuzzi FU, editor. *Mol Biol Evol*. 2018 Jun 1;35(6):1547–9.
31. Efron B, Halloran E, Holmes S. Bootstrap confidence levels for phylogenetic trees. *Proc Natl Acad Sci USA*. 1996;

32. Letunic I, Bork P. Interactive Tree Of Life (iTOL) v5: an online tool for phylogenetic tree display and annotation. *Nucleic Acids Res.* 2021 Jul 2;49(W1):W293–6.
33. Walker L, Subramaniam K, Viadanna P, Vann J, Marcquenski S, Godard D, et al. Characterization of an alloherpesvirus from wild lake sturgeon *Acipenser fulvescens* in Wisconsin (USA). *Dis Aquat Organ.* 2022 Jun 2;149:83–96.
34. Edgar RC. MUSCLE: a multiple sequence alignment method with reduced time and space complexity. *BMC Bioinformatics.* 2004;5(1):113.
35. Prediger E. How to design primers and probes for PCR and qPCR [Internet]. IDT Integrated DNA Technologies. 2018. Available from: <https://www.idtdna.com/pages/education/decoded/article/designing-pcr-primers-and-probes>
36. Guidelines for PCR Optimization with Taq DNA Polymerase [Internet]. New England BioLabs Inc. Available from: <https://www.neb.com/tools-and-resources/usage-guidelines/guidelines-for-pcr-optimization-with-taq-dna-polymerase>
37. Du K, Stöck M, Kneitz S, Klopp C, Woltering JM, Adolphi MC, et al. The sterlet sturgeon genome sequence and the mechanisms of segmental rediploidization. *Nat Ecol Evol.* 2020 Jun;4(6):841–52.
38. Hedrick RP, McDowell TS, Rosemark R, Aronstein D, Lannan CN. Two Cell Lines from White Sturgeon. *Trans Am Fish Soc.* 1991 Jul;120(4):528–34.
39. Lei C, Yang J, Hu J, Sun X. On the Calculation of TCID₅₀ for Quantitation of Virus Infectivity. *Virol Sin.* 2021 Feb;36(1):141–4.
40. Prediger E. Calculations: Converting from nanograms to copy number [Internet]. Integrated DNA Technologies. 2017 [cited 2023 Jan 3]. Available from: <https://www.idtdna.com/pages/education/decoded/article/calculations-converting-from-nanograms-to-copy-number>
41. Svec D, Tichopad A, Novosadova V, Pfaffl MW, Kubista M. How good is a PCR efficiency estimate: Recommendations for precise and robust qPCR efficiency assessments. *Biomol Detect Quantif.* 2015 Mar;3:9–16.
42. Soto E, Richey C, Stevens B, Yun S, Kenelty K, Reichley S, et al. Co-infection of *Acipenserid herpesvirus 2 (AciHV-2)* and *Streptococcus iniae* in cultured white sturgeon *Acipenser transmontanus*. *Dis Aquat Organ.* 2017 Mar 30;124(1):11–20.
43. Hanson L, Doszpoly A, Van Beurden SJ, de Oliveira Viadanna PH, Waltzek T. Chapter 9 - Alloherpesviruses of Fish. In: *Aquaculture Virology*. Academic Press; 2016. p. 153–72.
44. Eide KE, Miller-Morgan T, Heidel JR, Kent ML, Bildfell RJ, LaPatra S, et al. Investigation of Koi Herpesvirus Latency in Koi. *J Virol.* 2011 May 15;85(10):4954–62.

45. Reed AN, Izume S, Dolan BP, LaPatra S, Kent M, Dong J, et al. Identification of B Cells as a Major Site for Cyprinid Herpesvirus 3 Latency. *J Virol.* 2014 Aug 15;88(16):9297–309.
46. Costes B, Fournier G, Michel B, Delforge C, Raj VS, Dewals B, et al. Cloning of the Koi Herpesvirus Genome as an Infectious Bacterial Artificial Chromosome Demonstrates That Disruption of the Thymidine Kinase Locus Induces Partial Attenuation in *Cyprinus carpio koi*. *J Virol.* 2008 May 15;82(10):4955–64.
47. Delahaye C, Nicolas J. Sequencing DNA with nanopores: Troubles and biases. Andrés-León E, editor. *PLOS ONE.* 2021 Oct 1;16(10):e0257521.
48. Kellogg EA. Genome sequencing: Long reads for a short plant. *Nat Plants.* 2015 Dec;1(12):15169.
49. Kunec D, Hanson LA, van Haren S, Nieuwenhuizen IF, Burgess SC. An Overlapping Bacterial Artificial Chromosome System That Generates Vectorless Progeny for Channel Catfish Herpesvirus. *J VIROL.* 2008;82:10.
50. Subramaniam K, Venugopalan A, Davison AJ, Griffin MJ, Ford L, Waltzek TB, et al. Complete Genome Sequence of an Ictalurid Herpesvirus 1 Strain Isolated from Blue Catfish (*Ictalurus furcatus*). Stewart FJ, editor. *Microbiol Resour Announc.* 2019 Apr 11;8(15):e00082-19.
51. Schilling EM, Scherer M, Rothmund F, Stamminger T. Functional regulation of the structure-specific endonuclease FEN1 by the human cytomegalovirus protein IE1 suggests a role for the re-initiation of stalled viral replication forks. Kalejta RF, editor. *PLOS Pathog.* 2021 Mar 26;17(3):e1009460.
52. Tiwari V, Clement C, Scanlan PM, Kowlessur D, Yue BYJT, Shukla D. A Role for Herpesvirus Entry Mediator as the Receptor for Herpes Simplex Virus 1 Entry into Primary Human Trabecular Meshwork Cells. *J Virol.* 2005 Oct 15;79(20):13173–9.
53. Steinberg MW, Cheung TC, Ware CF. The signaling networks of the herpesvirus entry mediator (TNFRSF14) in immune regulation: HVEM networks in disease. *Immunol Rev.* 2011 Nov;244(1):169–87.
54. Reading PC, Khanna A, Smith GL. Vaccinia Virus CrmE Encodes a Soluble and Cell Surface Tumor Necrosis Factor Receptor That Contributes to Virus Virulence. *Virology.* 2002 Jan;292(2):285–98.
55. Yi Y, Qi H, Yuan J, Wang R, Weng S, He J, et al. Functional characterization of viral tumor necrosis factor receptors encoded by cyprinid herpesvirus 3 (CyHV3) genome. *Fish Shellfish Immunol.* 2015 Aug;45(2):757–70.
56. Zhou Y, Ouyang P, Tao Y, Yin L, Wang K, Geng Y, et al. Comparison the function of Cyprinid herpesvirus 3 encoded two viral tumor necrosis factor receptors. *Aquac Rep.* 2021 Nov;21:100878.

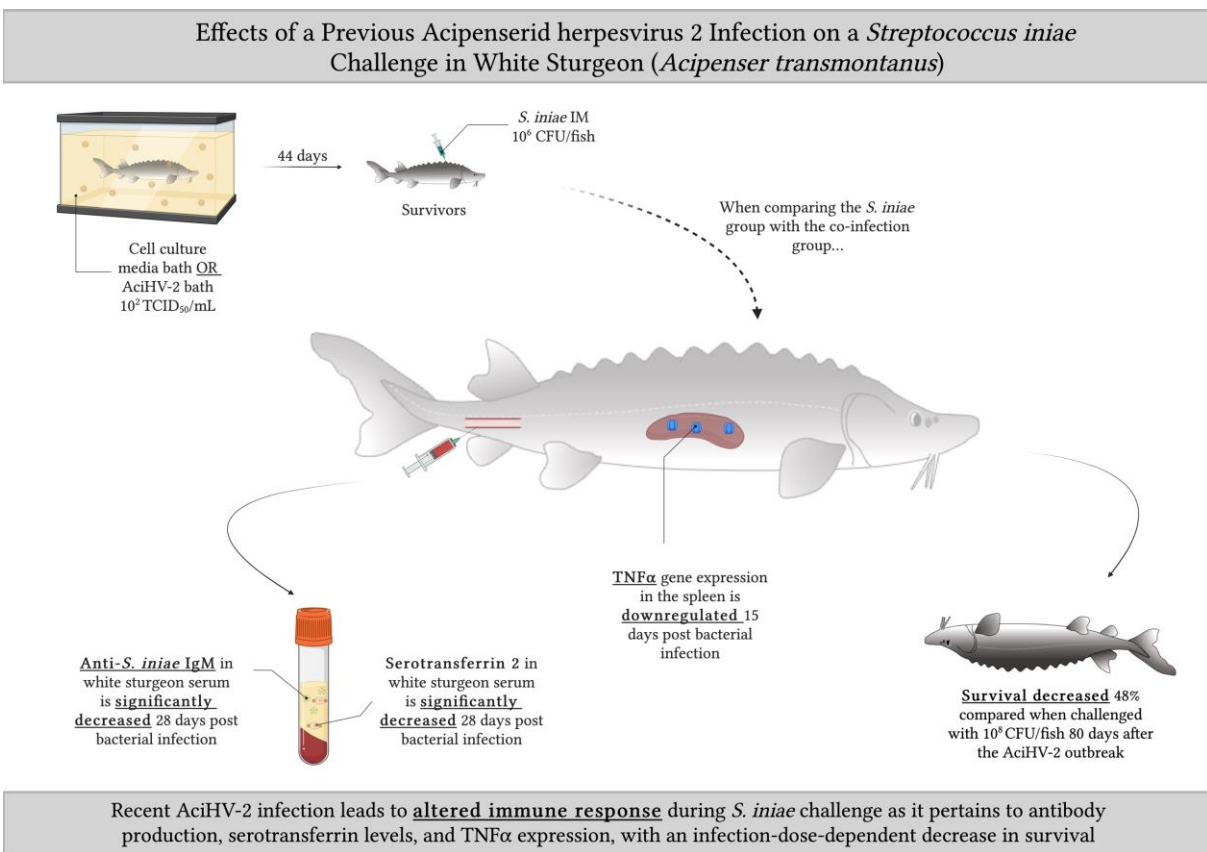
57. Nixon DE, McVoy MA. Terminally Repeated Sequences on a Herpesvirus Genome Are Deleted following Circularization but Are Reconstituted by Duplication during Cleavage and Packaging of Concatemeric DNA. *J Virol.* 2002 Feb 15;76(4):2009–13.
58. Yang L, Yang Q, Wang M, Jia R, Chen S, Zhu D, et al. Terminase Large Subunit Provides a New Drug Target for Herpesvirus Treatment. *Viruses.* 2019 Mar 5;11(3):219.
59. Keil T, Liu D, Lloyd M, Coombs W, Moffat J, Visalli R. DNA Encapsidation and Capsid Assembly Are Underexploited Antiviral Targets for the Treatment of Herpesviruses. *Front Microbiol.* 2020 Aug 12;11:1862.
60. Glenney GW, Barbash PA, Coll JA. A Quantitative Polymerase Chain Reaction Assay for the Detection and Quantification of Epizootic Epitheliotropic Disease Virus (EEDV; Salmonid Herpesvirus 3). *J Aquat Anim Health.* 2016 Mar;28(1):56–7.
61. Pavulraj S, Eschke K, Prah A, Flügger M, Trimpert J, van den Doel PB, et al. Fatal Elephant Endotheliotropic Herpesvirus Infection of Two Young Asian Elephants. *Microorganisms.* 2019 Sep 26;7(10):396.
62. Yuasa K, Kurita J, Kawana M, Kiryu I, Ohseko N, Sano M. Development of mRNA-specific RT-PCR for the detection of koi herpesvirus (KHV) replication stage. *Dis Aquat Organ.* 2012 Aug 13;100(1):11–8.
63. Cohen JI. Herpesvirus latency. *J Clin Invest.* 2020 May 4;130(7):3361–9.
64. Kralik P, Ricchi M. A Basic Guide to Real Time PCR in Microbial Diagnostics: Definitions, Parameters, and Everything. *Front Microbiol [Internet].* 2017 Feb 2 [cited 2022 Dec 13];8. Available from: <http://journal.frontiersin.org/article/10.3389/fmicb.2017.00108/full>
65. Bell DA, DeMarini DM. Excessive cycling converts PCR products to random length higher molecular weight fragments. *Nucleic Acids Res.* 1991;19(18):5079–5079.

CHAPTER 3. Effects of Acipenserid Herpesvirus 2 on the outcome of a *Streptococcus iniae* co-infection in white sturgeon (*Acipenser transmontanus*)

Abstract

Acipenserid herpesvirus 2 (AciHV-2) is a large double-stranded DNA virus in the family *Alloherpesviridae* that causes disease in young, naïve white sturgeon (*Acipenser transmontanus*). Mortality rates can approach 80% in catastrophic outbreaks, with survivors suspected to maintain latent infections. The gram-positive zoonotic bacterium *Streptococcus iniae* is another important sturgeon pathogen that causes severe myositis and up to 50% mortality during natural outbreaks. Over the past decade, co-infections of AciHV-2 and *S. iniae* have been reported in white sturgeon cultured in California, resulting in severe outbreaks of piscine streptococcosis. This phenomenon of herpesvirus and streptococcus co-infection appears to span multiple taxa, including humans, where Human herpesvirus 3 infection (VZV) has been identified as a negative prognostic indicator for pediatric Invasive Group A Streptococcal infections (IGASI). While a decrease in humoral immunity caused by VZV has been hypothesized as an important factor in IGASI cases, no natural animal model exists to study this process. Moreover, no studies have investigated these reported co-infections in white sturgeon. Therefore, the goal of this study was to investigate the effects of a previous AciHV-2 infection on the outcome of a subsequent *S. iniae* challenge in white sturgeon fingerlings. Intramuscular injections of fish with 10^8 colony forming units (CFU) of *S. iniae* yielded significant reductions in survival in fish previously exposed to AciHV-2 compared to fish that were not previously exposed to AciHV-2 (p-value < 0.001). This trend was not observed in comparable studies utilizing a lower *S. iniae* infection dose (10^6 CFU). However, this lower *S. iniae* dose resulted in a statistically significant transcriptional downregulation of TNF α in the

spleen of AciHV-2 survivors compared to fish that were not previously exposed to AciHV-2 (p-value = 0.0098). In addition, serological analysis revealed a statistically significant reduction in anti-*S. iniae* serum IgM and serum serotransferrin in fish exposed to *S. iniae* following AciHV-2 infection (p-value = 0.0134 and p-value = 0.0183, respectively). Further studies are warranted to determine what interactions yield decreased production of pathogen-specific IgM, serotransferrin, and TNF α in the convalescent host.



1. Introduction

The white sturgeon (*Acipenser transmontanus*) is an anadromous fish native to the Pacific Coast of North America¹ and a central part of the multi-million-dollar sturgeon aquaculture

industry. This species alone accounts for 95% of caviar and sturgeon meat production², and generates an annual revenue of over 200 million dollars in exports for the western region of the United States.³ These aquaculture practices provide substantial returns to producers, generate local employment opportunities, and allow for conservation of wild populations by offering a sustainable alternative to wild-caught fish. Continued expansion of the industry, however, is limited partially by infectious disease.

Acipenserid herpesvirus 2 (AciHV-2), also known as White sturgeon herpesvirus 2 or WSHV-2, is a large double-stranded DNA virus in the family *Alloherpesviridae* reported to cause epidermal ulceration, lethargy, inappetence, and erratic swimming^{5,6} in white sturgeon with up to 50% mortality during natural outbreaks⁷⁻⁹ and up to 80% mortality during experimental challenges (Data not shown). *Streptococcus iniae* (*S. iniae*), another important sturgeon pathogen, is a gram-positive, opportunistically zoonotic bacterium that can cause severe myositis in white sturgeon and up to 50% mortality during natural outbreaks.^{10,11} In the last decade, co-infections of AciHV-2 and *S. iniae* have been reported in cultured white sturgeon in California, resulting in severe outbreaks of piscine streptococcosis.¹² This is noteworthy as *S. iniae* infections are typically associated with stress events when causing severe disease in white sturgeon,^{10,11} suggesting that decreased immune response efficacy is needed for the bacteria to achieve pathogenicity in the white sturgeon host.

This herpesvirus-host-streptococcal interaction has also been described in humans in the context of pediatric Invasive Group A Streptococcal infections (IGASI), a condition with an increasing global prevalence over the past two decades.^{13,14} Clinical presentations vary, including necrotizing fasciitis^{15,16}, endocarditis¹⁷, toxic shock syndrome¹⁸, and cellulitis¹⁹. These infections can result in long-term morbidity, prolonged hospitalizations, and an approximately 4% mortality rate.^{18,20} A known risk factor for an unfavorable prognosis and an increased clinical severity is a

prior varicella zoster infection, caused by Human herpesvirus 3 (also known as Varicella-Zoster Virus - VZV), which has been detected in 15-30% of pediatric IGASI cases and increases the risk of acquiring IGASI by 58 fold.^{14,16,20} Canada, one of the few countries to enact a universal VZV vaccination program, reported a subsequent decrease in IGASI severity following its implementation, but no significant impact on the annual mean incidence rate or overall mortality rate.¹⁴ Health disparities and disinformation are factors to consider in the success of any vaccine program²¹ and there are several countries where VZV vaccines are still unavailable.

While a decrease in host humoral immunity caused by VZV infection has been hypothesized as a potential factor in IGASI²⁰, the mechanisms underlying the association between VZV infection and IGASI have not been elucidated. Similarly, while AciHV-2 has been detected in various cases throughout the years, little is known about this virus' pathogenesis and no studies have investigated its potential role in these reported co-infections in white sturgeon.

Herpesviruses are well known for their ability to employ a myriad of mechanisms to modulate the host's immune response to establish and maintain latency.^{22,23} In latency, a reversible state is achieved following an active outbreak wherein the full genome of the virus is maintained in the host cell with limited transcription and no production of viral particles.²³ Depending on the viral species, herpesviral DNA can be maintained as a circular episome (free in the nucleus or tethered to a chromosome) or integrated into the cellular chromosomes near the telomeric junction.²² Even though the switch to latency severely decreases gene expression, long-term persistence in the host is maintained in part by focusing efforts on protection from the immune system via immunomodulation, which can be initiated during the virus' lytic cycle or throughout the transition to latency. Latency has been extensively studied in mammalian herpesviruses, particularly in those affecting humans²²⁻²⁴, and continues to be a topic of active research. However, at present, little is

known about the *Alloherpesviridae* family members including AciHV-2.²⁵⁻²⁷ As a member of the *Herpesvirales* order, and based on previous research involving other important alloherpesviruses such as Cyprinid Herpesvirus 3 (CyHV-3)^{25,26}, it is suspected that AciHV-2 has the capacity to establish latency. While this process may not cause direct mortality or clinical signs, it may have detrimental effects when it comes to the host's ability to clear other pathogens, particularly if immunomodulation is occurring. This may be the case in both pediatric IGASI in humans and the white sturgeon AciHV-2/*S. iniae* co-infections, where the transcriptional profiles of the herpesviruses may influence humoral immune responses against the bacteria as well as impact other unrelated pathways involved in defense against streptococcosis.

These natural co-infections in the white sturgeon present a valuable opportunity for the development of an animal model aimed at studying the complex interactions occurring between the herpesvirus, the host's immune system, and the bacteria.²⁸ This model holds particular relevance considering that previous studies have proposed *S. iniae* as a good candidate for use in animal models designed for translational research involving *S. pyogenes*, *S. agalactiae*, and *S. pneumoniae* due to causing similar clinical presentations and having several homologous virulence factors.^{28,29} Lastly, investigating this phenomenon using the white sturgeon model simultaneously supports a vital sector of the United States aquaculture industry.

Therefore, this study aimed to assess the hypothesis that a prior, potentially latent, AciHV-2 infection in white sturgeon increases mortality caused by *S. iniae* by suppressing the host's immune response against the bacteria.

2. Materials and Methods

2.1 Viral Inoculum Preparation

White Sturgeon Skin (WSSK-1) cells were seeded in eight T75 flasks at approximately 90% confluency in Minimum Essential Media (MEM; Corning Inc, Corning, NY) supplemented with 7.5% Fetal Bovine Serum (FBS; Genesee, El Cajón, CA), L-glutamine (Gibco, Grand Island, NY), and Penicillin/Streptomycin (Gibco, Grand Island, NY) at 20°C. After 24 hours, these cells were used to propagate AciHV-2 isolate UCD3-30⁶ (passage number 8) from cryostock. An aliquot of 500 uL of cryostock was used per T75 flask. Ten days post-inoculation, the infected cell cultures were collected and centrifuged at 1900 g for 10 min. A 1 mL aliquot of the supernatant was used to determine the median tissue culture infectious dose of each viral inoculum using the Reed-Muench method.³⁰ The remaining supernatant was used in the challenges below.

2.2 Bacterial Inoculum Preparation

Streptococcus iniae WS-10A¹¹ was revived from frozen stock on trypticase soy agar supplemented with 5% sheep's blood (SBA; University of California, Biological Media Services) grown at 30°C for 48 hours. The colonies were resuspended in sterile phosphate-buffered saline (PBS) and adjusted to generate two different aliquots: one with an optical density (OD) of 0.98 at 540 nm (~10⁹ colony-forming units (CFU)/mL) and one with an OD of 0.15 at 600 nm (~10⁸ CFU/mL). The latter aliquot was further diluted 1:10 in sterile PBS to generate an aliquot of 10⁷ CFU/mL.

2.3 Fish

White sturgeon fry (n = 1000; average weight ~ 1 g) were obtained from a commercial producer and housed for four months in a 259-gallon circular tank under flow-through conditions supplied with well water (18 – 20°C). Supplemental aeration was provided to maintain 8 - 9 mg/L of dissolved oxygen. Fish were fed 4% of their body weight daily of a combination of ground and 1 mm salmon sink pellet feed (Skretting: a Nutreco company, Stavanger, Norway) via an automatic feeder. Water temperature was monitored daily and dissolved oxygen was measured weekly.

An arbitrary sample of 12 white sturgeon fry was selected for general health assessment and infectious agent screening. Briefly, fish were euthanized with 1000 mg/L (ppm) buffered tricaine methanesulfonate (MS-222, 1:1 sodium bicarbonate; Syndel USA, Ferndale, WA) and assessed grossly for external lesions. Skin scrapes and gill clips were evaluated microscopically for evidence of external parasites. Coelomic swabs were plated on tryptic soy agar supplemented with 5% sheep blood (Biological Media Service, University of California-Davis, CA) and incubated at 20°C for 7 days for bacterial assessment. Whole bodies were 1) pooled, 2) diluted 1:5 in MEM supplemented with 2% FBS, L-glutamine, and Penicillin/Streptomycin, 3) processed using a Stomacher 80 Laboratory Blender (Tekmar Company, Cincinnati, OH), 4) brought to a 1:50 final dilution in an antibiotic mixture (FBS, Gentamycin (10 mg/mL; Gemini Bio Products, West Sacramento, CA), Fungizone (amphotericin B 10 mg/mL; Sigma, St. Louis, MO) and HEPES (Mediatech Inc, Manassas, VA), 5) incubated overnight at 10°C, 6) and plated in duplicate onto WSSK-1³¹ and White Sturgeon Spleen (WSS-2)³¹ cells seeded 24 hours in advance at 90% confluency in 12-well plates with MEM supplemented with 2% FBS, L-glutamine, HEPES, and Penicillin/Streptomycin. In addition, the tissue pellet from the virus screening process was used to screen for AciHV-2 using a recently developed quantitative PCR.³² No external parasites,

pathogenic bacteria, or viruses were identified during this screening process. All protocols and procedures using these fish were ethically reviewed and approved by the University of California Institutional Animal Care and Use Committee.

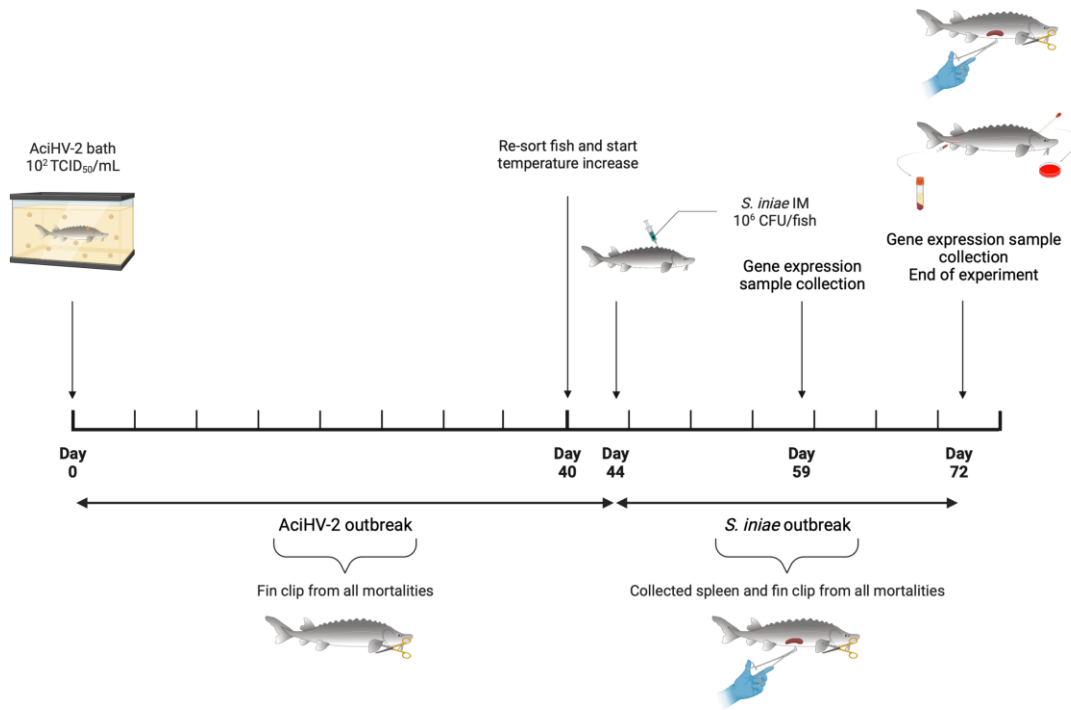


Figure 3.1 | Large-scale challenge timeline. White sturgeon fingerlings were exposed to an Acipenserid Herpesvirus 2 (AciHV-2) or sterile cell culture media immersion for 1 hour (Day 0). Mortality was recorded for 44 days and a pectoral fin clip was collected from every mortality for AciHV-2 quantitative polymerase chain reaction (qPCR) (AciHV-2 outbreak). Survivors of each group were sorted into triplicate tanks to generate four treatment groups (Negative control, AciHV-2, *S. iniae*, and AciHV-2/*S. iniae*) and the temperature was raised 1°C per day from 18–20°C to 22–24°C (Day 40–44). Fish then received 0.1 mL of either *S. iniae* suspension or sterile phosphate-buffered saline intramuscularly on the epaxial musculature (Day 44). Mortality was monitored for 28 days and pectoral fin clips and spleen samples were collected from each mortality for AciHV-2 and *S. iniae* qPCR, respectively (Day 44 - 72). Two fish per tank were euthanized on days 15 and 28 post-injection and spleen collected from each for reverse-transcription qPCR (Day 59 and 72, respectively). At least five moribund individuals per group were euthanized and submitted for histopathology in 10% buffered formalin. At 28 days post-injection, all survivors were euthanized (Day 72). Serum was obtained from 10 survivors of each group for enzyme-linked immunosorbent assay (ELISA) and Western Blot analysis. Re-isolation of bacteria from three survivors’ posterior kidney and brain swabs was performed in blood agar. Pectoral fin clips and spleen samples were collected from 10 survivors per group for molecular testing via AciHV-2 and *S. iniae* qPCR, respectively. This figure was created using BioRender with the white sturgeon depiction being a creation of Dr. Taylor Heckman.

2.4 Laboratory controlled challenges

The first challenge, henceforth referred to as the “pilot challenge”, was performed with 144 white sturgeon fingerlings (average weight = 10 g). A subgroup of 96 fish was exposed via static immersion bath to a 5.1×10^2 Median Tissue Culture Infectious Dose (TCID₅₀)/mL³⁰ of AciHV-2 for 1 hour. The remaining 48 fish were treated similarly, but exposed to an equal volume of sterile MEM supplemented with 2% FBS, L-glutamine, and Penicillin/Streptomycin for 1 hour to serve as negative controls. Fish were maintained at 18-20°C in 259-gallon circular tanks, fed 1% of their body weight of 1 mm-salmon sink pellet feed once daily, and monitored daily for morbidity and mortality for 80 days. A pectoral fin clip was collected from every mortality (n = 37) to quantify AciHV-2 viral load via qPCR³². Survivors of each group were then arbitrarily sorted into duplicate 35-gallon rectangular flow-through tanks (23 fish/group) to generate four treatment groups (Negative control, AciHV-2 infected, *S. iniae* infected, and AciHV-2/*S. iniae* co-infected). Fish were allowed to acclimate to their new environment for four days while the temperature was raised 1°C per day via commercial submersible water heaters (Aqueon, Franklin, WI) to 22-24°C. Fish in the *S. iniae* infected, and AciHV-2/*S. iniae* co-infected groups were challenged by intramuscular injection of *S. iniae* following previously published protocols using the 10⁹ CFU of *S. iniae* per mL suspension (0.1 mL per fish in the epaxial musculature for a final dose of 10⁸ CFU per fish). Fish were challenged under anesthesia (100 ppm buffered MS-222) after a netting stress event (two 30 sec periods out of the water within a net with 30 sec in the water within the net in between).¹⁰ Fish in the Negative control, and AciHV-2 infected groups were treated similarly but were injected with 0.1 mL of PBS. During the anesthetic event, a pectoral fin clip sample was collected from each fish for assessment of AciHV-2 pre-bacterial challenge via qPCR³². Mortality was monitored for 21 days and the cumulative percent mortality (CPM) per group was calculated.

Pectoral fin clips and spleen samples were collected from each mortality and stored at -80°C for molecular testing via AciHV-2³² and *S. iniae*³³ qPCR, respectively. All survivors were euthanized with 1000 ppm of buffered MS-222. Pectoral fin clips were collected from all survivors for testing of AciHV-2 via qPCR³².

The second challenge, henceforth referred to as the “large-scale challenge”, was performed with 720 white sturgeon fingerlings (average weight = 12 g). A subgroup of 360 fish was exposed to a 5.96×10^2 TCID₅₀ / mL bath³⁰ of AciHV-2 for 1 hour. The remaining 360 fish were exposed to the same volume of sterile MEM supplemented with 2% FBS, L-glutamine, and Penicillin/Streptomycin for 1 hour and served as negative controls. Fish were maintained at 18-20°C in 259-gallon circular tanks, fed 1% of their body weight of 1 mm-salmon sink pellet feed once daily, and monitored daily for morbidity and mortality for 44 days. A pectoral fin clip was collected from every mortality (n = 180) to quantify AciHV-2 viral load via qPCR³². Survivors of each group were then arbitrarily sorted into triplicate 35-gallon rectangular flow-through tanks (20 fish/tank) to generate four treatment groups (Negative control, AciHV-2 infected, *S. iniae* infected, and AciHV-2/*S. iniae* co-infected; 60 fish/group). As in the pilot challenge, fish were allowed to acclimate to their new environment for four days while the temperature was raised 1°C per day until reaching 22-24°C. Fish in the *S. iniae* infected, and AciHV-2/*S. iniae* co-infected groups were challenged with *S. iniae* using the 10⁷ CFU of *S. iniae* per mL suspension (0.1 mL per fish in the epaxial musculature for a final dose of 10⁶ CFU per fish) under anesthesia (100 ppm buffered MS-222) after the previously described netting stress event.¹⁰ This administered bacterial dose was lower than in the pilot challenge in order to reduce mortalities and thus have enough fish for immune response assessment sampling. Fish in the Negative control, and AciHV-2 infected groups were treated similarly, but were injected with 0.1 mL of PBS. Mortality was monitored for 28 days

and the cumulative percent mortality (CPM) per group was calculated. Pectoral fin clips and spleen samples were collected from each mortality and stored at -80°C for molecular testing via AciHV-2³² and *S. iniae*³³ qPCR, respectively. Two fish per tank were euthanized with 1000 ppm buffered MS-222 on day 15 post-injection. The spleen of each euthanized fish was collected aseptically and incubated individually in 0.5 mL of RNAlater (ThermoFisher Scientific, Waltham, MA) overnight at 4°C before being transferred to -80°C for storage for subsequent reverse-transcription qPCR (RT-qPCR) analysis. In addition, a pectoral fin clip and spleen sample were collected from each euthanized fish for molecular testing via AciHV-2³² and *S. iniae*³³ qPCR, respectively. At least five moribund individuals per group were euthanized throughout the study and submitted for histological analysis in 10% neutral-buffered formalin (pH 7.2) after fixing for a minimum of 24 hours. Tissues were processed routinely, embedded in paraffin, sectioned at 4 µm, and stained with hematoxylin and eosin (H&E) or Gram stain. Slides were scored based on four categories: “degree of erosion/ulceration”, “distribution of erosion/ulceration”, “percentage of section affected”, and “muscle necrosis”. At 28 days post-injection, all survivors were euthanized with 1000 ppm of buffered MS-222. Ten euthanized individuals per group of this time point were used for the collection of blood, fin clip samples, spleen samples, and swabs as follows. At least 0.8 mL of blood was collected individually in microcentrifuge tubes (with no anticoagulant) from the caudal vein. Clotted blood was then centrifuged at 10,000 g for 5 min and the serum was stored individually at -20°C until enzyme-linked immunosorbent assay (ELISA) and Western Blot analysis. Re-isolation of bacteria from the posterior kidney and brain swabs was performed in SBA. Pectoral fin clips and spleen samples were collected for molecular testing via AciHV-2³² and *S. iniae*³³ qPCR, respectively. A spleen sample was also collected aseptically and immersed in 0.5 mL of RNAlater (ThermoFisher Scientific, Waltham, MA) overnight at 4°C before being

transferred to -80°C for storage until reverse-transcription qPCR (RT-qPCR) analysis. A graphical representation of the timeline of the large-scale challenge can be found in Figure 3.1.

2.5 Pathogen quantification and gene expression assay

Genomic DNA from fin and spleen samples was isolated using the DNeasy Blood & Tissue kit (QIAGEN, Hilden, Germany) with the following modifications: tissues were incubated with ATL buffer and proteinase K at 56°C for 1 hour and samples were incubated with AL buffer at 56°C for 10 minutes. Isolated DNA was stored at -20°C until analysis using the recently developed AciHV-2 qPCR³² and the previously published *S. iniae* qPCR³³. Positive controls were included in each assay, consisting of purified genomic DNA extracted from the original inoculums described above in sections 2.1 and 2.2 (10^7 copies/reaction). The DNA concentration and quality of each sample and control were assessed spectrophotometrically (Nanodrop; ThermoFisher Scientific, Waltham, MA) and all samples and controls were diluted in sterile water to 50 ng/ μ L before being used in the qPCR reactions, for a total of 250 ng of total DNA per 12 μ L reaction. All samples and controls were run in triplicate.

Total RNA from spleen samples, as well as genomic DNA, were isolated using the AllPrep DNA and RNA Mini Kit (QIAGEN, Hilden, Germany). The DNA and RNA concentration and quality of each sample were assessed spectrophotometrically (Nanodrop). The material was considered of sufficient quality if the ratio of absorbance at 260nm and 280 nm (260/280 ratio) was between 1.8 – 2.0 for DNA and between 2.0 – 2.2 for RNA. The DNA samples were used for qPCR as described above. The RNA samples were reverse transcribed to cDNA using the High-capacity RNA-to-cDNA kit (ThermoFisher Scientific, Waltham, MA). The cDNA samples were then diluted 1:2 in sterile water and used to quantify transcript abundance of cytokines, acute-phase proteins, and other molecules involved in various immune pathways from the innate and

adaptive responses (Serum Amyloid A - *saa*, Major Histocompatibility Complex Class II - *mhcII*, Interleukin 17 - *il17*, Interferon Regulatory Factor 8 - *irf8*, and Tumor Necrosis Factor alpha - *tnfa*) via previously published reverse-transcription qPCR (RT-qPCR)^{34,35} protocols. The expression of the Elongation Factor and Beta Actin genes was used to normalize the gene expression data and all samples were run in duplicate. The primer sequences used in this study are listed in Table 3.1.

Table 3.1 | Primers used for gene expression assay.

Gene name	Sequence (5' – 3') of forward primer	Sequence (5' – 3') of reverse primer
Serum Amyloid A	GGCCAATTATATCGGTGCAG	AAACTCTGCCAAGCTTCACG
Major Histocompatibility Complex Class II	TCTGCTACGTCATTGGCTTC	TAGGATACATCAGCCGTCACC
Cathelicidin	ATAGTGATTCTGGCGATGG	TTGGGCAAACGTCTCCTTC
Interleukin 17	TAACCCTCCCTCATGTCAGC	AATCCCCCTACCAAAAACG
Interferon Regulatory Factor 8	CGGACTCTTGTGGGAAAATG	ATGGAAGCGTCGATTCTTG
Tumor Necrosis Factor alpha	AAGCCCAGATGGACCAAAAG	TTGAGCTGCTCTTGTTTCCC
Elongation Factor	GGACTCCACTGAGCCACCT	GGGTTGTAGCCGATCTTCTTG
Beta actin	CATTGTCACCAACTGGGATG AC	ACACGCAGCTCATTGTAGAAG GT

2.6 Enzyme-linked immunosorbent assay

An indirect ELISA was performed following previously published protocols³⁶ with some modifications. Briefly, *S. iniae* (isolate WS-10A) was grown from stock on SBA at 28°C for 48 hours. The bacteria was resuspended in coating buffer (1% poly-L-lysine in carbonate-bicarbonate) to an optical density (OD) of 0.245 at 600 nm. Immulon 2HB Flat Bottom Microtiter 96-well plates (Thermofisher Scientific, Waltham, MA) were coated with 100 µL of bacterial suspension per well and incubated overnight at 4°C.

The plates were washed three times with low-salt wash buffer (LSWB; 0.02 M Trizma base, 0.38 M NaCl, 0.05% Tween-20, pH 7.3) and a 250 µL suspension of blocking buffer (5% skim milk powder in double-distilled water) added to each well before incubation at room temperature for 3 hours. Following incubation, the plates were washed again three times with LSBW. The white sturgeon serum samples collected at the end of the challenge were diluted 1:200 in LSBW containing 1% bovine serum albumin (BSA; Sigma) and 100 µL of the diluted serum or sterile PBS was added to respective plate wells in duplicate. Plates were then incubated overnight at 4°C.

The plates were washed five times with high-salt wash buffer (HSWB; 0.02 M Trizma base, 0.5 M NaCl, 0.01% Tween-20, pH 7.7), including a 5 min soak on the last wash. Mouse anti-sturgeon IgM monoclonal antibodies (Aquatic Diagnostics Ltd, UK) were diluted 1:75 in PBS and 100 µL added to each well. The plates were incubated at room temperature for 1 hour before washing five times with HSWB, including a 5 min soak. Goat anti-mouse IgG with conjugated horseradish peroxidase (Sigma-Aldrich, St. Louis, MO) was diluted 1:3000 in LSBW with 1% BSA and 100 µL was added to each well. The plates were incubated at room temperature for 1 hour and then washed with HSWB five times, including a 5 min soak on the last wash. Each well received 100 µL of substrate solution (ABTS 1-component microwell peroxidase substrate kit;

SeraCare Life Sciences, Milford, MA) and the plates were incubated at room temperature for 30 min. The reaction was terminated by adding 100 μ L of stop solution (0.01% Sodium Dodecyl Sulfate in distilled water) to each well. Absorbance at 410 nm was measured using a Cytation 5 Cell Imaging Multimode Reader (BioTek, Winooski, VT) and standardized against the PBS controls.

2.7 Acute-phase protein analysis

Serum serotransferrin (STF-2) levels were determined following previously published protocols.³⁵ Briefly, the protein concentration in each serum sample was determined using the Pierce BCA Protein Assay Kit (ThermoFisher Scientific, Waltham, MA). An aliquot of 25 μ g of total protein per sample was denatured in Laemmli buffer (Bio-Rad Laboratories, Hercules, CA) for 5 min at 95 °C. Samples were loaded into Mini-PROTEAN® TGX Stain-Free™ 4–15% gels (Bio-Rad Laboratories, Hercules, CA) and separated using the Mini-PROTEAN® Tetra Cell gel apparatus (Bio-Rad Laboratories, Hercules, CA) for 50 min at 150 v. Total protein per sample was imaged using the stain-free application on the ChemiDoc MP imager (Bio-Rad Laboratories, Hercules, CA). Gels were then activated and transferred onto 0.22 μ m nitrocellulose (STF) membranes (Azure Biosystems, Dublin, CA) using the Trans-Blot® Turbo™ Mini-size Transfer Stacks and the Trans-Blot® Turbo™ Transfer System (Bio-Rad Laboratories, Hercules, CA) for 3 min. Total protein per sample was imaged again as described above. Membranes were immediately transferred to the blocking buffer of 5% non-fat dry milk in PBS with Tween (PBSTW; 1.37 M NaCl, 27 mM KCl, 100 mM Na₂HPO₄, 18 mM KH₂PO₄, pH 7.4, 0.1% (w/v) Tween 20) and incubated with gentle agitation for 2 h at room temperature. Each blot was then incubated with the following primary/secondary antibody combination: 1) chicken anti-sturgeon

serotransferrin (1:500, Somru BioScience Inc., Charlottetown, PE, CA) and 2) donkey anti-chicken IgY⁺⁺(IgG) (H + L) (1:10,000 Jackson ImmunoResearch Laboratories, Inc.). The primary antibody was diluted in its blocking buffer (5% non-fat dry milk in PBS with Tween) and incubated for 18 hours at 4 °C with gentle agitation, while the secondary antibody was diluted in its blocking buffer (5% non-fat dry milk in PBS with Tween) and incubated for 1 h at room temperature with gentle agitation. All protein bands were visualized using Clarity™ Western ECL Substrate Chemiluminescent Detection Reagent (Bio-Rad Laboratories, Hercules, CA) prior to image acquisition and visualized using a ChemiDoc MP Imaging System (Bio-Rad Laboratories, Hercules, CA). Image analysis was performed using Image Lab™ Software (Bio-Rad Laboratories, Hercules, CA). The data is presented as the ratio of protein of interest expressed as a “fold difference” to the loading control, normalized to total protein levels.

2.8 Statistical analysis

The CPM was assessed using Kaplan-Meier survival analysis with a Mantel-Cox test. All data, except survival data, was assessed for normality with a D’Agostino-Pearson omnibus K2 test. Differences between groups for the viral and bacterial loads were determined using unpaired t-tests and Mann-Whitney tests as appropriate for the desired comparison. The significance of differences in relative gene expression levels between treatments was calculated using a one-way ANOVA or a Kruskal-Wallis test as appropriate followed by a Holm-Sídák’s multiple comparison test (with a single pooled variance) or a Dunn’s multiple comparison test, respectively. The IgM quantification between groups was assessed with a one-way ANOVA and a Sídák’s multiple comparison test (with a single pooled variance). The STF-2 quantification between groups was assessed with a Kruskal-Wallis test and a Dunn’s multiple comparison test. The histopathologist

was not blinded as to treatment group identity and the histopathological scores were compared via one-way ANOVA and a Sidak's multiple comparison test (with a single pooled variance). All results were considered significant at p-values ≤ 0.05 .

3. Results

3.1 Challenge

During the AciHV-2 portion of both challenges, the sturgeon in the AciHV-2 infected group began showing clinical signs seven days post-immersion. Clinical signs included erythema (Figure 3.2A), lethargy, splenomegaly (Figure 3.2B), decreased feed intake, buoyancy abnormalities, epidermal ulcerations (Figure 3.2C), and acute mortality. In addition, it was common to find moderate to severe colonization of the mouth and opercular cavities by oomycetes (Figure 3.2D)

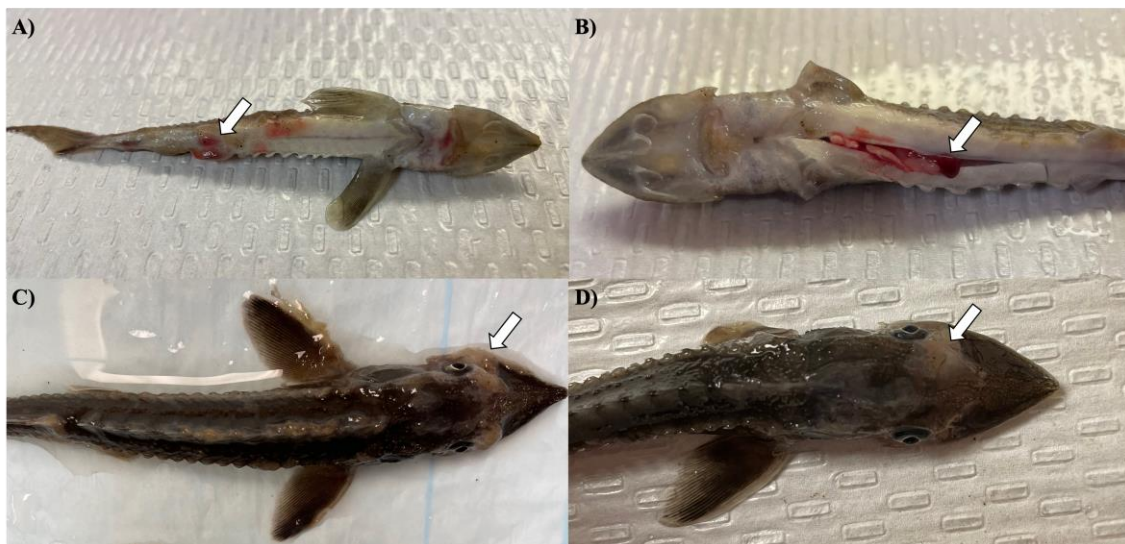


Figure 3.2 | Clinical signs in white sturgeon during Acipenserid Herpesvirus 2 (AciHV-2) challenge. White sturgeon fingerlings were exposed to a 10^2 TCID₅₀ / mL bath for 1 hour. Morbidity and mortality were monitored for 44 (large-scale challenge) to 80 (pilot challenge) days after immersion. These are representative images of clinical signs observed in both challenges during the AciHV-2 outbreak portion of the experiments. A) Erythema surrounding pelvic fins in a fresh mortality. B) Splenomegaly in a fresh mortality. Pectoral fins had been clipped for diagnostic purposes post-mortem. C) Epidermal ulceration medial to the left eye in a fresh mortality. D) oomycetes colonization in an euthanized fish. The white arrows point towards the lesions described.

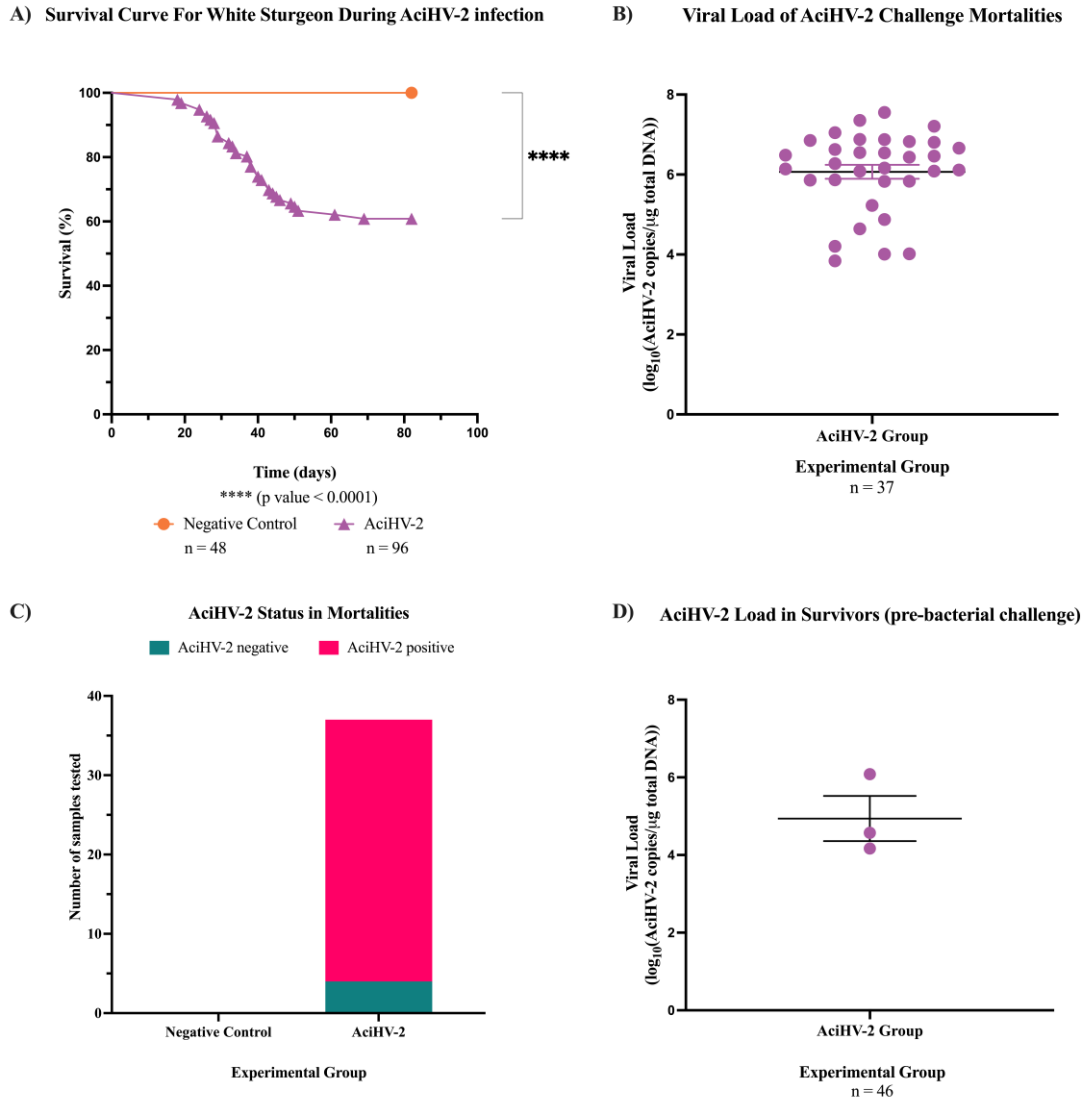


Figure 3.3 | Acipenserid Herpesvirus 2 (AciHV-2) challenge during pilot challenge. A 1-hour static immersion challenge with 10^2 median tissue culture infectious dose (TCID₅₀)/mL of Acipenserid Herpesvirus 2 (AciHV-2) was performed (n=96). A negative control group was treated similarly but sterile cell culture media was used instead of virus suspension (n=48). Mortality was monitored for 80 days and mortalities were tested for AciHV-2 via qPCR of pectoral fin DNA. Survivors were tested for AciHV-2 via quantitative polymerase chain reaction (qPCR) of DNA extracted from the pectoral fin of each fish. A) The solid shapes represent the mean cumulative mortality at each day, with standard error of the mean plotted. The different experimental groups are color-coded. A statistically significant reduction in survival is seen in the AciHV-2 exposed group when compared with the negative control group. B) The solid dots represent the mean viral load of sampled mortalities, with the standard error of the mean plotted. Four mortalities in the AciHV-2 group had undetermined Ct values and are not displayed in this graph. The mean viral load among mortalities was 10^6 copies. C) The bars represent the number of samples tested for AciHV-2 via qPCR, color coded by qPCR result. This shows that 89% of the mortalities in the AciHV-2 group tested positive for AciHV-2 via qPCR. D) The solid dots represent the mean viral load of sampled survivors, with the standard error of the mean plotted. Only three individuals tested positive with a mean viral load of $10^{4.9}$ copies.

in fish displaying severe clinical signs. The experimental group experienced a 40% (pilot challenge) and 50% (large-scale) reduction in survival compared to the negative control, with mortalities starting 18 days post-infection in the pilot challenge (Figure 3.3A) and eight days post-infection in the large-scale challenge (Figure 3.4A). Survivors had no overt clinical signs 52 days (pilot challenge) and 40 days (large-scale challenge) post-immersion, with only sporadic mortalities observed in the following days before the bacterial co-infection (Figures 3.3A and 3.4A, respectively). When assessing viral load in the mortalities, 89% in the pilot challenge (Figure 3.3C) and 94% in the large-scale challenge (Figure 3.4C) tested positive via qPCR with a mean viral load of 10^6 copies in the pilot challenge (Figure 3.3B) and $10^{5.4}$ copies (large-scale challenge, Figure 3.4B) per μg of total DNA. Two fish in the negative control group died during the large-scale challenge, with both testing negative for AciHV-2 via qPCR (Figure 3.4C). Finally, a screening of AciHV-2 via qPCR was performed in the pilot challenge prior to the bacterial infection, with only 0.06% of fish testing positive for AciHV-2 (Figure 3.3D).

During the co-infection portion, sturgeon infected with *S. iniae* began developing clinical signs 24 hours post-injection in both the pilot and the large-scale challenges (Figure 3.5A). Clinical signs included lethargy, inappetence or anorexia, injection site ulceration (Figure 3.5B-D), and acute mortality. A statistically significant difference was observed in survival between the negative control and the treatment groups in both challenges. In the pilot challenge, the co-infection group had a statistically significant decrease in survival of 41% compared to the *S. iniae* group and 36% compared to AciHV-2 group (Figure 3.6A). Mortality trends in the large-scale challenge were consistent with the pilot challenge, with the co-infected group displaying a 7.8% reduction in survival compared to the *S. iniae* group and a 9.1% reduction compared to the AciHV-2 group. However, this difference was statistically significant only when compared with the AciHV-2 group

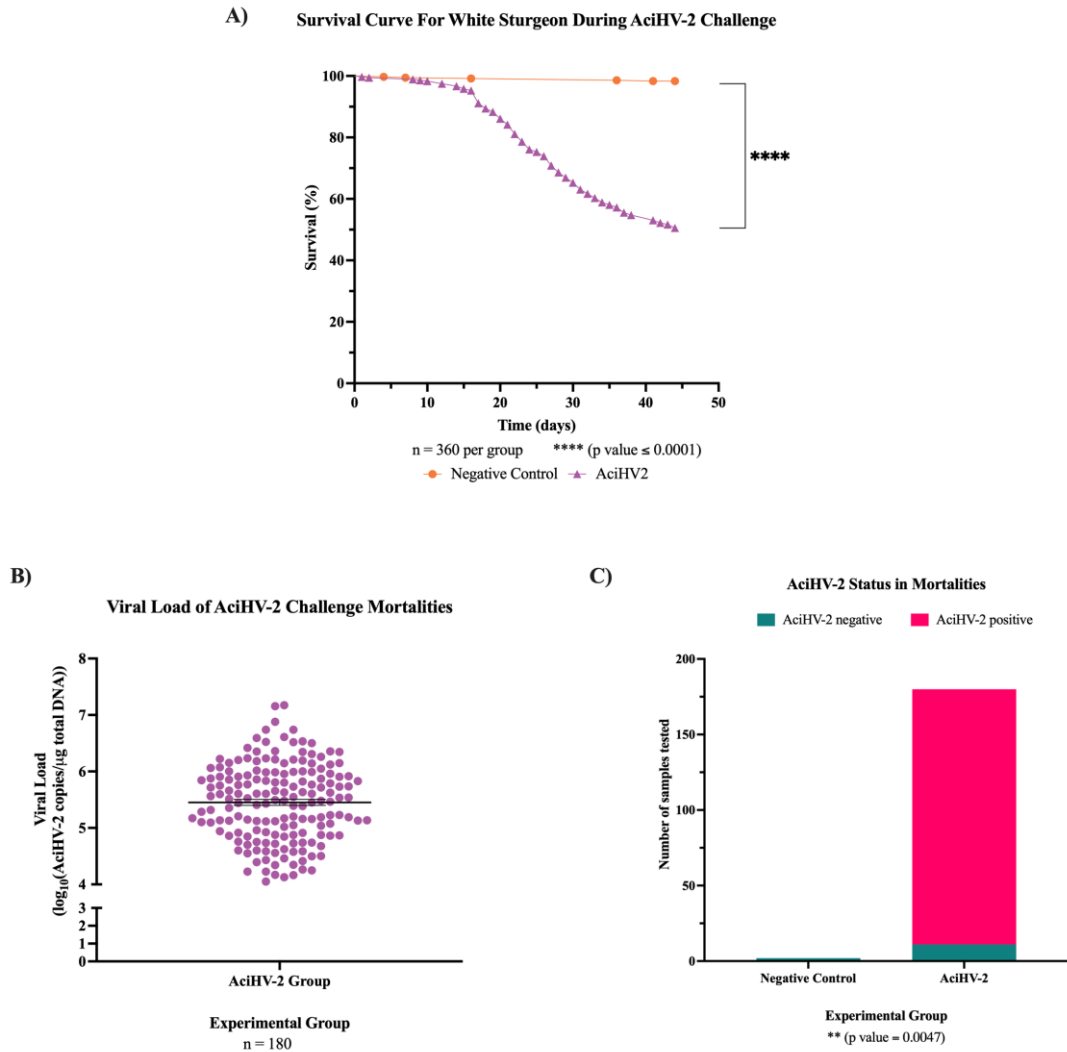


Figure 3.4 | Acipenserid Herpesvirus 2 (AciHV-2) challenge during large-scale challenge. An immersion challenge model was performed by exposing white sturgeon fingerlings to a 10^2 TCID₅₀ / mL bath or a sterile cell culture media bath for 1 hour. Mortality was monitored for 44 days after immersion and mortalities tested for AciHV-2 via quantitative polymerase chain reaction (qPCR). Survivors were weighed at the end of the challenge. A) The solid shapes represent the mean cumulative mortality at each day, with standard error of the mean plotted. The different experimental groups are color-coded. A statistically significant reduction in survival is seen in the AciHV-2 exposed group when compared with the negative control group. B) The solid dots represent the mean viral load of sampled mortalities, with the standard error of the mean plotted. Both mortalities in the negative control group and 11 mortalities in the AciHV-2 group had undetermined Ct values and are not displayed in this graph. The mean viral load among mortalities was $10^{5.4}$ copies. C) The bars represent the number of samples tested for AciHV-2 via qPCR, color-coded by qPCR result. This shows that 94% of the mortalities in the AciHV-2 group tested positive for AciHV-2 via qPCR, while none of the mortalities in the negative control group tested positive for AciHV-2 via qPCR. There is a strong association between an AciHV-2 positive status and the experimental group.

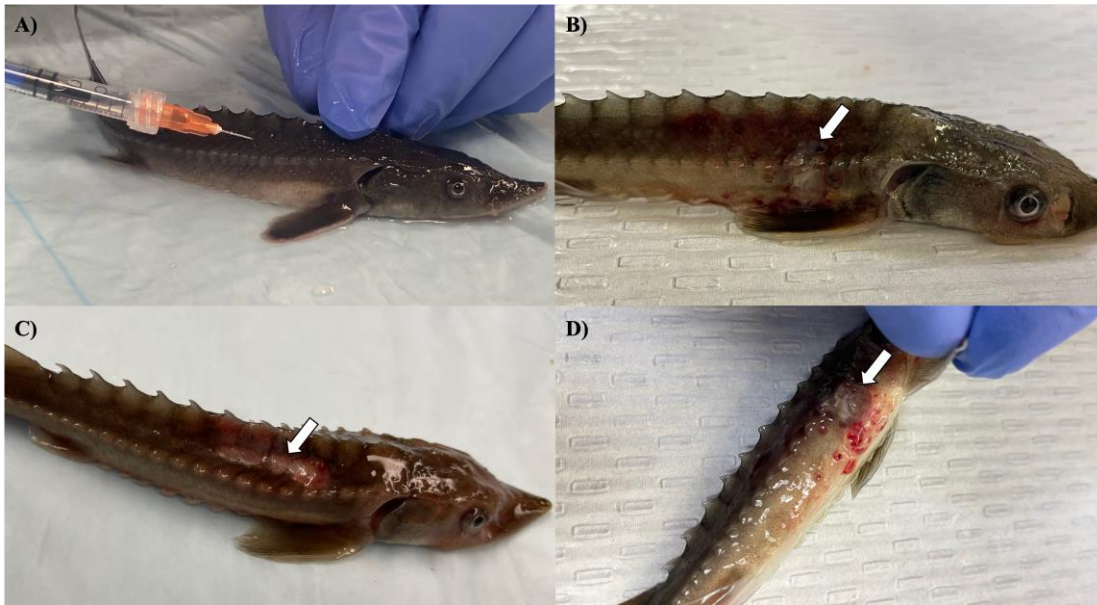


Figure 3.5 | Clinical signs in white sturgeon during Acipenserid Herpesvirus 2 (AciHV-2) and *Streptococcus iniae* co-infection challenge. White sturgeon fingerlings were exposed to a 10^2 TCID₅₀ AciHV-2 / mL bath for 1 hour or an equivalent volume of sterile cell culture media. Survivors were then injected with 10^6 CFU *S. iniae* per fish or 0.1 mL of sterile Phosphate Buffered Saline. Clinical signs and mortality were monitored for 28 days. A) Injection site for the *S. iniae* intramuscular challenge in an anesthetized white sturgeon fingerling. B) Mild cutaneous ulceration at the injection site in a fresh mortality. C) Moderate to severe ulceration at the injection site in a fresh mortality. D) Moderate to severe ulceration at the injection site with subdermal hemorrhage. The white arrows point towards the lesions described.

and not when compared to the *S. iniae* group (Figure 3.7A). In addition, mortalities started in the co-infection group 24 hours earlier than in the *S. iniae* group during both the pilot and large-scale challenges (Figure 3.6A and 3.6A, respectively). In terms of viral and bacterial loads of the challenge mortalities, there was no statistical difference in loads between groups (Figure 3.6B-C and 3.6B-C). During the pilot challenge, only four individuals tested positive for AciHV-2 and there was no statistical difference in viral load between groups (p-value = 0.5538, Figure 3.6D). During the large-scale challenge, all euthanized individuals for gene expression sampling tested negative for AciHV-2 and *S. iniae* via qPCR (n = 6 per group at 15 days post-bacterial infection and n = 10 per group at 28 days post-bacterial infection).

Histopathological analysis of at least five moribund or fresh mortalities per group during the

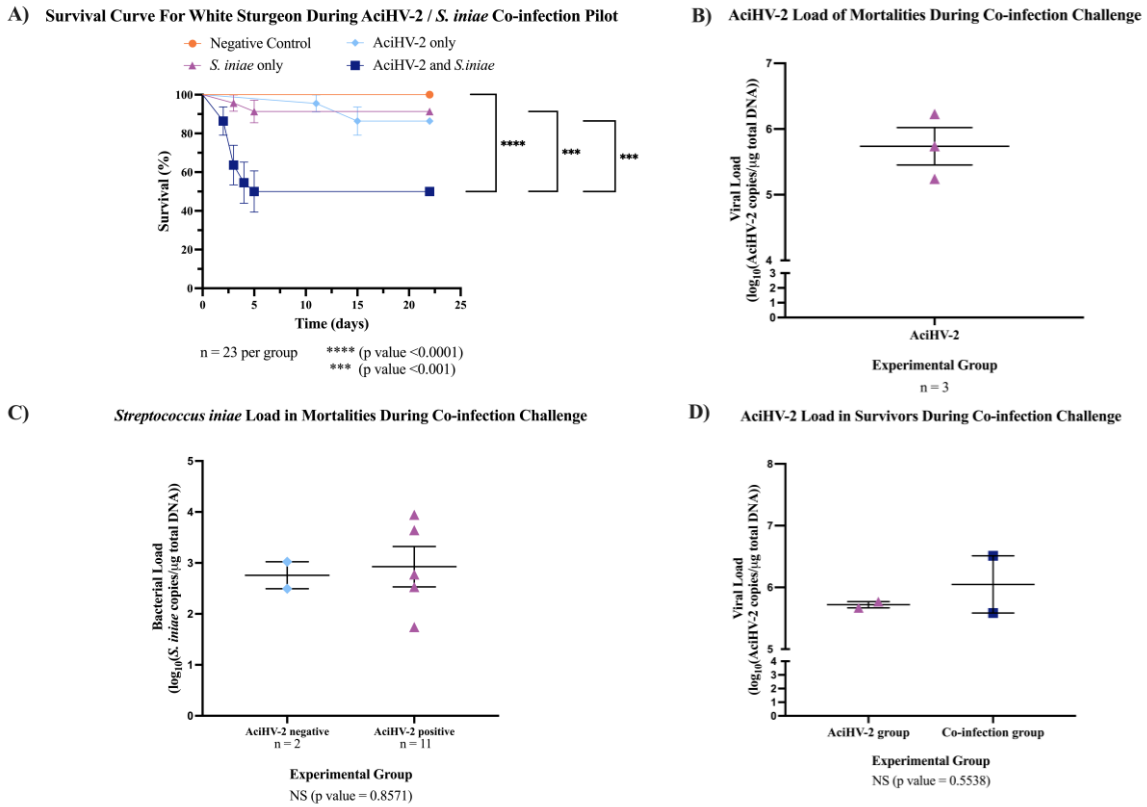


Figure 3.6 | Acipenserid Herpesvirus 2 (AciHV-2) and *Streptococcus iniae* (*S. iniae*) co-infection pilot challenge. An immersion challenge model was performed by exposing white sturgeon fingerlings to a 10^2 TCID₅₀ / mL AciHV-2 bath or a sterile cell culture media bath for 1 hour. Survivors of this challenge at 80 days were re-sorted into groups of 23 fish per treatment. Fish received either 10^8 CFU of *S. iniae* or sterile Phosphate Buffered Saline in the epaxial musculature. Mortality was monitored for 21 days after injection and mortalities were tested for AciHV-2 and *S. iniae* via quantitative polymerase chain reaction (qPCR). A) The solid shapes represent the mean cumulative mortality at each day, with standard error of the mean plotted. The different experimental groups are color-coded. The black stars indicate statistical significance between the bracketed groups and p values are stated below. Results reveal that the *S. iniae* group that was previously infected with AciHV-2 had a statistically significant decrease in survival of 41% compared to *S. iniae* alone and of 36% compared to AciHV-2 alone. B) The solid dots represent the mean viral load of sampled mortalities, with the standard error of the mean plotted. Only the AciHV-2 group mortalities tested positive for AciHV-2 via qPCR. C) The solid dots represent the mean bacterial load of sampled mortalities, with the standard error of the mean plotted. There was no statistical difference in bacterial loads between groups. This also shows that 100% and 45% of the mortalities in the *S. iniae* and in the co-infection groups, respectively, tested positive for *S. iniae*. There is a strong association between an *S. iniae* positive status and the experimental group (p value ≤ 0.0001). D) The solid dots represent the mean viral load of sampled survivors, with the standard error of the mean plotted. Experimental groups are color-coded. There was no statistical difference in viral load between groups.

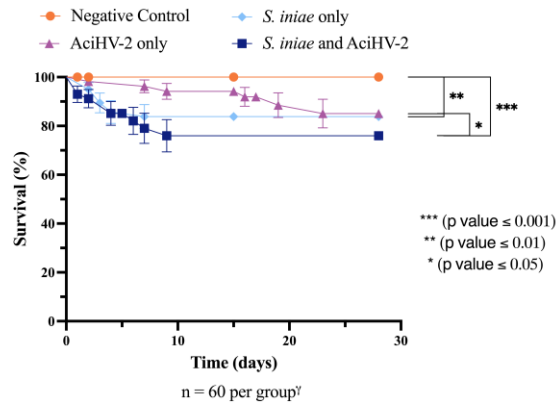
large-scale challenge revealed that erosion and ulceration scores were only statistically significantly increased in the groups infected with AciHV-2 (Figure 3.8A-C, p-value < 0.0001). In

addition, while lesions in fish exposed to *S. iniae* were most often characterized by muscle necrosis, none of the infected groups had statistically significant muscle necrosis scores present in the sections analyzed when compared to the negative control (Figure 3.8D). However, it is important to note that the injection site may have been absent in certain slides evaluated, affecting the overall score per group. Representative images of the lesions used for histopathological scoring can be found in Figure 3.9. In fish infected with AciHV-2, lesions were often centered on the epithelium and were characterized by areas of erosion and ulceration (Figure 3.10C-D and 3.10G). Secondary colonization of these areas of ulceration by bacteria (Figure 3.10D and 3.10G) and/or oomycetes (Figure 3.10C) was common. In fish infected with *S. iniae*, lesions were most pronounced at the injection site and were characterized by degeneration and necrosis of the myocytes surrounding the injection site, as well as large numbers of coccoid bacteria (Figure 3.10E and 3.10H). There also appeared to be large numbers of intravascular coccoid bacteria, consistent with septicemia. Fish infected with both AciHV-2 and *S. iniae* typically exhibited epithelial lesions and/or injection site lesions.

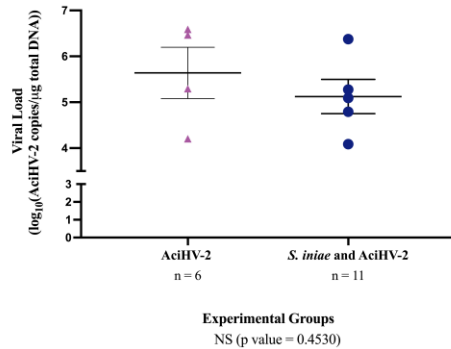
3.2 Immune-related gene expression assessment

At 15 days post-bacterial infection during the large-scale challenge, there was a statistically significant downregulation of *tnf- α* transcripts in the spleen of fish in the co-infection group compared to both single pathogen groups (Figure 3.11A, p-value = 0.0098). In addition, there was a statistically significant downregulation of *irf8* transcripts in the co-infection group compared to the negative control group (Figure 3.11B, p-value = 0.0374). Finally, there was a statistically significant downregulation of *saa* transcripts in all infected groups compared to the negative control group (Figure 3.11D, p-value 0.0472). These changes were not present at 28 days, but there

A) Survival Curve For White Sturgeon During Co-infection Challenge



B) AciHV-2 Load of Mortalities During Coinfection Challenge



C) *S. iniae* Load of Mortalities During Coinfection Challenge

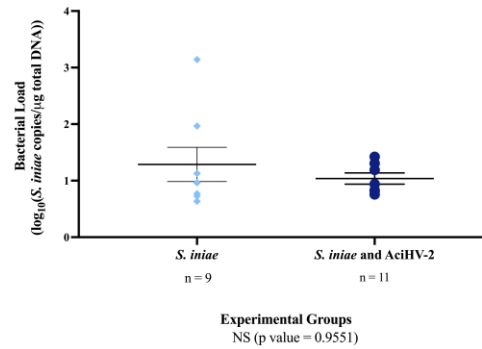
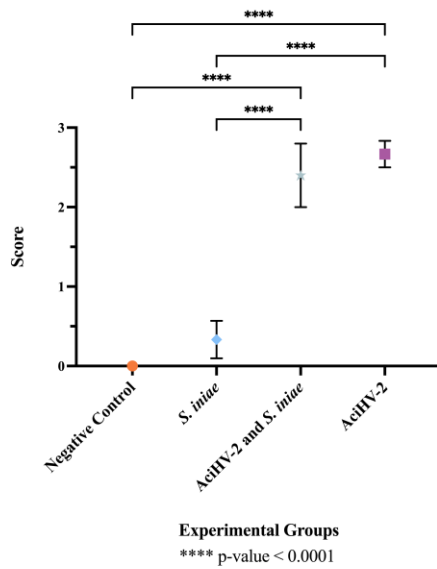
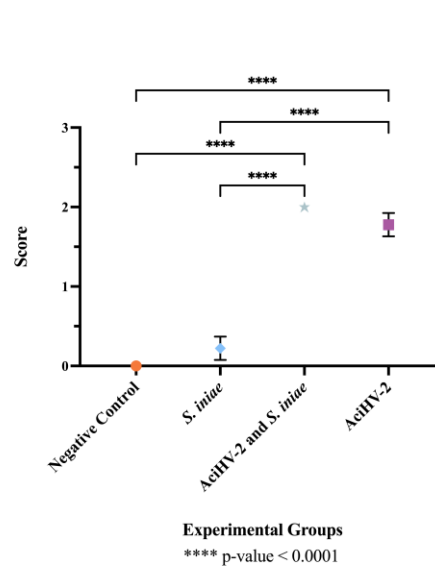


Figure 3.7 | Acipenserid Herpesvirus 2 (AciHV-2) and *Streptococcus iniae* (*S. iniae*) co-infection large-scale challenge. An immersion challenge model was performed by exposing white sturgeon fingerlings to a 10^2 TCID₅₀ / mL AciHV-2 bath or a sterile cell culture media bath for 1 hour. Survivors of this challenge at 44 days were re-sorted into groups of 60 fish (triplicate tanks of 20 fish each) per treatment. Fish received either 10^6 CFU of *S. iniae* or sterile Phosphate Buffered Saline in the epaxial musculature. Mortality was monitored for 28 days after injection and mortalities tested for AciHV-2 and *S. iniae* via quantitative polymerase chain reaction (qPCR). A) The solid shapes represent the mean cumulative mortality at each day, with standard error of the mean plotted. The different experimental groups are color coded. A statistically significant reduction in survival is seen in all infected groups when compared to the negative control, except for the AciHV-2 group. When comparing infected groups among themselves, the co-infection group has the lowest survival, showing a statistically significant reduction compared to the AciHV-2 group. B) The solid dots represent the mean viral load of sampled mortalities, with the standard error of the mean plotted. There was no statistical difference in viral loads between groups. This also shows that 67% and 45% of the mortalities in the AciHV-2 and in the co-infection groups, respectively, tested positive for AciHV-2. There is a strong association between an AciHV-2 positive status and the experimental group (p value = 0.0027). C) The solid dots represent the mean bacterial load of sampled mortalities, with the standard error of the mean plotted. There was no statistical difference in bacterial loads between groups. This also shows that 89% and 45% of the mortalities in the *S. iniae* and in the co-infection groups, respectively, tested positive for *S. iniae*. There is a strong association between an *S. iniae* positive status and the experimental group (p value ≤ 0.0001).

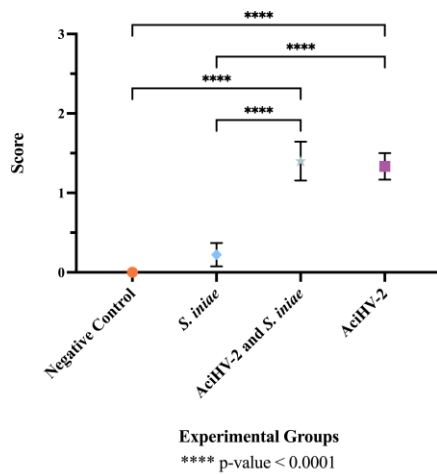
A) Histopathologic Score of Degree of Erosion/Ulceration



B) Histopathologic Score of Distribution of Erosion/Ulceration



C) Histopathologic Score of Percentage of Section Affected



D) Histopathologic Score of Muscle Necrosis

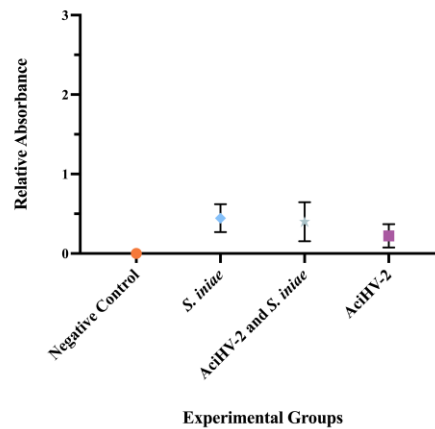


Figure 3.8 | Histopathologic evaluation of tissues from mortalities of the co-infection challenge.

An immersion challenge model was performed by exposing white sturgeon fingerlings to a 10^2 TCID₅₀ / mL Acipenserid herpesvirus 2 (AcHV-2) bath or a sterile cell culture media bath for 1 hour. Survivors of this challenge at 44 days were re-sorted into groups of 60 fish (triplicates of 20 fish) per treatment. Fish received either 10^6 CFU of *S. iniae* or sterile Phosphate Buffered Saline in the epaxial musculature. Mortality was monitored for 28 days after injection and at least 5 mortalities from each challenged group (*S. iniae* group and AcHV-2 group: n = 9 each; co-infection group: n = 5) were submitted for histopathologic analysis. The negative control representatives (n = 10) were submitted as euthanized survivors at the end of the study. A) The “degree of erosion/ulceration” category was scored from 0-3 per slide where 0 represented no erosion or ulceration, 1 represented loss of superficial epithelial cells (erosion), 2 represented loss of epidermis/mucosal epithelium (ulceration), and 3 represented loss of dermis/underlying connective tissue. B) The “distribution of erosion/ulceration” category was scored from 1-2 per slide where 0 represented no erosion or ulceration, 1 represented focal erosion or ulceration, and 2 represented multifocal erosion or ulceration. C) The “percentage of section affected” category was scored from 0-4 per slide where 0

represented no erosion or ulceration, 1 represented less than 25% of the section affected, 2 represented between 25% and 50% of the section affected, 3 represented between 51% and 75% of the section affected, and 4 represented more than 75% of the section affected. D) The “muscle necrosis” category was scored from 0-1 per slide where 0 represented no muscle necrosis present, and 1 represented muscle necrosis present. Results reveal that the degree of, distribution of, and percentage of section affected with erosion/ulceration appears to be driven by the AciHV-2 infection. In addition, none of the infected groups had significant muscle necrosis present in the sections analyzed. Values represent mean with standard error of the mean plotted.

was a statistically significant downregulation of *saa* transcripts in the groups infected with *S. iniae* compared to the AciHV-2 group (Figure 3.12D, p-value 0.0323).

3.3 Humoral immunity assessment

Assessment of anti-*S. iniae* IgM present in the serum of challenged fish revealed a statistically significant reduction in anti-*S. iniae* serum IgM in fish from the coinfection group compared to fish in the *S. iniae* group (Figure 3.13, p-value = 0.0134).

3.4 Acute-phase protein analysis

Assessment of serotransferrin in the serum of survivors of the co-infection challenge revealed a statistically significant decrease in the groups previously exposed to AciHV-2 compared to the negative control and *S. iniae* groups (Figure 3.14, p-value < 0.05).

4. Discussion

The *Herpesvirales* order is characterized by the ability to establish latency, which can lead to changes in immunocompetency of the host.²² Although the specific interactions involving AciHV-2 have not been investigated, reports of co-infections in white sturgeon¹² parallel reports of pediatric IGASI²⁰, suggesting an interaction between the infectious agents and the host that impacts disease outcome. Notably, neither of these clinical presentations across taxa have

undergone exploration in a controlled environment and it is posited that this co-infection scenario in white sturgeon may provide valuable insights for future studies related to human pediatric IGASI. Therefore, a pilot challenge was performed to assess the hypothesis that a previous,

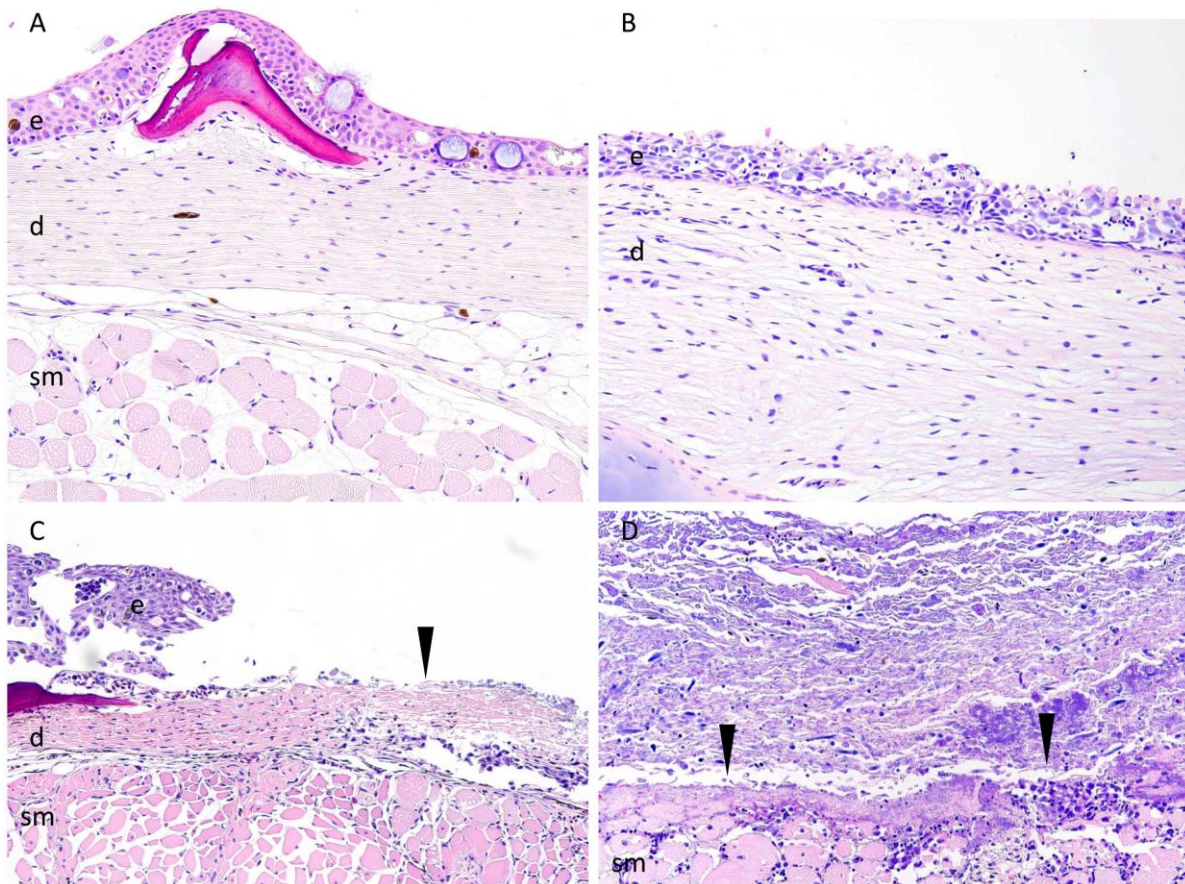


Figure 3.9 | Representative microscopic findings and the corresponding scoring of the described epithelial lesions during co-infection challenge. An immersion challenge model was performed by exposing white sturgeon fingerlings to a 10^2 TCID₅₀ / mL Acipenserid herpesvirus 2 (AcicHV-2) bath or a sterile cell culture media bath for 1 hour. Survivors of this challenge at 44 days were re-sorted into groups of 60 fish (triplicates of 20 fish) per treatment. Fish received either 10^6 CFU of *S. iniae* or sterile Phosphate Buffered Saline in the epaxial musculature. Mortality was monitored for 28 days after injection and at least 5 mortalities from each challenged group (*S. iniae* group and AcicHV-2 group: n = 9 each; co-infection group: n = 5) were submitted for histopathologic analysis. The negative control representatives (n = 10) were submitted as euthanized survivors at the end of the study. A) the negative control group showing no overt pathology with intact epidermis (e), dermis (d), and muscle (sm). B) the co-infection group showing epidermal erosion - thinning of the epidermis (e) and loss of superficial epithelial cells with dermis (d) intact. C) the AcicHV-2 group showing epidermal ulceration - loss of epidermis (black arrowhead) with dermis and muscle present/intact. D) the AcicHV-2 group showing loss of epidermis and dermis with muscle exposed (sm) (black arrowheads). All images are with H&E.

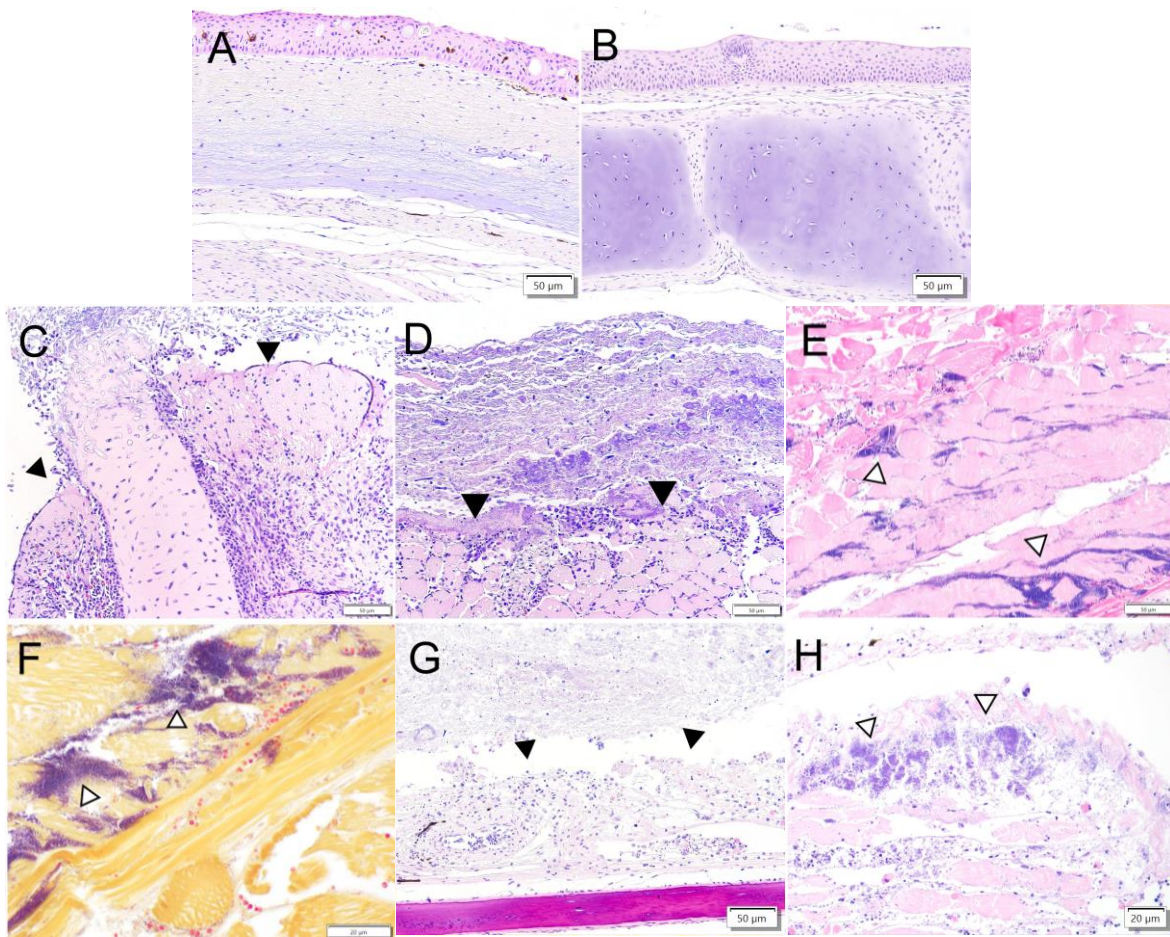


Figure 3.10 | Histopathological findings during co-infection challenge. An immersion challenge model was performed by exposing white sturgeon fingerlings to a 10^2 TCID₅₀ / mL Acipenserid herpesvirus 2 (AciHV-2) bath or a sterile cell culture media bath for 1 hour. Survivors of this challenge at 44 days were re-sorted into groups of 60 fish (triplicates of 20 fish) per treatment. Fish received either 10^6 CFU of *S. iniae* or sterile Phosphate Buffered Saline in the epaxial musculature. Mortality was monitored for 28 days after injection and at least 5 mortalities from each challenged group (*S. iniae* group and AciHV-2 group: n = 9 each; co-infection group: n = 5) were submitted for histopathologic analysis. The negative control representatives (n = 10) were submitted as euthanized survivors at the end of the study. A and B) the negative control showed no overt pathology (H&E). C and D) the AciHV-2 group showed ulceration - loss of epithelium (black arrowheads), and exposure of underlying connective tissue/cartilage (C) or skeletal muscle (D) with secondary oomycete (C) or bacterial (D) colonization (H&E). E) the *S. iniae* group showed regionally extensive rhabdomyonecrosis with large numbers of intralesional coccoid bacteria (white arrowheads) (H&E). F) the *S. iniae* group showed regionally extensive rhabdomyonecrosis with large numbers of intralesional Gram-positive bacteria (white arrowheads) (Gram stain). G) the co-infection group showed ulceration - loss of epidermis (black arrowheads), and exposure of underlying connective tissue/cartilage with secondary colonization by bacteria (H&E). H) the co-infection group showed regionally extensive rhabdomyonecrosis with large numbers of intralesional coccoid bacteria (white arrowheads) (H&E).

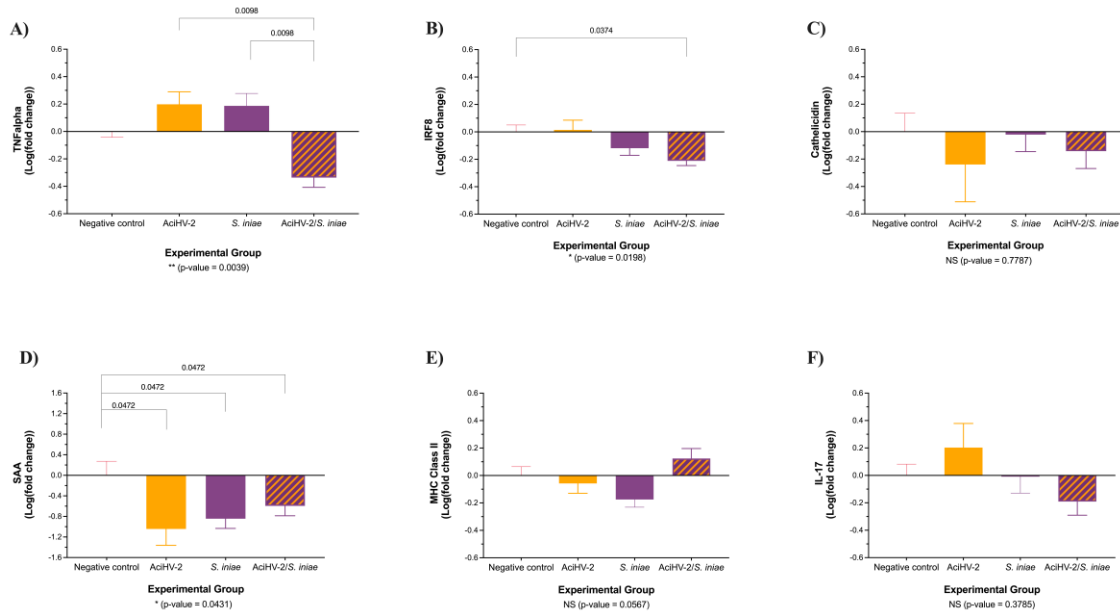


Figure 3.11 | Gene expression at 15 days post co-infection challenge. An immersion challenge model was performed by exposing white sturgeon fingerlings to a 10^2 TCID₅₀ / mL bath or a sterile cell culture media bath for 1 hour. Survivors of this challenge at 44 days were re-sorted into groups of 60 fish (triplicates of 20 fish) per treatment. Fish received either 10^6 CFU of *S. iniae* or sterile Phosphate Buffered Saline in the epaxial musculature. Mortality was monitored for 28 days after injection. Two fish per tank (six fish per group) were euthanized at 15 days post-injection and spleens were collected for reverse transcription quantitative polymerase chain reaction (RT-qPCR) of important players in the immune response, using elongation factor and beta-actin as housekeeping genes. Results are plotted as the mean and standard error of the mean. Results reveal a statistically significant transcriptional downregulation of Tumor Necrosis Factor alpha (TNFalpha - A) in the coinfection group compared to the single pathogen groups, as well as some differential transcription of interferon regulatory factor 8 (IRF8 - B) and serum amyloidA (SAA - D) when compared to the negative control.

potentially latent, AciHV-2 infection in white sturgeon fingerlings would increase mortality during a subsequent *S. iniae* infection. Results revealed that the co-infection group had a statistically significant decrease in survival of 41% compared to the *S. iniae* group and of 36% compared to AciHV-2 group (Figure 3.6A), evincing that a previous, potentially latent, AciHV-2 infection has a profound impact on the outcome of a subsequent *S. iniae* infection in white sturgeon. These results are consistent with observations from natural cases of piscine streptococcosis in white sturgeon that also had AciHV-2¹², as well as with reports on *S. iniae*-virus co-infections in other

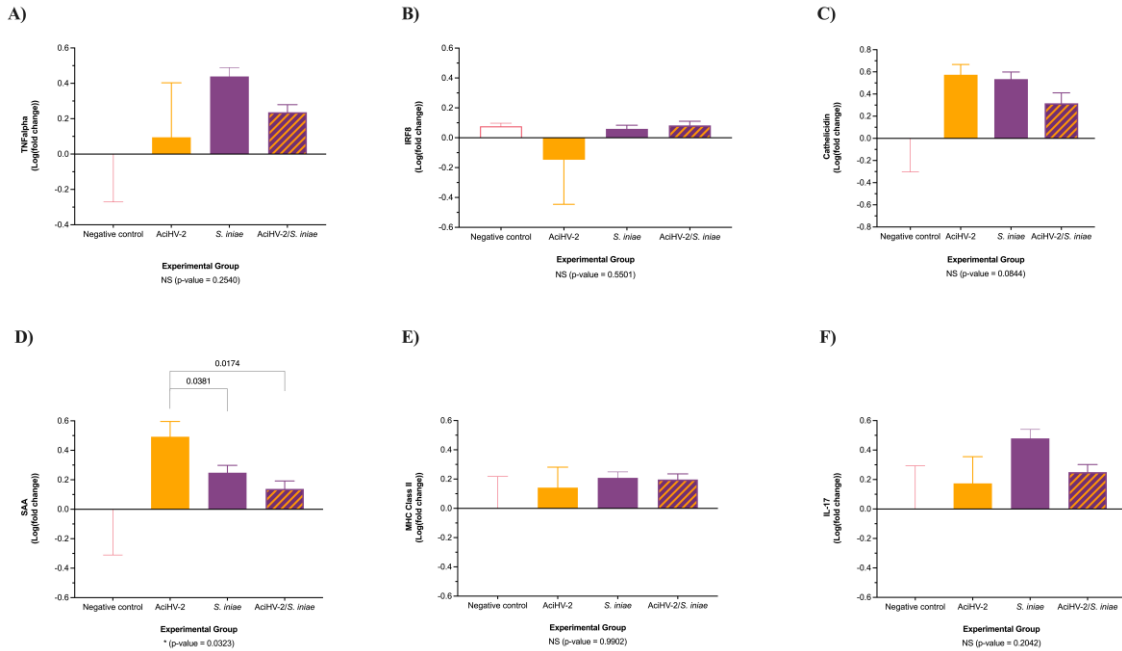


Figure 3.12 | Gene expression at 28 days post co-infection challenge. An immersion challenge model was performed by exposing white sturgeon fingerlings to a 10^2 TCID₅₀ / mL bath or a sterile cell culture media bath for 1 hour. Survivors of this challenge at 44 days were re-sorted into groups of 60 fish (triplicates of 20 fish) per treatment. Fish received either 10^6 CFU of *S. iniae* or sterile Phosphate Buffered Saline in the epaxial musculature. Mortality was monitored for 28 days after injection. Ten fish per group were euthanized at 28 days post-injection and spleens were collected for reverse transcription quantitative polymerase chain reaction (RT-qPCR) of important players in the immune response, using elongation factor and beta actin as housekeeping genes. Results are plotted as the mean and standard error of the mean. Results reveal a statistically significant transcriptional downregulation of serum amyloid A (SAA - D) in the groups infected with bacteria when compared to the AciHV-2 group.

fish species. For example, Japanese flounder (*Paralichthys olivaceus*) experiences statistically increased mortality when infected with *S. iniae* 1 week after an aquabirnavirus (ABV) infection compared with fish infected with *S. iniae* alone.³⁷ However, to the authors’ knowledge, the study described herein is the first to investigate this phenomenon in the context of a herpesvirus infection in sturgeon during what is suspected to be the latent phase (80 days post-infection, 30 days past the last mortality of the active outbreak, with no AciHV-2 detectable in fin tissue of the majority of survivors – Figure 3.4A and 3.4D).

A large-scale challenge was conducted to explore potential impacts of AciHV-2 on targeted aspects of the immune system, aiming to identify factors that may lead to alterations in the interactions between the host and *S. iniae*. For the large-scale challenge presented here, while following similar trends to the pilot challenge (Figure 3.6A), there was no significant difference in survival between the co-infection group and the *S. iniae* group (Figure 3.7A). The primary differences between the pilot and large-scale challenge experiments were time between viral and bacterial infection (80 vs 44 dpi, respectively) and bacterial dose (10^8 vs 10^6 CFU/fish,

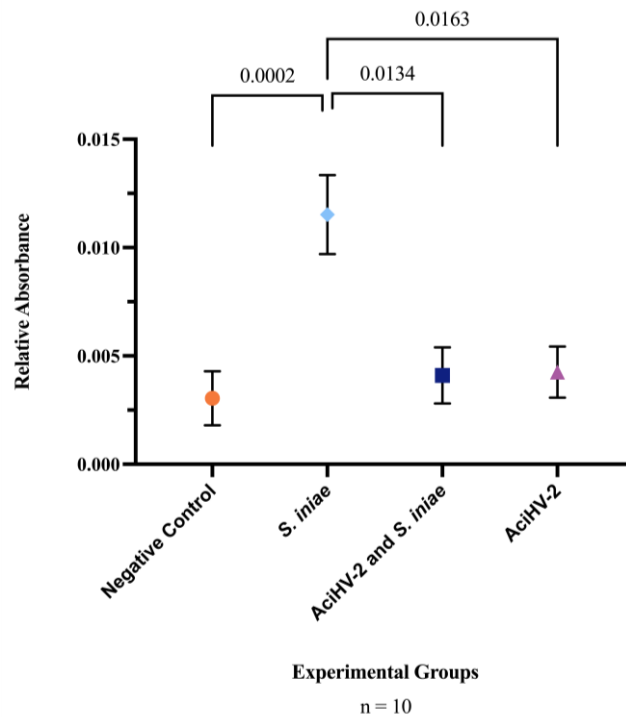


Figure 3.13 | Detection of serum anti-*S. iniae* IgM in survivors of co-infection challenge. An immersion challenge model was performed by exposing white sturgeon fingerlings to a 10^2 TCID₅₀ / mL bath or a sterile cell culture media bath for 1 hour. Survivors of this challenge at 44 days were re-sorted into groups of 60 fish (triplicates of 20 fish) per treatment. Fish received either 10^6 CFU of *S. iniae* or sterile Phosphate Buffered Saline in the epaxial musculature. Mortality was monitored for 28 days after injection and whole blood was collected from the caudal vein of 10 survivors per group. Serum was obtained from the whole blood samples and an indirect enzyme-linked immunosorbent assay (ELISA) was performed to detect anti-*S. iniae* IgM. The solid shapes represent the mean relative absorbance using an OD₄₀₅₋₄₁₀, with standard error of the mean. The p values calculated between groups is stated in each comparison bracket. Results reveal that the *S. iniae* group that was previously infected with AciHV-2 had a statistically significant decrease in serum anti-*S. iniae* IgM levels compared to the group that received *S. iniae* alone.

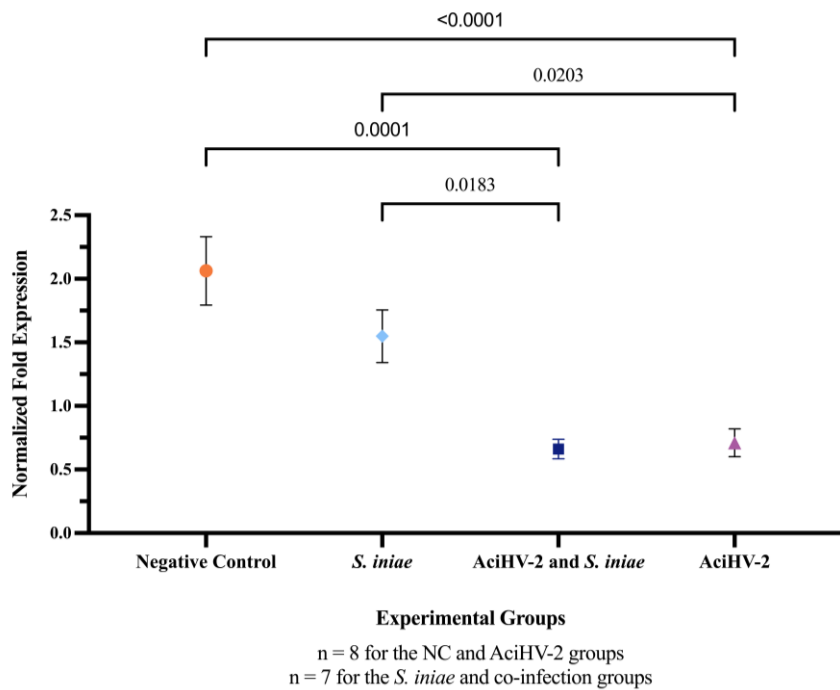


Figure 3.14 | Detection of serum serotransferrin in survivors of co-infection challenge. An immersion challenge model was performed by exposing white sturgeon fingerlings to a 10^2 TCID₅₀ / mL bath or a sterile cell culture media bath for 1 hour. Survivors of this challenge at 44 days were re-sorted into groups of 60 fish (triplicates of 20 fish) per treatment. Fish received either 10^6 CFU of *S. iniae* or sterile Phosphate Buffered Saline in the epaxial musculature. Mortality was monitored for 28 days after injection and whole blood was collected from the caudal vein of 10 survivors per group. Serum was obtained from the whole blood samples and Western Blotting was performed to identify Serotransferrin 2 (STF-2) in the samples. The solid shapes represent the mean normalized fold expression, with standard error the mean plotted. The p values calculated between groups are stated in each comparison bracket. Results reveal that the co-infection and AciHV-2 groups had a statistically significant decrease in serum STF-2 levels compared to the group that received *S. iniae* alone and the negative control.

respectively). While the overall lower mortality rate may preclude statistical significance, this still raises interesting questions into the effect of timing and bacterial infectious dose in co-infections, which have been investigated before for other co-infections involving *S. iniae*.

In terms of the bacterial infectious dose, a study assessing *S. iniae* infections in tilapia (*Oreochromis niloticus*) showed that infection dose impacted the mortality rate only if fish were stocked at high densities.³⁸ High-density environments have been associated with immunosuppression in fish elicited by a physiologic stress response.³⁹ Taken together, the two

studies described herein combined appear to support that both factors (high bacterial infectious dose and immunomodulation) must be present in order to significantly impact mortality.

In terms of the timing of the infection, in the ABV-*S. iniae* study using Japanese flounder mentioned above, the authors observed that if flounder were infected with *S. iniae* 3 weeks post ABV infection rather than 1-week, there were no differences in mortality between co-infection and single pathogen groups.³⁷ The authors suggest that active replication of ABV, which happens during early infection, may be required to induce immunosuppression and worsen the outcome of the *S. iniae* infection. In the large-scale challenge, fish were infected with *S. iniae* 44 days after the AciHV-2 immersion compared to 80 days post-immersion in the pilot challenge. It is possible that the transcriptional profile of AciHV-2 is different this early after an active outbreak and the immunomodulatory effects are thus distinct from later in its life cycle, which has been described for multiple herpesviruses of mammals.^{40,41} Further comparative studies are warranted to tease apart the contribution to mortality of bacterial infectious dose and of bacterial infection timing in relation to viral infection during this co-infection scenario, as the extent of variation between the pilot and the large-scale study in this project prevents additional conclusions.

It is well described that latency is not a static, but rather a dynamic state where the virus is mostly dormant, yet the transcriptional profile is not fixed. For example, low levels of lytic gene expression have been detected in cells harboring Herpes Simplex Virus 1 (HSV-1) in the absence of any other evidence of reactivation.⁴² Furthermore, studies have shown that within a population of HSV-1 latently infected cells, a sub-population of those cells can go through transient reactivation while the remaining cells still lack detectable infectious virus or viral lytic transcripts.⁴² Given this information, the term latency is applicable only at the cellular level rather than the tissue level. This is important to consider when assessing the effects of the viral population

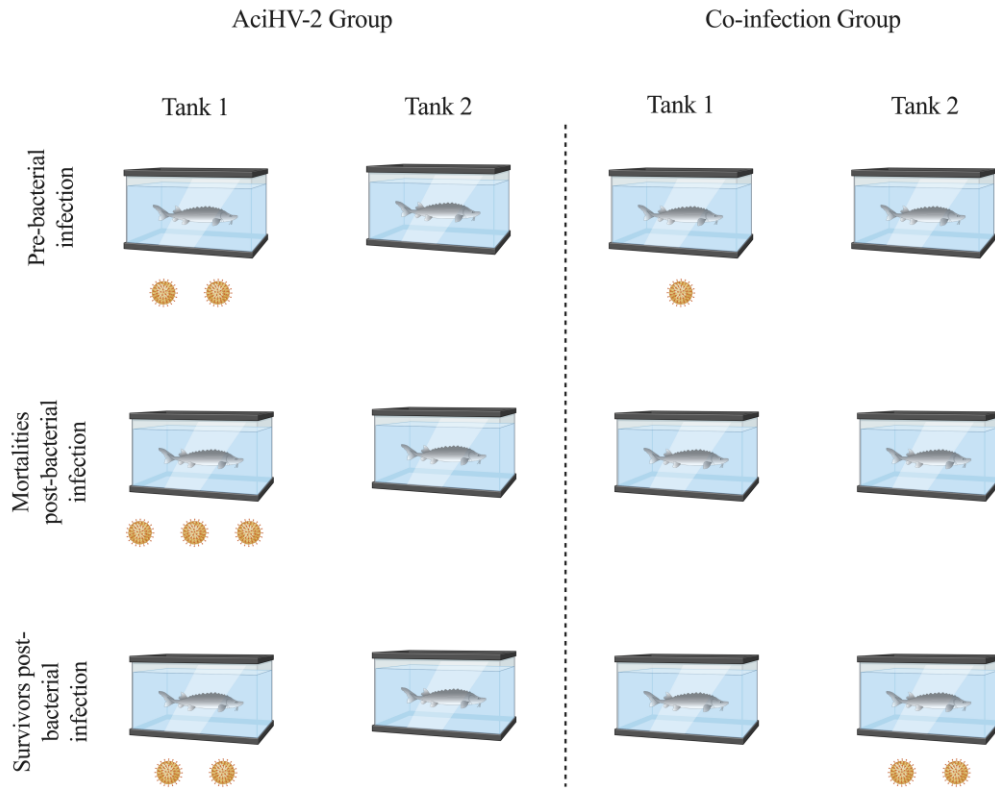


Figure 3.15 | Pilot challenge Acipenserid Herpesvirus 2 (AciHV-2) positivity distribution. White sturgeon fingerlings were exposed to an AciHV-2 or sterile cell culture media immersion for 1 hour. Mortality was recorded for 80 days. Survivors of each group were sorted into duplicate tanks to generate four treatment groups (Negative control, AciHV-2, *S. iniae*, and AciHV-2/*S. iniae*). Fish then received 0.1 mL of either *S. iniae* suspension or sterile phosphate-buffered saline intramuscularly on the epaxial musculature. Pectoral fin clips were collected from every fish injected for detection of AciHV-2 via qPCR. Mortality was monitored for 21 days and pectoral fin clips were collected from all mortalities and survivors for AciHV-2 qPCR. This figure was created using BioRender with the white sturgeon depiction being a creation of Dr. Taylor Heckman. The virus depiction below each tank represents the number of fish that tested positive for AciHV-2 during the indicated timepoint.

on the immune system of the host. In theory, at any time after the initial outbreak, herpesviruses have the capacity to benefit from the immunomodulation obtained through the expression of specific latency-associated transcripts while going through reactivation events that ensure passing progeny to new hosts. In the current study, it is hypothesized that potentially latent AciHV-2 interacts with the immune system of the white sturgeon in a way that changes the fish's interaction with *S. iniae*. In the pilot challenge, fin clips were collected from all survivors prior to the bacterial

infection (Figure 3.3D), from all mortalities after the bacterial infection (Figure 3.6B), and from all survivors after the bacterial infection (Figure 3.6D) to test AciHV-2 detection via qPCR as a marker of reactivation. When assessing the distribution of positive fish throughout the tanks, it is most notably observed that for the co-infection group there is one fish in Tank 1 that was positive during the pre-bacterial infection timepoint that is not detected positive again (Figure 3.15, Tank 1 of the co-infection group) and two fish in Tank 2 that test negative during the pre-bacterial infection timepoint but positive during the survivor timepoint (Figure 3.15, Tank 2 of the co-infection group). The fish detected positive during late stages of the study are evidence of the population undergoing some level of herpesviral reactivation. Further studies are needed to show that AciHV-2 achieves latency in a cell population and then to evaluate if latency is maintained in a subpopulation of cells while these reactivation events occur.

Mammalian herpesviruses have multiple pathways for regulating host cellular immune competency, resulting in immune system evasion.⁴³⁻⁴⁵ This has also been demonstrated to a lesser extent for certain herpesviruses that affect fish.⁴⁶⁻⁴⁸ The evasion mechanisms are diverse, including complement activation inhibition, impaired antigen presentation via numerous pathways, apoptosis and natural killer cell inhibition, interferon signaling interference, and others.^{49,50} From the host side, results revealed a significant transcriptional downregulation of *tnf α* at 15 days post-bacterial infection in the co-infection group compared to the *S. iniae* group (Figure 3.11A). This transcriptional downregulation is not maintained at 28 days post-bacterial infection (Figure 3.12A). The cytokine TNF α , a potent inflammatory modulator known for its prominent pro-inflammatory role while also participating in regulating the extent and duration of the immune response, is primarily produced by activated macrophages, T lymphocytes, and natural killer cells.

However, it is also expressed at lower levels by various other cells, including fibroblasts, smooth muscle cells, and even tumor cells. Some studies have specifically looked at the augmenting effects of TNF α on B cell proliferation and immunoglobulin production,⁵¹ which suggests that the transcriptional downregulation of *tnf α* in the spleen at 15 days post-bacterial infection in this study could impact antibody response. This was supported by the significant decrease in serum anti-*S. iniae* IgM in fish from the co-infection group compared to fish in the single-pathogen group (Figure 3.13) as had been suggested for pediatric IGASI²⁰ in humans. While a decrease in humoral immunity could be playing a role in this co-infection during the late stages of the disease, it is most concerning for survivors of the co-infection who were to encounter *S. iniae* again as older fish in the caviar production pipeline. It is unclear at this time if decreased humoral immunity would be significant in the acute onset of disease in naïve fish, which is precisely where most mortalities occur (first 10 days post-bacterial infection, Figure 3.6A and 3.6A). It is important to note, however, that teleost B cells have demonstrated phagocytic and intracellular killing capacity⁵², which may play a role in early immune response against *S. iniae*. More studies are warranted to determine which B cell populations are being affected during these co-infection and to establish the timeline of humoral immunity development in white sturgeon against *S. iniae*.

Recently, sequencing of the full genome of AciHV-2 demonstrated that one of the open reading frames of AciHV-2, ORF 101, has the TNFRSF14_teleost conserved domain.⁵³ This is present in members of the TNF Receptor superfamily, which are common targets for viral manipulation due to their important roles in the regulation of immune responses as well as viral entry.^{54,55} While further characterization of ORF 101 in AciHV-2 is needed to understand its expression patterns and effects on the host, other teleost herpesviruses have been shown to influence *tnf α* expression. For example, Cyprinid Herpesvirus 3 (CyHV-3) has been shown to encode two TNFR homologs,

of which one causes upregulation of *tnfa*.⁴⁸ To our knowledge, AciHV-2 alone has not been shown to change expression patterns of *tnfa* in the spleen, but this changes during the co-infection state. Further studies are indicated to determine what interactions lead to the decreased transcript abundance of *tnfa* and of pathogen-specific IgM in the host, and to understand the temporal transcriptional patterns of the host and AciHV-2, particularly as it pertains to the expression of *tnfa* and ORF 101. Assessing translation to determine if these gene expression changes lead to effects at the protein level is also warranted.

The impact of co-infection on the production of the acute-phase protein serotransferrin 2 (STF-2), which has been shown to play a role in the inflammatory response during certain infections in white sturgeon,³⁴ was also assessed. Fish exposed to AciHV-2 (both single pathogen and co-infection) had a significant decrease in STF-2 serum levels compared to the Negative control and *S. iniae* groups at 28 days post-bacterial infection (Figure 3.14). This finding provides an alternate or perhaps complementary hypothesis on the mechanism behind the decreased anti-*S. iniae* IgM levels in the serum of fish in the co-infection group (Figure 3.13). Serotransferrin 2 is a protein in the transferrin family, which is known for its iron transportation role. Because of its ability to bind iron, serotransferrin is considered part of the immune response where it creates an iron-limited environment that is not conducive to pathogen replication, including *S. iniae*.⁵⁶ This has been identified as a mechanism against herpesvirus as well.⁵⁷ Nonetheless, even though this direct mechanism could explain the worsened disease state observed in the co-infection group, serotransferrin has an additional function related to immunity against herpesviruses: it has been described to be a primary activator of fish macrophages, an important antigen-presenting cell to CD4+ T cells in fish.⁵⁶ Evidence indicating that CD4+ T cells are vital for herpesvirus control continues to emerge.⁵⁸ This is particularly highlighted in both susceptibility to and reactivation of

herpesviruses when the human host has a CD4+ T cell deficiency.⁵⁹ CD4+ T cells play a role in herpesvirus control not only by using helper functions, but also by using direct effector functions that impact viral replication via secreted interferon (IFN) gamma and TNF α .⁶⁰ Finally, CD4+ T cells are also involved in a robust and appropriate humoral response, being shown to be necessary for the generation of plasma and memory B cells, as well as germinal center establishment and responses.⁶¹ Given the importance of CD4+ T cell response in the control of herpesviral infections, both during the lytic and latent stages, it has been described that herpesviruses have a variety of strategies to manipulate CD4+ T cell responses.⁵⁸ A potential mechanism by which AciHV-2 – white sturgeon – *S. iniae* interactions lead to an inferior antibody response against *S. iniae* during a co-infection may involve the potential effects of AciHV-2 on the general CD4+ T cell population via a decrease in serotransferrin. Affected CD4+ T cells have been reported to have decreased production of TNF α as well as inhibited cytotoxic effector functions in human and murine cytomegalovirus infections.⁵⁸ While speculative, this may indicate that the downregulation of TNF α may be related to the poor activation of both fish macrophages and CD4+ T cells.

The results from this study identify an altered immune response in the co-infection group, including the hypothesized impaired humoral immunity against *S. iniae* and additional impacts to important players of the innate immune response. Further studies are indicated to determine what interactions lead to the decreased production of pathogen-specific IgM in the host. Piscine streptococcosis is a significant emerging disease of white sturgeon with the capacity to cause outstanding losses in white sturgeon aquaculture, particularly considering its effect on subadult populations. A comprehensive understanding of the conditions that lead to significant disease by *S. iniae* and the underlying mechanisms responsible for creating an optimal environment for its occurrence will provide focus for prevention and therapeutic programs in aquaculture farms.

References

1. Kelly J. White Sturgeon [Internet]. California Department of Fish and Wildlife. [cited 2022 Jan 20]. Available from: <https://wildlife.ca.gov/Conservation/Fishes/Sturgeon/White-Sturgeon>
2. Ethier V. Farmed Sturgeon [Internet]. Monterey Bay Aquarium Seafood Watch; 2014 [cited 2022 Jan 20]. Available from: <https://seafood.ocean.org/wp-content/uploads/2016/10/Sturgeon-Farmed-US.pdf>
3. Carocci F, Lagrange C, Levavasseur V, Yakimushkin A. Sturgeons (*Acipenseriformes*) [Internet]. Food and Agriculture Organization of the United Nations. Available from: <https://www.fao.org/3/Y5261E/y5261e06.htm>
4. The 17 Goals [Internet]. United Nations Department of Economic and Social Affairs | Sustainable Development. 2023 [cited 2023 Aug 23]. Available from: <https://sdgs.un.org/goals>
5. Lepa A, Siwicki AK. Fish herpesvirus diseases: a short review of current knowledge. *Acta Vet Brno*. 2012;81(4):383–9.
6. Watson L, Yun S, Groff J, Hedrick R. Characteristics and pathogenicity of a novel herpesvirus isolated from adult and subadult white sturgeon *Acipenser transmontanus*. *Dis Aquat Organ*. 1995;22:199–210.
7. Goodwin A. Herpesviruses in Fish. Southern Regional Aquaculture Center; 2012.
8. Hanson LA, Rudis MR, Vasquez-Lee M, Montgomery RD. A broadly applicable method to characterize large DNA viruses and adenoviruses based on the DNA polymerase gene. *Virology*. 2006 Dec;3(1):28.
9. Mugetti D, Pastorino P, Menconi V, Pedron C, Prearo M. The Old and the New on Viral Diseases in Sturgeon. *Pathogens*. 2020 Feb 21;9(2):146.
10. Nguyen DT, Marancik D, Soto E. Intracoelomic- and Intramuscular-Injection Challenge Model of Piscine Streptococcosis in White Sturgeon Fingerlings. *J Aquat Anim Health*. 2020 Sep;32(3):133–8.
11. Pierezan F, Shahin K, Heckman TI, Ang J, Byrne BA, Soto E. Outbreaks of severe myositis in cultured white sturgeon (*Acipenser transmontanus* L.) associated with *Streptococcus iniae*. *J Fish Dis*. 2020 Apr;43(4):485–90.
12. Soto E, Richey C, Stevens B, Yun S, Kenelty K, Reichley S, et al. Co-infection of Acipenserid herpesvirus 2 (AciHV-2) and *Streptococcus iniae* in cultured white sturgeon *Acipenser transmontanus*. *Dis Aquat Organ*. 2017 Mar 30;124(1):11–20.
13. Suárez-Arrabal MC, Sánchez Cámara LA, Navarro Gómez ML, Santos Sebastián M del M, Hernández-Sampelayo T, Cercenado Mansilla E, et al. Enfermedad invasiva por *Streptococcus pyogenes*: cambios en la incidencia y factores pronósticos. *An Pediatr*. 2019 Nov;91(5):286–95.

14. Frère J, Bidet P, Tapiéro B, Rallu F, Minodier P, Bonacorsi S, et al. Clinical and Microbiological Characteristics of Invasive Group A Streptococcal Infections Before and After Implementation of a Universal Varicella Vaccine Program: Table 1. *Clin Infect Dis*. 2016 Jan 1;62(1):75–7.
15. Wilson GJ, Talkington DF, Gruber W, Edwards K, Dermody TS. Group A Streptococcal Necrotizing Fasciitis Following Varicella in Children: Case Reports and Review. *Clin Infect Dis*. 1995 May 1;20(5):1333–8.
16. Sturgeon JP, Segal L, Verma A. Going Out on a Limb: Do Not Delay Diagnosis of Necrotizing Fasciitis in Varicella Infection. *Pediatr Emerg Care*. 2015 Jul;31(7):503–7.
17. Laskey AL, Johnson TR, Dagartzikas MI, Tobias JD. Endocarditis Attributable to Group A Hemolytic Streptococcus After Uncomplicated Varicella in a Vaccinated Child. *PEDIATRICS*. 2000 Sep;106(3):4.
18. Strom MA, Hsu DY, Silverberg JI. Prevalence, comorbidities and mortality of toxic shock syndrome in children and adults in the USA: Epidemiology of Toxic Shock Syndrome. *Microbiol Immunol*. 2017 Nov;61(11):463–73.
19. Oyake S, Oh-i T, Koga M. A Case of Varicella Complicated by Cellulitis and Scarlet Fever Due to *Streptococcus pyogenes*. *J Dermatol*. 2000 Nov;27(11):750–2.
20. Laupland KB, Davies HD, Low DE, Schwartz B, Green K, the Ontario Group A Streptococcal Study Group, et al. Invasive Group A Streptococcal Disease in Children and Association With Varicella-Zoster Virus Infection. *Pediatrics* [Internet]. 2000 May 1 [cited 2023 Apr 25];105(5). Available from: <https://publications.aap.org/pediatrics/article/105/5/e60/66024/Invasive-Group-A-Streptococcal-Disease-in-Children>
21. Nicoli F, Appay V. Immunological considerations regarding parental concerns on pediatric immunizations. *Vaccine*. 2017 May;35(23):3012–9.
22. Cohen JI. Herpesvirus latency. *J Clin Invest*. 2020 May 4;130(7):3361–9.
23. Speck SH, Ganem D. Viral latency and its regulation: lessons from the gammaherpesviruses. *Cell Host Microbe*. 2010 Jul 22;8(1):100–15.
24. Jarvis MA, Nelson JA. Chapter 42: Molecular basis of persistence and latency. In: *Human Herpesviruses: Biology, Therapy, and Immunoprophylaxis* [Internet]. Cambridge: Cambridge University Press; 2007. Available from: https://www.ncbi.nlm.nih.gov/books/NBK47414/?report=reader#_NBK47414_pubdet_
25. Eide KE, Miller-Morgan T, Heidel JR, Kent ML, Bildfell RJ, LaPatra S, et al. Investigation of Koi Herpesvirus Latency in Koi. *J Virol*. 2011 May 15;85(10):4954–62.
26. Reed AN, Izume S, Dolan BP, LaPatra S, Kent M, Dong J, et al. Identification of B Cells as a Major Site for Cyprinid Herpesvirus 3 Latency. *J Virol*. 2014 Aug 15;88(16):9297–309.

27. Stingley RL, Griffin BR, Gray WL. Channel catfish virus gene expression in experimentally infected channel catfish, *Ictalurus punctatus* (Rafinesque). *J Fish Dis*. 2003 Aug;26(8):487–93.
28. Miller JD, Neely MN. Large-Scale Screen Highlights the Importance of Capsule for Virulence in the Zoonotic Pathogen *Streptococcus iniae*. *Infect Immun*. 2005 Feb;73(2):921–34.
29. Baiano JCF, Barnes AC. Towards Control of *Streptococcus iniae*. *Emerg Infect Dis*. 2009 Dec;15(12):1891–6.
30. Lei C, Yang J, Hu J, Sun X. On the Calculation of TCID₅₀ for Quantitation of Virus Infectivity. *Virol Sin*. 2021 Feb;36(1):141–4.
31. Hedrick RP, McDowell TS, Rosemark R, Aronstein D, Lannan CN. Two Cell Lines from White Sturgeon. *Trans Am Fish Soc*. 1991 Jul;120(4):528–34.
32. Quijano Carde EM, Anenson K, Waldbieser G, Brown CT, Griffin M, Henserson E, et al. Design and Validation of a qPCR Assay for Diagnosis of Acipenserid Herpesvirus 2 in White Sturgeon (*Acipenser transmontanus*) Tissues. In Santiago, Chile; 2022.
33. López-Porras A, Elizondo C, Chaves AJ, Camus AC, Griffin MJ, Kenelty K, et al. Application of multiplex quantitative polymerase chain reaction methods to detect common bacterial fish pathogens in Nile tilapia, *Oreochromis niloticus*, hatcheries in Costa Rica. *J World Aquac Soc*. 2019 Jun;50(3):645–58.
34. Soto E, Coleman D, Yazdi Z, Purcell SL, Camus A, Fast MD. Analysis of the white sturgeon (*Acipenser transmontanus*) immune response during immunostimulation and *Veronaea botryosa* infection. *Comp Biochem Physiol Part D Genomics Proteomics*. 2021 Dec;40:100879.
35. Soto E, Fast MD, Purcell SL, Denver Coleman D, Yazdi Z, Kenelty K, et al. Expression of immune markers of white sturgeon (*Acipenser transmontanus*) during *Veronaea botryosa* infection at different temperatures. *Comp Biochem Physiol Part D Genomics Proteomics*. 2022 Mar;41:100950.
36. Heckman TI, Shahin K, Henderson EE, Griffin MJ, Soto E. Development and efficacy of *Streptococcus iniae* live-attenuated vaccines in Nile tilapia, *Oreochromis niloticus*. *Fish Shellfish Immunol*. 2022 Feb;121:152–62.
37. Pakingking R, Takano R, Nishizawa T, Mori K ichiro, Iida Y, Arimoto M, et al. Experimental Coinfection with Aquabirnavirus and Viral Hemorrhagic Septicemia Virus (VHSV), *Edwardsiella tarda* or *Streptococcus iniae* in Japanese Flounder *Paralichthys olivaceus*. *Fish Pathol*. 2003;38(1):15–21.
38. Shoemaker CA, Evans JJ, Klesius PH. Density and dose: factors affecting mortality of *Streptococcus iniae* infected tilapia *Oreochromis niloticus*. *Aquaculture*. 2000;188:229–35.
39. Aidos L, Cafiso A, Serra V, Vasconi M, Bertotto D, Bazzocchi C, et al. How Different Stocking Densities Affect Growth and Stress Status of *Acipenser baerii* Early Stage Larvae. *Animals*. 2020 Jul 28;10(8):1289.

40. Ye F, Lei X, Gao SJ. Mechanisms of Kaposi's Sarcoma-Associated Herpesvirus Latency and Reactivation. *Adv Virol*. 2011;2011:1–19.
41. Rozman B, Nachshon A, Levi Samia R, Lavi M, Schwartz M, Stern-Ginossar N. Temporal dynamics of HCMV gene expression in lytic and latent infections. *Cell Rep*. 2022 Apr;39(2):110653.
42. Bloom DC. Chapter Two - Alpha herpesvirus Latency: A Dynamic State of Transcription and Reactivation. In: *Advances in Virus Research* [Internet]. Elsevier; 2016 [cited 2023 Aug 16]. p. 53–80. Available from: <https://linkinghub.elsevier.com/retrieve/pii/S0065352715000901>
43. Alibek K, Baiken Y, Kakpenova A, Mussabekova A, Zhussupbekova S, Akan M, et al. Implication of human herpesviruses in oncogenesis through immune evasion and suppression. *Infect Agent Cancer*. 2014;9(1):3.
44. Crow MS, Lum KK, Sheng X, Song B, Cristea IM. Diverse mechanisms evolved by DNA viruses to inhibit early host defenses. *Crit Rev Biochem Mol Biol*. 2016 Nov;51(6):452–81.
45. Alcami A. Viral mimicry of cytokines, chemokines and their receptors. *Nat Rev Immunol*. 2003 Jan;3(1):36–50.
46. Lu JF, Jin TC, Zhou T, Lu XJ, Chen JP, Chen J. Identification and characterization of a tumor necrosis factor receptor like protein encoded by Cyprinid Herpesvirus 2. *Dev Comp Immunol*. 2021 Mar;116:103930.
47. Piazzon MC, Wentzel AS, Tijhaar EJ, Rakus KŁ, Vanderplasschen A, Wiegertjes GF, et al. Cyprinid Herpesvirus 3 II10 Inhibits Inflammatory Activities of Carp Macrophages and Promotes Proliferation of Igm⁺ B Cells and Memory T Cells in a Manner Similar to Carp II10. *J Immunol*. 2015 Oct 15;195(8):3694–704.
48. Zhou Y, Ouyang P, Tao Y, Yin L, Wang K, Geng Y, et al. Comparison the function of Cyprinid herpesvirus 3 encoded two viral tumor necrosis factor receptors. *Aquac Rep*. 2021 Nov;21:100878.
49. Sehrawat S, Kumar D, Rouse BT. Herpesviruses: Harmonious Pathogens but Relevant Cofactors in Other Diseases? *Front Cell Infect Microbiol*. 2018 May 25;8:177.
50. Chang WLW, Baumgarth N, Yu D, Barry PA. Human Cytomegalovirus-Encoded Interleukin-10 Homolog Inhibits Maturation of Dendritic Cells and Alters Their Functionality. *J Virol*. 2004 Aug 15;78(16):8720–31.
51. Pasparki M, Alexopoulou L, Episkopou V, Kollias G. Immune and Inflammatory Responses in TNF-deficient Mice: A Critical Requirement for TNF in the Formation of Primary B Cell Follicles, Follicular Dendritic Cell Networks and Germinal Centers, and in the Maturation of the Humoral Immune Response. *J Exp Med*. 1996 Oct;184:1397–411.
52. Ye J, Li J. Recent Advances on Phagocytic B Cells in Teleost Fish. *Front Immunol*. 2020;11.

53. Quijano Carde EM. Whole-genome Sequencing of Acipenserid Herpesvirus 2 and Identification of Potential Host Homologs. In: American Fisheries Society | Fish Health Section: Fish Health Seminar Series. Virtual; 2022.
54. Rakus K, Ronsmans M, Forlenza M, Boutier M, Piazzon MC, Jazowiecka-Rakus J, et al. Conserved Fever Pathways across Vertebrates: A Herpesvirus Expressed Decoy TNF- α Receptor Delays Behavioral Fever in Fish. *Cell Host Microbe*. 2017 Feb;21(2):244–53.
55. Tiwari V, Clement C, Scanlan PM, Kowlessur D, Yue BYJT, Shukla D. A Role for Herpesvirus Entry Mediator as the Receptor for Herpes Simplex Virus 1 Entry into Primary Human Trabecular Meshwork Cells. *J Virol*. 2005 Oct 15;79(20):13173–9.
56. Stafford JL, Belosevic M. Transferrin and the innate immune response of fish: identification of a novel mechanism of macrophage activation. *Dev Comp Immunol*. 2003 Jun;27(6–7):539–54.
57. Maffettone C, De Martino L, Irace C, Santamaria R, Pagnini U, Iovane G, et al. Expression of iron-related proteins during infection by bovine herpes virus type-1. *J Cell Biochem*. 2008 May 1;104(1):213–23.
58. Walton S, Mandaric S, Oxenius A. CD4 T Cell Responses in Latent and Chronic Viral Infections. *Front Immunol* [Internet]. 2013 [cited 2023 Mar 15];4. Available from: <http://journal.frontiersin.org/article/10.3389/fimmu.2013.00105/abstract>
59. Komanduri KV, Feinberg J, Hutchins RK, Frame RD, Schmidt DK, Viswanathan MN, et al. Loss of Cytomegalovirus-Specific CD4⁺ T Cell Responses in Human Immunodeficiency Virus Type 1–Infected Patients with High CD4⁺ T Cell Counts and Recurrent Retinitis. *J Infect Dis*. 2001 Apr 15;183(8):1285–9.
60. Casazza JP, Betts MR, Price DA, Precopio ML, Ruff LE, Brenchley JM, et al. Acquisition of direct antiviral effector functions by CMV-specific CD4⁺ T lymphocytes with cellular maturation. *J Exp Med*. 2006 Dec 25;203(13):2865–77.
61. Elong Ngonu A, Young MP, Bunz M, Xu Z, Hattakam S, Vizcarra E, et al. CD4⁺ T cells promote humoral immunity and viral control during Zika virus infection. Fernandez-Sesma A, editor. *PLOS Pathog*. 2019 Jan 24;15(1):e1007474.

CHAPTER 4. Transcriptomic Analysis of White Sturgeon (*Acipenser transmontanus*) Skin Cells during Acipenserid Herpesvirus 2 Infection *in vitro*

Abstract

White sturgeon (*Acipenser transmontanus*), the predominant species in the production of caviar and sturgeon meat in the USA, has been affected by outbreaks of Acipenserid herpesvirus 2 (AciHV-2) since its description in the early 1990s. Previous studies have demonstrated the immunomodulatory effects of AciHV-2 on white sturgeon juveniles. In this study, an *in vitro* model was used to investigate the transcriptional profiles of the host (white sturgeon skin cells [WSSK-1]) and the virus during an active infection. From the host perspective, differential transcript expression analysis was performed, and it was detected that 2,507 transcripts were upregulated during infection while 287 transcripts were downregulated during infection. Gene ontology was employed using the zebrafish (*Danio rerio*) as a reference, and only 792 of the differentially expressed transcripts were identified via homology. Of particular interest is one of the downregulated transcripts identified to be a homolog of a member of the tumor necrosis factor receptor superfamily (TNFRSF21). This gene has been associated with apoptosis triggering and T-helper cell activation. Considering AciHV-2 has a homolog of a member of the TNFRSF (TNFRSF14), this is a good candidate for further characterization and investigation. In addition, several additional transcripts associated with negative regulation of the immune response were identified to be upregulated in infected cells and should be investigated in depth. From the pathogen perspective, the transcriptional profile confirms all predicted open reading frames (ORFs) previously proposed by our group. Moreover, at 10 days post-infection, all ORFs are detected as transcriptionally expressed at various levels of expression. This serves as a foundation

for additional transcriptional studies and presents the WSSK-1 cell lines as a good model for future *in vitro* studies.

1. Introduction

An important commodity within the multi-million-dollar aquaculture industry in the United States (USA) is the culture of white sturgeon (*Acipenser transmontanus*), an anadromous fish native to the Pacific Coast of North America¹ and the primary species used for the production of globally recognized high-quality caviar². White sturgeon caviar is one of the few aquaculture products exported internationally by the USA, and it is estimated that white sturgeon aquaculture on the West Coast generates over 200 million dollars in yearly revenue.³ However, aquaculture in the USA is relatively under-exploited compared to aquaculture industries in China, Norway, Chile, and Brazil. Based on statistics from the Food and Agriculture Organization (FAO) for 2023, the USA ranked fourth for aquaculture production in the Americas yet was the top global importer of fish and fishery products.⁴ For instance, China is the world's largest producer of freshwater fish generating over 51×10^6 tonnes in 2021, compared with a modest 4.5×10^5 tonnes produced by the USA in the same year. Moreover, over 90% of seafood consumed by the USA is imported, resulting in economic and food supply vulnerability. This dichotomy has resulted in a deficit exceeding 17 billion dollars, but suggests tremendous growth potential for USA aquaculture that if exploited would both benefit the country's economy and increase food security for Americans.^{4,5}

Infectious disease is one of the primary factors limiting aquaculture production, resulting in significant economic deficits in the form of lost feed days, costly therapeutics, and direct losses associated with mortality.⁶ Acipenserid herpesvirus 2 (AciHV-2) is a large double-stranded DNA virus in the family *Alloherpesviridae* reported to cause epidermal ulceration, lethargy, inappetence,

and erratic swimming^{7,8} with up to 50% mortality during natural outbreaks in white sturgeon.⁹ Little is known about AciHV-2's pathogenesis, particularly as it pertains to its ability to immunomodulate the host, even though it is well established that herpesviruses have multiple pathways for regulating host cellular immune competency, resulting in immune system evasion and in some cases even oncogenesis.¹⁰⁻¹⁴ The evasion mechanisms are diverse, including complement activation inhibition, impaired antigen presentation via numerous pathways, apoptosis haltering, natural killer cell inhibition, interferon signaling interference, and more.^{15,16} In terms of AciHV-2 specifically, a previous study demonstrated that fish exposed to AciHV-2 have a transcriptional downregulation of tumor necrosis factor alpha (TNF α), a decrease in pathogen-specific serum IgM, and a decrease in serum serotransferrin when exposed to a subsequent heterologous infection (specifically *Streptococcus iniae*).¹⁷

To further characterize the changes AciHV-2 drives in the immune capabilities of the white sturgeon, this study aimed to 1) determine the differential gene expression pattern of the host using an *in vitro* model with white sturgeon skin cells (WSSK-1 cells) 10 days post-infection with AciHV-2, and 2) to determine the expression pattern of AciHV-2 predicted open reading frames (ORFs) at that same time point.

2. Materials and Methods

2.2 RNA Sample Generation

White sturgeon skin cells^{18,19} were grown from stock and maintained in “Minimum essential media” (MEM; Corning Inc, Corning, NY) supplemented with 7.5% Fetal Bovine Serum (FBS; Genesee, El Cajón, CA), L-glutamine (Gibco, Grand Island, NY), and penicillin/streptomycin (Gibco, Grand Island, NY) at 20°C. Seeding of WSSK-1 cells in T75 flasks was done at

approximately 90% confluency in MEM supplemented with 2% FBS, L-glutamine, and penicillin/streptomycin. After 24 hours, triplicate biological replicates of WSSK-1 cells in T75 flasks were inoculated with Acipenserid Herpesvirus 2 (isolate UCD3-30⁸ passage number 0) at an infection dose of 10⁵ Median Tissue Culture Infectious Dose (TCID₅₀) mL⁻¹. Concurrently, triplicate biological replicates of WSSK-1 cells were inoculated with MEM supplemented with 2% FBS, L-glutamine, and penicillin/streptomycin and used as uninfected controls. Ten days post-inoculation, cell cultures were collected individually and centrifuged at 1900 g for 10 min. The pellets were immediately frozen at -80°C for 48 hours and subsequently shipped to Azenta LLC (South Plainfield, NJ) overnight on dry ice for analysis.

2.2 RNA Sequencing and Bioinformatic Analysis

The RNA extraction and RNA sequencing of the samples were performed by Azenta LLC. Briefly, total RNA was extracted from frozen cell pellets using the QIAGEN RNeasy Plus Universal Mini Kit (QIAGEN, Hilden, Germany). RNA samples were quantified using Qubit 2.0 Fluorometer (Life Technologies, Carlsbad, CA), and RNA integrity was verified with the 4200 TapeStation (Agilent Technologies, Palo Alto, CA). The rRNA depletion sequencing library was prepared by using the QIAGEN FastSelect rRNA HMR Kit (QIAGEN, Hilden, Germany). The RNA sequencing library was prepared using the NEBNext Ultra II RNA Library Preparation Kit for Illumina following the manufacturer's recommendations (NEB, Ipswich, MA). Sequencing libraries were validated using the Agilent TapeStation 4200 (Agilent Technologies, Palo Alto, CA), and quantified using Qubit 2.0 Fluorometer (ThermoFisher Scientific, Waltham, MA) as well as by quantitative PCR (KAPA Biosystems, Wilmington, MA). The sequencing libraries were multiplexed and clustered on one lane of a flow cell. After clustering, the flow cell was loaded on

the Illumina HiSeq 4000 instrument according to the manufacturer's instructions. The samples were sequenced using a 2x150 Paired-End configuration. Image analysis and base calling were conducted by the Control Software (HCS). Raw sequence data (.bcl files) generated from Illumina HiSeq was converted into fastq files and de-multiplexed using the Illumina bcl2fastq program (v.2.20). One mismatch was allowed for index sequence identification.

Sequence quality was assessed using FastQC. Sequence reads were trimmed to remove possible adapter sequences and nucleotides with poor quality using Trimmomatic (v.0.36). The trimmed reads were then mapped to the white sturgeon reference genome (NCBI Accession ID GCA_020113195.1) or the AciHV-2 genome (NCBI Accession number OQ626810) using the Bowtie2 aligner (v.2.2.6). Unique gene hit counts were calculated by using featureCounts from the Subread package (v.1.5.2). The hit counts were summarized and reported using the gene_id feature in the annotation file. Only unique reads that fell within gene regions were counted.

The hit count data obtained from Azenta LLC. was imported to RStudio (v.2023.06.1+524). Data was log-transformed, filtered to include transcripts present in all replicates per treatment group, and normalized by the weighted trimmed mean of the log expression ratios (TMM)²⁰. This normalization of filtered data was performed using the packages edgeR (v.3.42.4)²¹ and matrixStats (v.1.0.0), and visualized using ggplot2 (v.3.4.3)²² from the tidyverse (v.2.0.0) and cowplot (v.1.1.1). Hierarchical clustering with the maximum distance method and the complete agglomeration method, and principal component analysis were performed using the dist, hclust, and prcomp built-in functions of R, and visualized using the packages ggplot2 (v.3.4.3) from the tidyverse (v.2.0.0), plotly (v.4.10.2), and DT(v.0.30). Differential gene expression (DGE) for host counts between uninfected and infected samples was performed using the package limma (v.3.56.2)²³ and visualized using the packages ggplot2 (v.3.4.3) from the tidyverse (v.2.0.0), plotly

(v.4.10.2), DT(v.0.30), gt (v.0.10.0), and RColorBrewer (v.1.1.3), gplots(3.1.3). Gene Ontology was performed on omicsbox after using Blast2Go to annotate the DGE data using the reference organism zebrafish (*Danio rerio*, package org.Dr.eG.db v.3.17.0).^{24,25} The zebrafish was used due to the white sturgeon genome being at the scaffold level and not annotated. Visualization of gene ontology was done with the package rrvgo (v.1.12.2).²⁶ Finally, visualization of viral transcripts' expression was done on Prism 10 (version 10.0.2 (171)). The script used in this study is available upon request.

Table 4.1 | RNA sequencing read statistics.

Sample	Total reads after sequencing	Mean quality score for reads	Percent of bases with a mean quality score of at least 30	Total reads after filtering	Percent of bases mapped to the host genome	Percent of bases mapped to the viral genome
Uninfected-1	144,918,878	36.66	91.79	141,322,134	42.33	N/A
Uninfected-2	145,064,854	36.50	91.60	141,169,072	42.26	N/A
Uninfected-3	140,635,856	36.37	91.23	135,632,302	40.60	N/A
Infected-1	125,606,744	35.31	90.82	118,768,992	57.09	27.54
Infected-2	130,734,296	35.75	91.16	125,619,400	55.30	24.01
Infected-3	132,803,622	35.30	90.84	127,066,623	55.30	22.04

3. Results

3.1 Read quality and mapping statistics

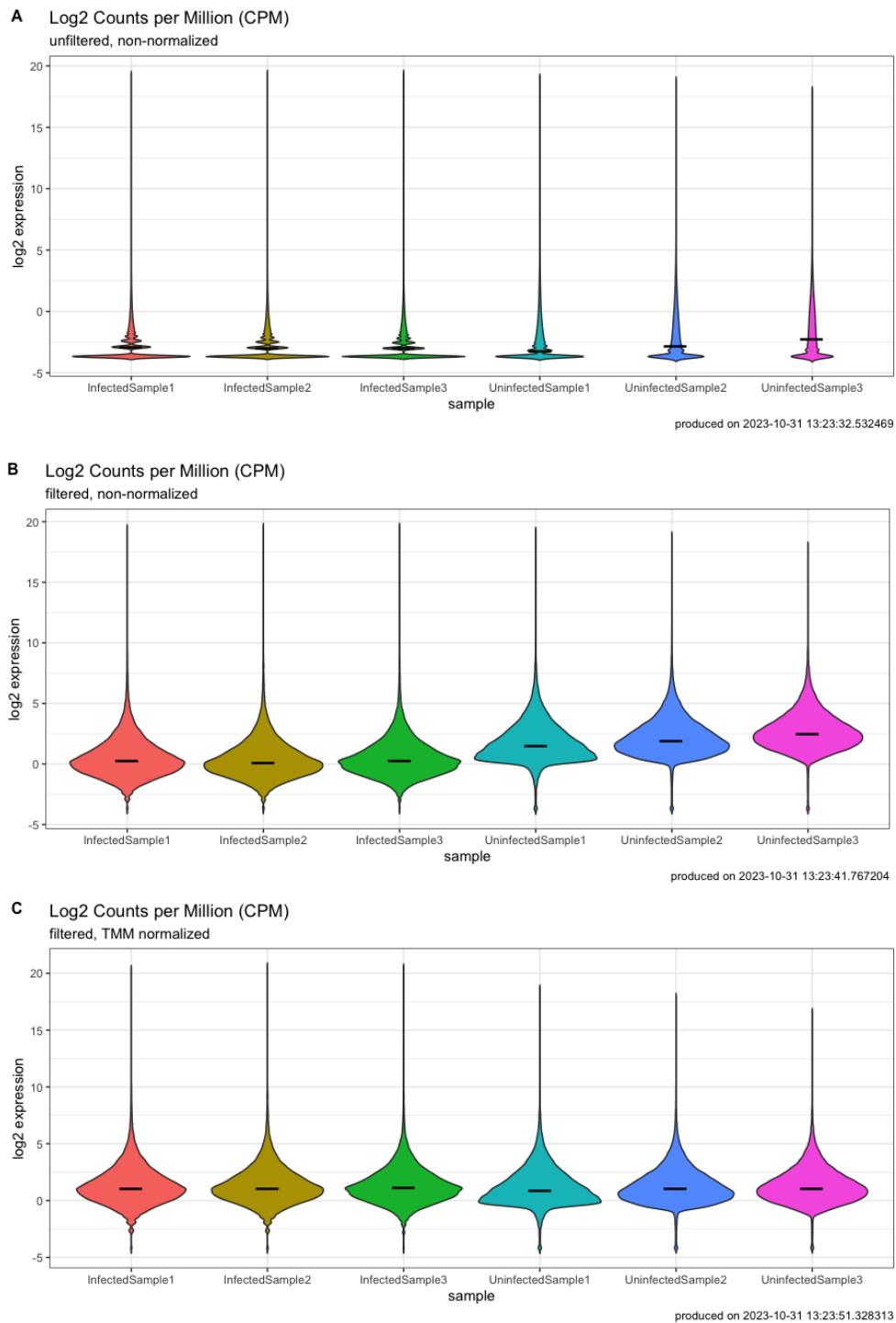


Figure 4.1 | Filtering and normalization of host counts. An *in vitro* Acipenserid Herpesvirus 2 infection was performed on white sturgeon skin cells. Total RNA was collected at 10 days post-infection and sequencing was conducted. After A) mapping reads to the white sturgeon scaffold-level genome, the counts were B) filtered by eliminating counts with low level or inconsistent expression among replicates and C) normalized via the weighted trimmed mean of the log expression ratios method. For all graphs, the horizontal bar represents log₂ expression.

All samples were successfully sequenced with over 90% of the reads having a mean quality score (Q) above 35 (Table 4.1).²⁷ This resulted in all samples having over 118 million reads to use for analysis (Table 4.1), well above Azenta Lifescience's recommendation of 30 million reads per sample for analysis of gene expression in large genomes. When mapping the reads to the host or the viral genome as appropriate for the sample type, 40.6 – 42.3% of the reads from the uninfected samples and 55 – 57% of the reads from the infected samples mapped to the host genome, while only 22 – 27.5% of the reads from the infected samples mapped to the viral genome (Table 4.1). For the process of mapping to the host genome, it was expected that the percentage of bases mapping to the reference genome would be between 70 – 90%.²⁸ The discrepancy is most likely a result of the white sturgeon genome being available only at the scaffold level. In terms of the infected samples, it is expected that a minor percentage of reads in the sample would belong to the virus.

3.2 Filtering and normalization of the counts

After filtering the counts to keep only transcripts expressed in all replicates per group, a subset of 10.22% of the transcripts from the host (Figure 4.1A-B) and 2.65% of the transcripts from the virus (Figure 4.2A-B) were used for the analysis. Subsequently, TMM normalization was employed to be able to compare between samples more accurately (Figure 4.1C and 4.2C).

3.3 Identification of differentially expressed transcripts in the host

Hierarchical clustering was performed on the samples to determine how similar they were to each other, and results reveal that the samples cluster together by infection status (Figure 4.3). This

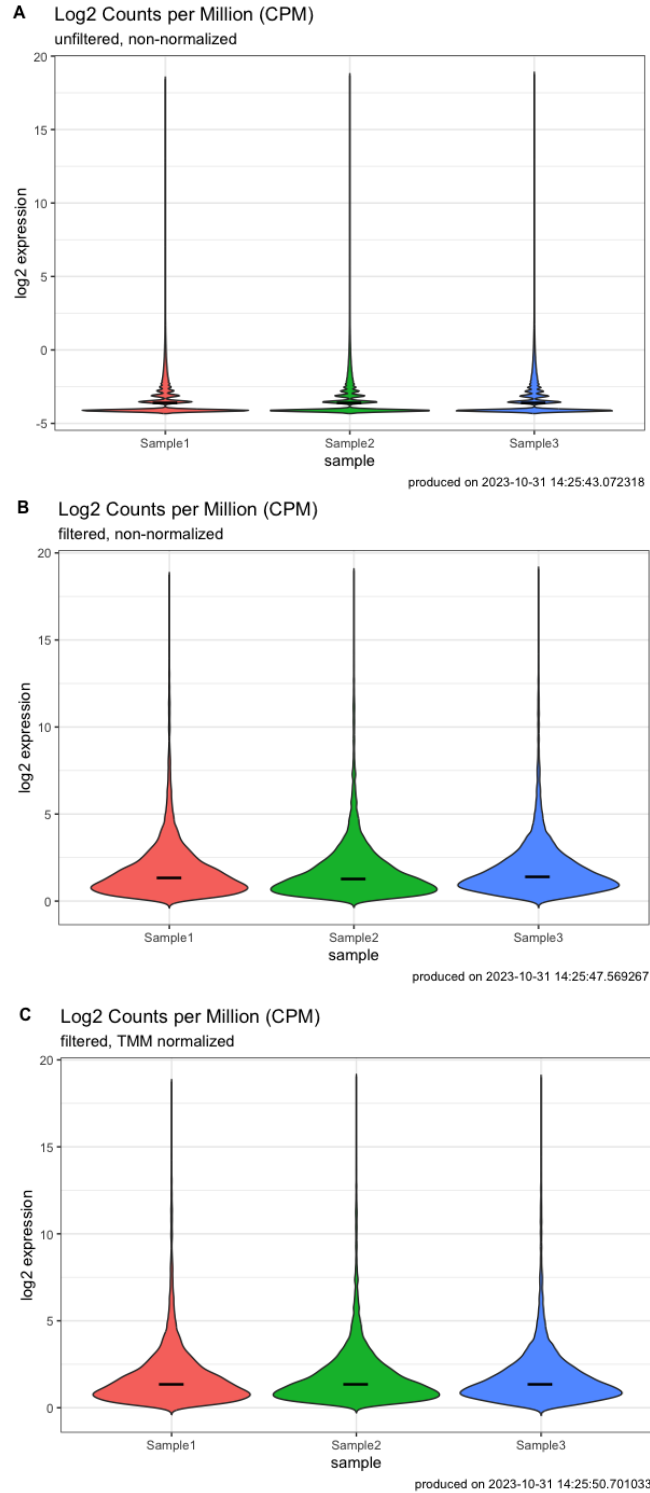


Figure 4.2 | Filtering and normalization of viral counts. An *in vitro* Acipenserid Herpesvirus 2 (AciHV-2) infection was performed on white sturgeon skin cells. Total RNA was collected at 10 days post-infection and sequencing was conducted. After A) mapping reads to the AciHV-2 genome, the counts were B) filtered by eliminating counts with low level or inconsistent expression among replicates and C) normalized via the weighted trimmed mean of the log expression ratios method. For all graphs, the horizontal bar represents log₂ expression.

clustering is confirmed when looking at the principal component analysis, where the principal component 1 (PC1), which accounts for 59.3% of the variation in the data, is the infection status (Figure 4.4). The PC2, which accounts for 17.2% of the variation in the data, appears to be driven by uninfected sample 1, which can be seen on the left upper corner of the plot (Figure 4.4).

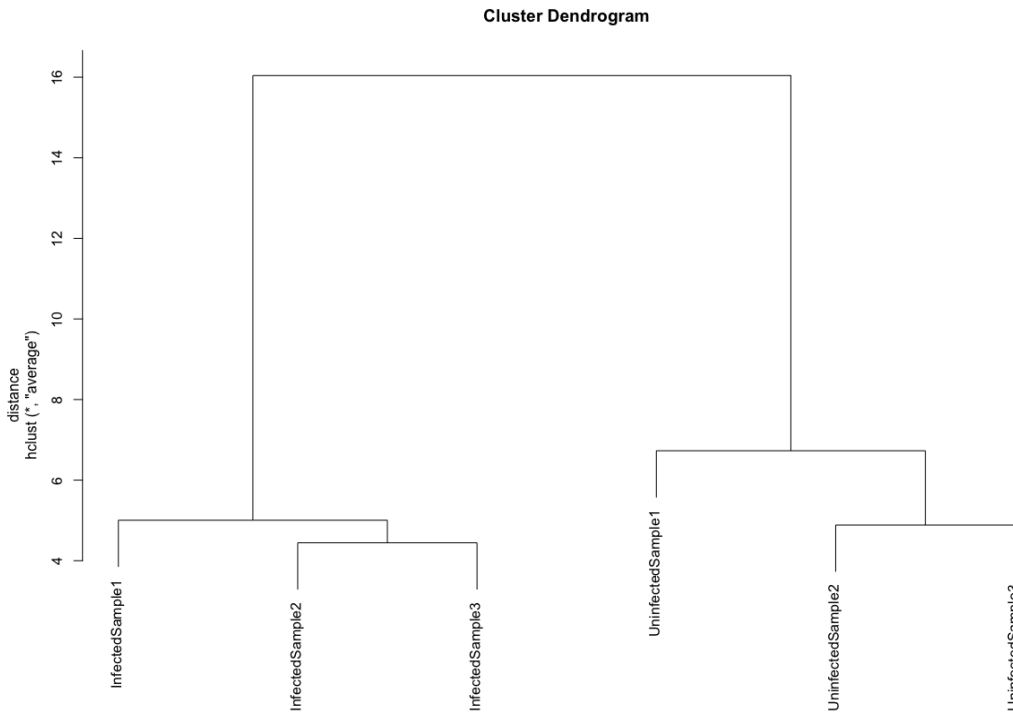


Figure 4.3 | Hierarchical clustering of samples. An *in vitro* Acipenserid Herpesvirus 2 infection was performed on white sturgeon skin cells. Total RNA was collected at 10 days post-infection and sequencing was conducted. Reads were mapped to a reference genome and counts filtered and normalized. Distance between samples was calculated using the “maximum” method on the data matrix and clustering was performed using the “complete” agglomeration method. Results show that samples cluster by infection status.

Of the 36,779 transcripts of the host used for analysis, 2,794 transcripts were found to be differentially expressed when using a p-value of 0.01 as a cutoff (Figure 4.5). A subset of 2,507 transcripts was upregulated, while a subset of 287 transcripts was downregulated (Figure 4.6). The heat map of differentially expressed transcripts (Figure 4.6), clustering by infection status, also

confirms the previously shown hierarchal clustering (Figure 4.3). The differentially expressed transcripts were subjected to blastx with an E value cutoff of 10^{-10} when compared to the zebrafish (*Danio rerio*). Only 792 transcripts had a homolog match in the zebrafish, and these were then used to predict the function of the matched transcripts via assessment of the gene ontology (GO) annotations in the reference genome. When looking at the various GO domains, both annotated terms and parent terms were evaluated.

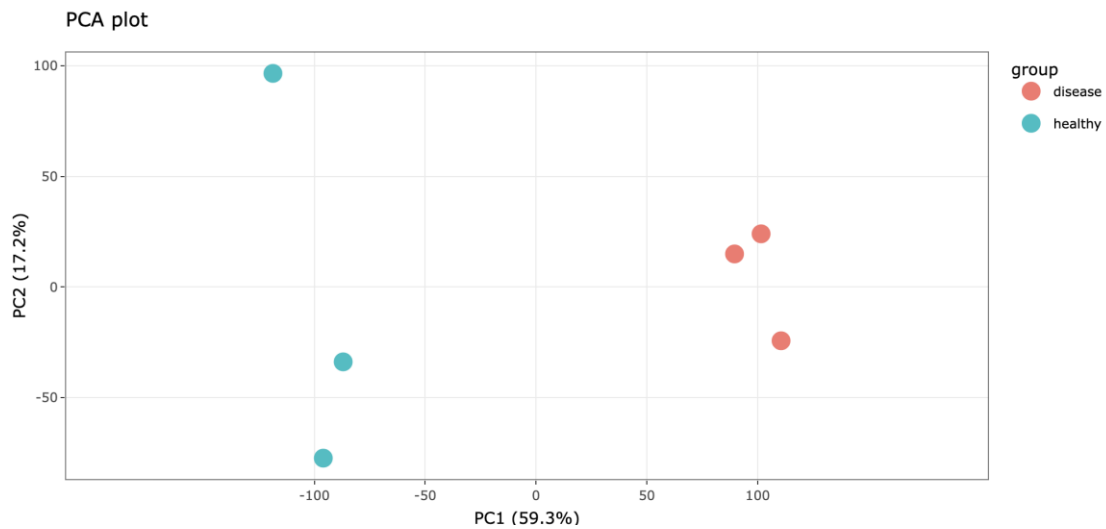


Figure 4.4 | Principal component analysis. An *in vitro* Acipenserid Herpesvirus 2 infection was performed on white sturgeon skin cells. Total RNA was collected at 10 days post-infection and sequencing was conducted. Reads were mapped to a reference genome and counts filtered and normalized. Principal component analysis (PCA) was performed and samples were plotted as principal component (PC) 1 vs PC2. Groups are color-coded, and legend refers to uninfected samples as “healthy” and infected samples as “disease”. Results show that the PC1 accounts for 59.3% of the variation in the data and is driven by infection status, while PC2 accounts for 17.2% of the variation in the data and is driven by uninfected sample 1 (right upper corner).

In the biological process (BP) domain, 89 unique parent terms were upregulated (Figure 4.7), of which “regulation of gene expression” and “response to stimulus” had the most transcripts upregulated. Within “regulation of gene expression”, the term “regulation of DNA-templated transcription” was most predominant. Within “response to stimulus”, the term “signal transduction” was most predominant. For the same BP domain, 39 unique parent terms were

downregulated (Figure 4.8), of which “DNA metabolic process” had the most transcripts downregulated related to “regulation of DNA-templated transcription”.

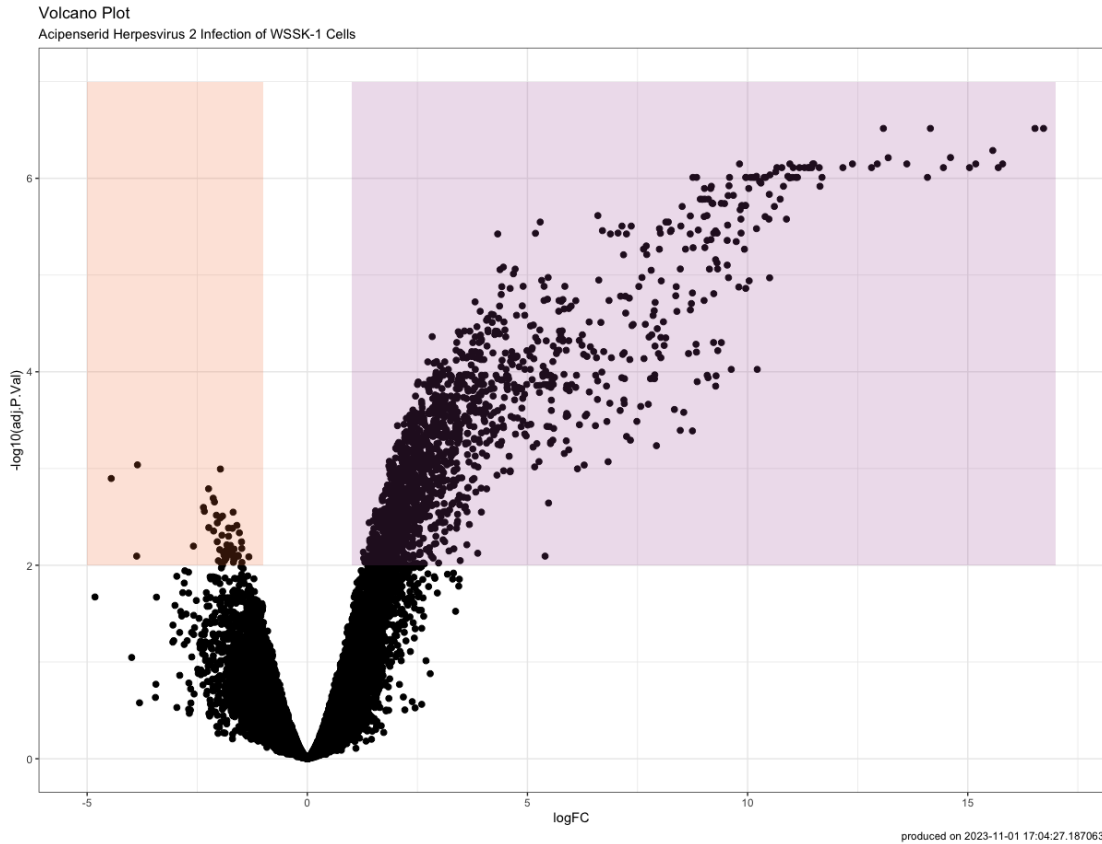


Figure 4.5 | Volcano plot. An *in vitro* Acipenserid Herpesvirus 2 infection was performed on white sturgeon skin cells. Total RNA was collected at 10 days post-infection and sequencing was conducted. Reads were mapped to a reference genome and counts filtered and normalized. Differential gene expression analysis was performed and differentially expressed transcripts were plotted. Transcripts to the right of the “0” on the log(FC) axis are upregulated in the infected samples, while transcripts to the left of the “0” on the log(FC) axis are downregulated in the infected samples. The colored boxes indicate those differentially expressed transcripts where the upregulation (purple) or downregulation (tan) was statistically significant with a p-value cutoff of 0.01. Results show that 2,794 transcripts were statistically significantly differentially expressed, with 2,507 being upregulated and 287 being downregulated in the infected samples.

In the molecular function (MF) domain, 56 unique parent terms were upregulated (Figure 4.9), of which “magnesium ion binding”, “nucleoside diphosphate kinase activity”, and “folic acid binding” had the most transcripts upregulated. Within “magnesium ion binding, the term “metal ion binding” was most predominant. Within “nucleoside diphosphate kinase activity”, the term

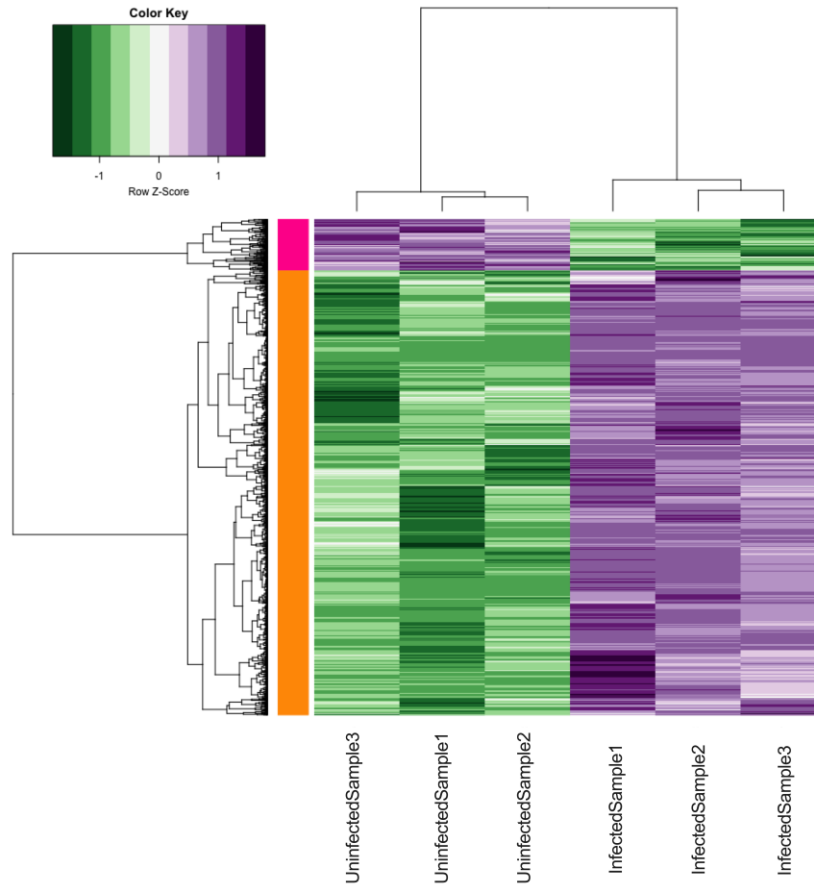


Figure 4.6 | Heat map. An *in vitro* Acipenserid Herpesvirus 2 infection was performed on white sturgeon skin cells. Total RNA was collected at 10 days post-infection and sequencing was conducted. Reads were mapped to a reference genome and counts filtered and normalized. Differential gene expression analysis was performed and differentially expressed transcripts were plotted by row z score, with purple representing statistically significantly upregulated transcripts and green representing statistically significantly downregulated transcripts, both on a gradient of significance. The gold and pink groupings represent the modules as it pertains to group comparison, with the gold representing transcripts upregulated in the infected state and pink representing transcripts downregulated in the infected state. Results show that 2,794 transcripts were statistically significantly differentially expressed, with 2,507 being upregulated and 287 being downregulated in the infected samples. Clusters are formed on the x axis, showing grouping by infection status, while clusters are formed on the y axis by similarity between transcripts.

“transferase activity” was most predominant. Finally, within “folic acid binding”, the terms “nucleotide binding” and “ATP binding” were most predominant. For the same MF domain, 26 unique parent terms were downregulated (Figure 4.10), of which “magnesium ion binding”, “methyltransferase activity”, and “pyridoxal phosphate binding” had the most transcripts downregulated. Within “magnesium ion binding”, the term “metal ion binding” was most

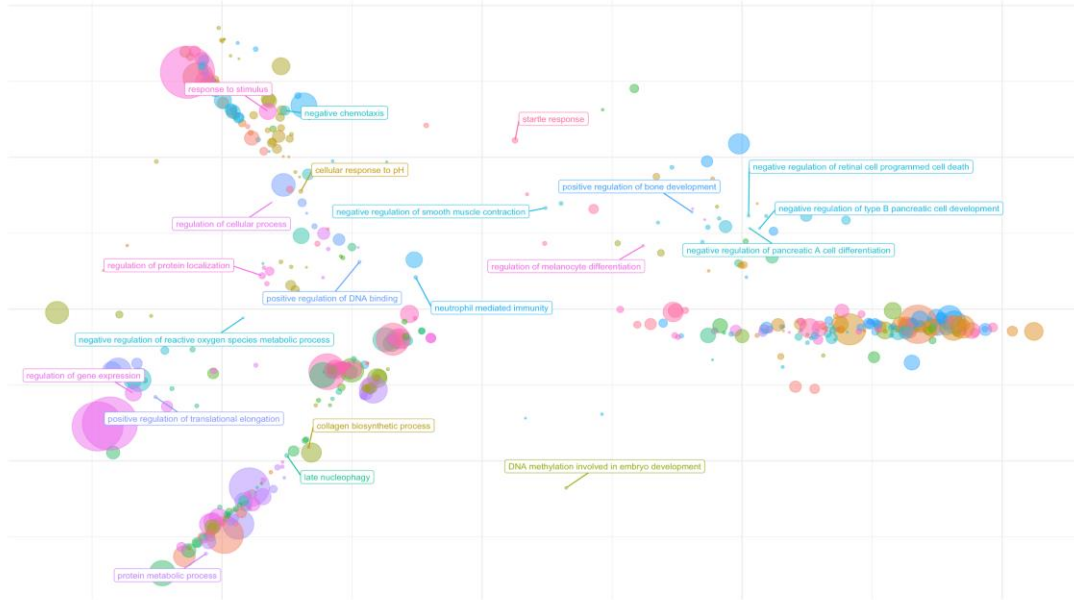


Figure 4.7 | Scatter plot of gene ontology terms of the biological process domain for upregulated transcripts. An *in vitro* Acipenserid Herpesvirus 2 infection was performed on white sturgeon skin cells. Total RNA was collected at 10 days post-infection and sequencing was conducted. Reads were mapped to a reference genome and counts filtered and normalized. Differential gene expression analysis was performed, and the sequences for the differentially expressed genes were then subjected to blastx against the zebrafish (*Danio rerio*) annotated genome for subsequent gene ontology (GO) analysis. Parent GO terms of the biological process (BP) domain for the upregulated transcripts obtained via the rrvgo package were plotted as scattered points. The distance between the points represents the similarity between the GO terms, while the size of the points represents the number of transcripts annotated with that GO term. Due to the amount of terms present, not all are plotted as labels (data available upon request).

predominant”. Within “methyltransferase activity”, the term “transferase activity” was most predominant. Finally, within “pyridoxal phosphate binding”, the term “ATP binding” was most predominant.

In the cellular component (CC) domain, 36 unique parent terms were upregulated (Figure 4.11), of which “membrane”, “nucleus”, and “cytoplasm” had the most transcripts upregulated. Within each of those parent terms, the terms “membrane”, “nucleus”, and “cytoplasm” were most predominant, respectively. For the same CC domain, 18 unique parent terms were downregulated (Figure 4.12), of which “membrane”, “nuclear speck”, and “intracellular anatomical structure” had the most transcripts downregulated. Within “membrane”, the term “membrane” was most

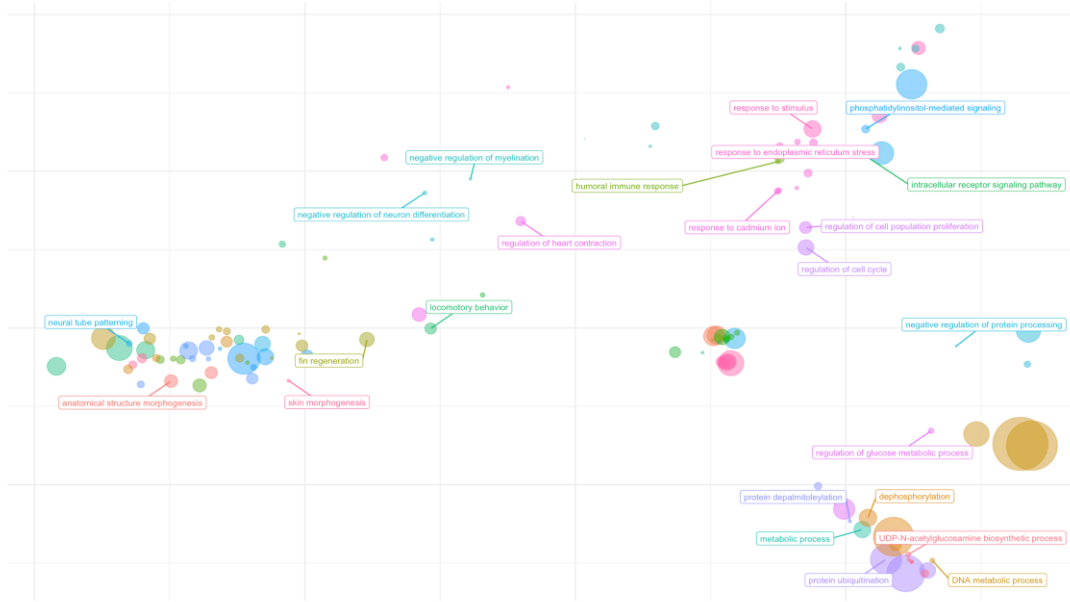


Figure 4.8 | Scatter plot of gene ontology terms of the biological process domain for downregulated transcripts. An *in vitro* Acipenserid Herpesvirus 2 infection was performed on white sturgeon skin cells. Total RNA was collected at 10 days post-infection and sequencing was conducted. Reads were mapped to a reference genome and counts filtered and normalized. Differential gene expression analysis was performed, and the sequences for the differentially expressed genes were then subjected to blastx against the zebrafish (*Danio rerio*) annotated genome for subsequent gene ontology (GO) analysis. Parent GO terms of the biological process (BP) domain for the downregulated transcripts obtained via the rrvgo package were plotted as scattered points. The distance between the points represents the similarity between the GO terms, while the size of the points represents the number of transcripts annotated with that GO term. Due to the amount of terms present, not all are plotted as labels (data available upon request).

predominant. Within “nuclear speck”, the term “nucleus” was the most predominant. Inally, within “intracellular anatomical structure”, the term “cytoplasm” was most predominant.

Since the focus of this study was to gain an initial understanding of the transcriptional changes in the sturgeon cells in response to infection, gene ontology analysis was further narrowed to terms associated with immune-related pathways. Of the 792 transcripts with identified gene ontology terms, only 18 transcripts were associated with immunity (Table 4.2). Seventeen were upregulated and one was downregulated in the infected samples.

Table 4.2 | Differentially expressed transcripts with gene ontology terms associated with immunity.

Transcript ID	Homologous protein in the zebrafish	Annotation of gene ontology terms in the biological process domain
14690	AGN48009.1 retinoic acid-inducible protein Ib	regulation of DNA-templated transcription canonical NF-kappaB signal transduction RIG-I signaling pathway defense response to virus type II interferon-mediated signaling pathway type I interferon-mediated signaling pathway
29111 and 31252	AKA09352.1 LGP2 variant 2	immune system process regulation of cellular process defense response to virus negative regulation of RIG-I signaling pathway antiviral innate immune response
35094	NP_001009988.1 forkhead box protein O3a	negative regulation of transcription by RNA polymerase II RNA polymerase II-specific chordate embryonic development regulation of neuron apoptotic process negative regulation of defense response to virus regulation of nervous system development primitive hemopoiesis

		negative regulation of canonical Wnt signaling pathway
54804	NP_956065.1 ras-related C3 botulinum toxin substrate 1	neutrophil homeostasis neutrophil mediated immunity pro-T cell differentiation actin filament organization myoblast fusion motor neuron axon guidance regulation of cell shape response to wounding positive regulation of lamellipodium assembly Rac protein signal transduction rhombomere boundary formation cortical cytoskeleton organization actomyosin structure organization regulation of establishment or maintenance of cell polarity regulation of actin cytoskeleton organization cell migration involved in gastrulation defense response to bacterium engulfment of apoptotic cell macrophage chemotaxis defense response to fungus

		<p>regulation of neutrophil chemotaxis</p> <p>positive regulation of neutrophil extravasation</p>
67205	<p>AJG05936.1</p> <p>Tnfrsf21, partial</p>	<p>sprouting angiogenesis</p> <p>adaptive immune response</p> <p>humoral immune response</p> <p>establishment of endothelial blood-brain barrier</p> <p>negative regulation of B cell proliferation</p> <p>negative regulation of myelination</p> <p>negative regulation of T cell proliferation</p> <p>neuron apoptotic process</p> <p>oligodendrocyte apoptotic process</p>
82053	<p>NP_001287801.1</p> <p>interferon-induced protein with tetratricopeptide repeats 10</p>	<p>defense response to virus</p>
89770	<p>AAH65902.1</p> <p>Irf7 protein</p>	<p>regulation of DNA-templated transcription</p> <p>response to virus</p> <p>regulation of T cell differentiation</p> <p>negative regulation of hematopoietic stem cell differentiation</p>
124825	<p>XP_009301676.1</p> <p>DNA-dependent protein kinase catalytic subunit</p>	<p>telomere maintenance</p> <p>double-strand break repair via nonhomologous end joining</p>

		<p>intrinsic apoptotic signaling pathway in response to DNA damage</p> <p>phosphorylation</p> <p>B cell differentiation</p> <p>T cell receptor V(D)J recombination</p> <p>immunoglobulin heavy chain V-D-J recombination</p>
144308 and 306841	<p>NP_001315640.1</p> <p>interferon-induced protein with tetratricopeptide repeats 9</p>	<p>defense response to virus</p>
216249 and 319437	<p>AGN48007.1</p> <p>melanoma differentiation-associated protein 5b</p>	<p>regulation of DNA-templated transcription</p> <p>innate immune response</p> <p>defense response to virus</p> <p>MDA-5 signaling pathway</p> <p>antiviral innate immune response</p>
243309	<p>NP_001295492.1</p> <p>interferon-induced helicase C domain-containing protein 1</p>	<p>immune system process</p> <p>regulation of DNA-templated transcription</p> <p>defense response to other organism</p>
282025	<p>NP_001122200.1</p> <p>interferon induced protein 44c1</p>	<p>immune response</p>
298491	<p>NP_001333171.1</p> <p>protein THEMIS</p>	<p>immune system process</p>

298842	XP_001334871.1 histone H2A-like	DNA repair DNA recombination nucleosome assembly brain development innate immune response defense response to Gram-positive bacterium meiotic cell cycle disruption of plasma membrane integrity in another organism
305853	ABJ97316.1 viperin	innate immune response positive regulation of immune response defense response to virus

Transcripts are color-coded by differential expression directionality in the infected samples (purple = upregulated; green = downregulated).

3.4 Identification of expressed ORFs in the virus

In terms of the transcriptional profile of the virus, transcripts were detected for every predicted ORF. Predicted locations were confirmed for all detected ORFs except for ORF 90, which mapped to the correct predicted location but one nucleotide short (119,083-116,294 instead of 119,083-116,295). In addition, ORF 67, which is predicted to be the DNA polymerase gene, and ORF 71,

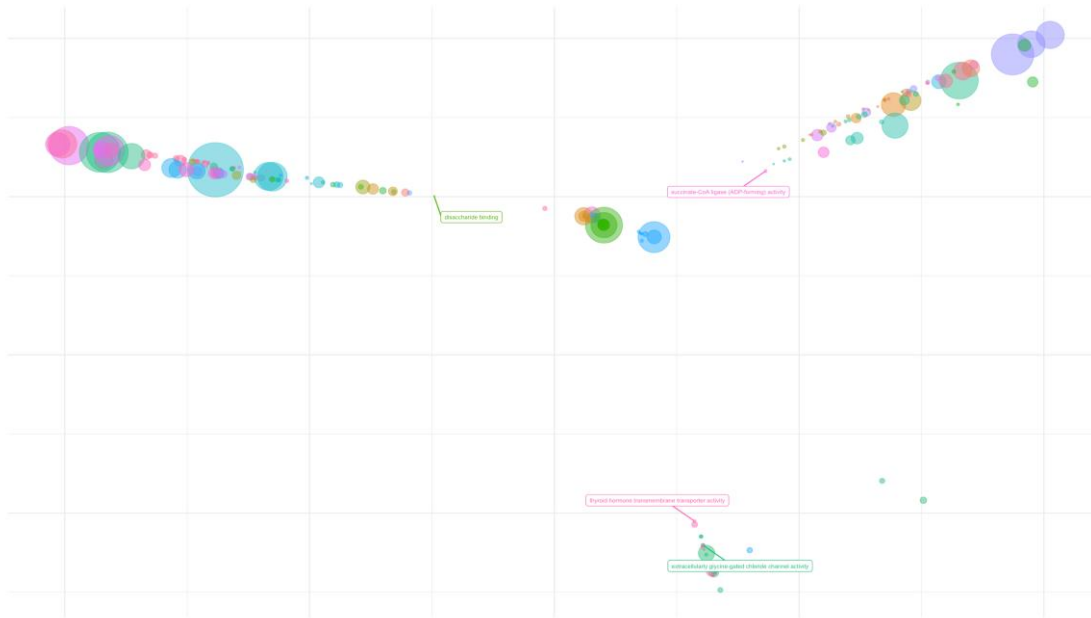


Figure 4.9 | Scatter plot of gene ontology terms of the molecular function domain for upregulated transcripts. An *in vitro* Acipenserid Herpesvirus 2 infection was performed on white sturgeon skin cells. Total RNA was collected at 10 days post-infection and sequencing was conducted. Reads were mapped to a reference genome and counts filtered and normalized. Differential gene expression analysis was performed, and the sequences for the differentially expressed genes were then subjected to blastx against the zebrafish (*Danio rerio*) annotated genome for subsequent gene ontology (GO) analysis. Parent GO terms of the molecular function (MF) domain for the upregulated transcripts obtained via the rrvgo package were plotted as scattered points. The distance between the points represents the similarity between the GO terms, while the size of the points represents the number of transcripts annotated with that GO term. Due to the amount of terms present, not all are plotted as labels (data available upon request).

which is predicted to be the terminase gene, had no transcripts that spanned the entire ORF regions. Instead, as expected, transcripts were detected that mapped to each predicted exon with variations in the predicted locations (Table 4.3).

The three ORFs with the highest expression in the time point used for this study were ORF 9, ORF 39, and ORF 82 (Figure 4.13), predicted to be a hypothetical protein (no homology to other characterized proteins described), a capsid maturation protease, and a protein kinase, respectively. The three ORFs with the lowest expression in the time point used for this study were ORF 89U, ORF 1U, and ORF 91 (Figure 4.13), all predicted to be hypothetical proteins.

Table 4.3 | DNA polymerase and transcriptase viral transcript locations when mapped to the viral genome.

Exon	Predicted location	Mapped location
DNA Polymerase – Exon 1	72,382 – 75,131	72,328 – 75,153
DNA Polymerase – Exon 2	75,215 – 76,946	75,282 – 76,946
Terminase – Exon 1	80,298 – 81,097	80,266 – 81,171
Terminase – Exon 2	97,597 – 98,163	97,843 – 98,238
Terminase – Exon 3	98,842 – 99,642	98,884 – 99,648

4. Discussion

As expected from most pathogens, herpesviruses have been reported to induce changes in the transcriptional profiles of infected cells.^{29–31} This is due not only to the natural responses from the host in order to clear the pathogen, but also to encoded molecules and proteins in the herpesviruses genomes whose function is to alter the host’s response.^{16,32} AciHV-2, a member of the *Herpesvirales* order and a significant agent in various white sturgeon mortality events^{8,33,34}, has been shown to potentially have immune-related host homologs³⁵ and to impact the white sturgeon response to heterologous infections¹⁷. Therefore, the objective of this study was to gain an initial understanding of the differential gene expression of the host during an acute infection *in vitro*. An additional objective was to assess the transcriptional profile of the virus at 10 days post-infection *in vitro* and confirm the previously predicted ORFs.³⁵

Sturgeon is one of the most ancient extant teleost families, with the divergence of this group from the rest of the actinopterygians dating to over 320 million years ago.³⁶ One particularity of

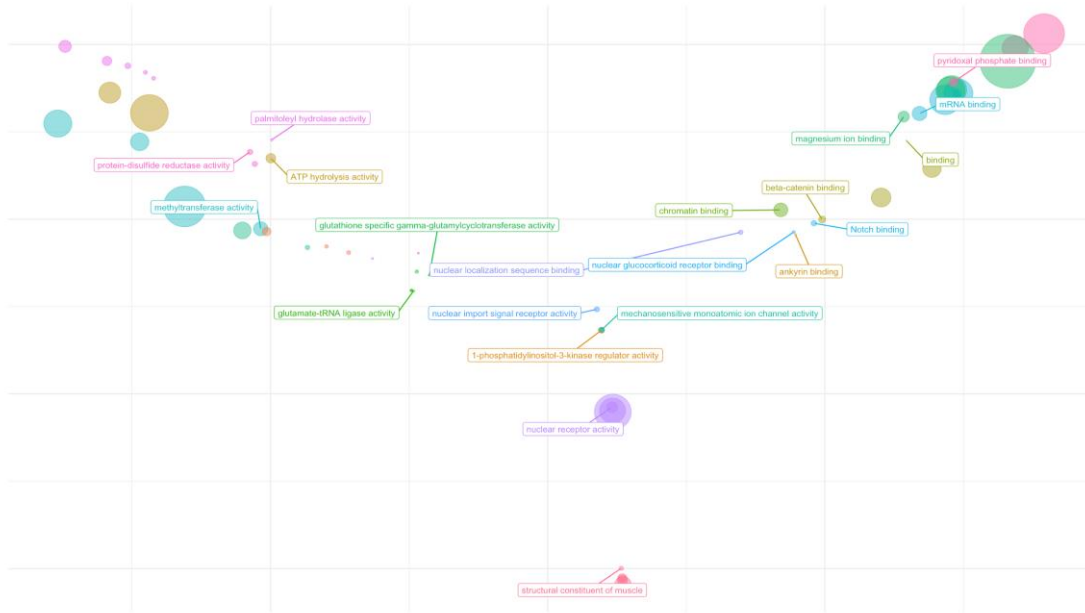


Figure 4.10 | Scatter plot of gene ontology terms of the molecular function domain for downregulated transcripts. An *in vitro* Acipenserid Herpesvirus 2 infection was performed on white sturgeon skin cells. Total RNA was collected at 10 days post-infection and sequencing was conducted. Reads were mapped to a reference genome and counts filtered and normalized. Differential gene expression analysis was performed, and the sequences for the differentially expressed genes were then subjected to blastx against the zebrafish (*Danio rerio*) annotated genome for subsequent gene ontology (GO) analysis. Parent GO terms of the molecular function (MF) domain for the downregulated transcripts obtained via the rrvgo package were plotted as scattered points. The distance between the points represents the similarity between the GO terms, while the size of the points represents the number of transcripts annotated with that GO term. Due to the amount of terms present, not all are plotted as labels (data available upon request).

the sturgeon group is their history of various polyploidization events, with some species being dodecaploid, which makes whole genome studies more challenging.³⁶ For this reason, the white sturgeon genome, released in September 2021, is only available at the scaffold level with no annotations. Therefore, this study determined differential transcript expression in WSSK-1 cells 10 days after being infected with AciHV-2 and focused on those transcripts associated with immune pathways when compared to the zebrafish annotated genome.²⁵ As expected, most of the 17 immune-related upregulated transcripts (Table 4.2) are associated with response to viral infections including homologs for four interferon-induced transcripts³⁷, one interferon regulatory

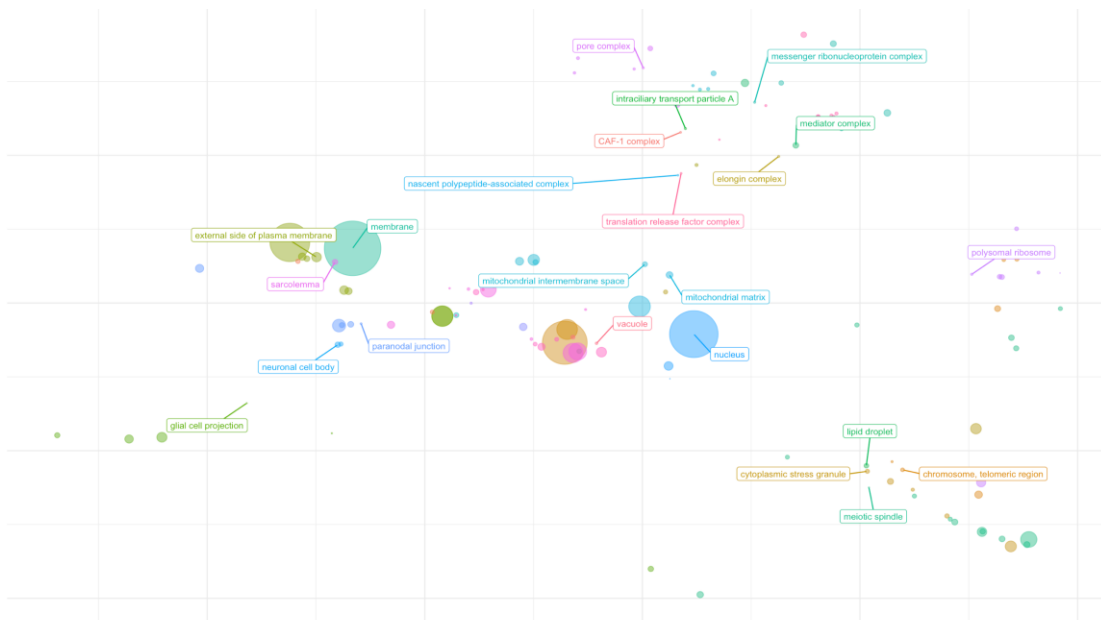


Figure 4.11 | Scatter plot of gene ontology terms of the cellular component domain for upregulated transcripts. An *in vitro* Acipenserid Herpesvirus 2 infection was performed on white sturgeon skin cells. Total RNA was collected at 10 days post-infection and sequencing was conducted. Reads were mapped to a reference genome and counts filtered and normalized. Differential gene expression analysis was performed, and the sequences for the differentially expressed genes were then subjected to blastx against the zebrafish (*Danio rerio*) annotated genome for subsequent gene ontology (GO) analysis. Parent GO terms of the cellular component (CC) domain for the upregulated transcripts obtained via the rrvgo package were plotted as scattered points. The distance between the points represents the similarity between the GO terms, while the size of the points represents the number of transcripts annotated with that GO term. Due to the amount of terms present, not all are plotted as labels (data available upon request).

factor³⁸, three retinoic acid-inducible gene (RIG)-like receptor family members^{39,40}, one Forkhead box protein family member⁴¹, one Ras-related C3 botulinum toxin substrate (RAC) subfamily member⁴², one DNA-dependent protein kinase^{43,44}, a thymocyte selection associated transcript, one histone-like transcript (H2A-like), and a viperin-like transcript⁴⁵. Three of these are of special interest due to previous reports on their ability to assist viral infection under the right conditions: the Laboratory of genetics and physiology 2 (LGP2) transcript, the RAC-1 transcript, and the H2A-like transcript.

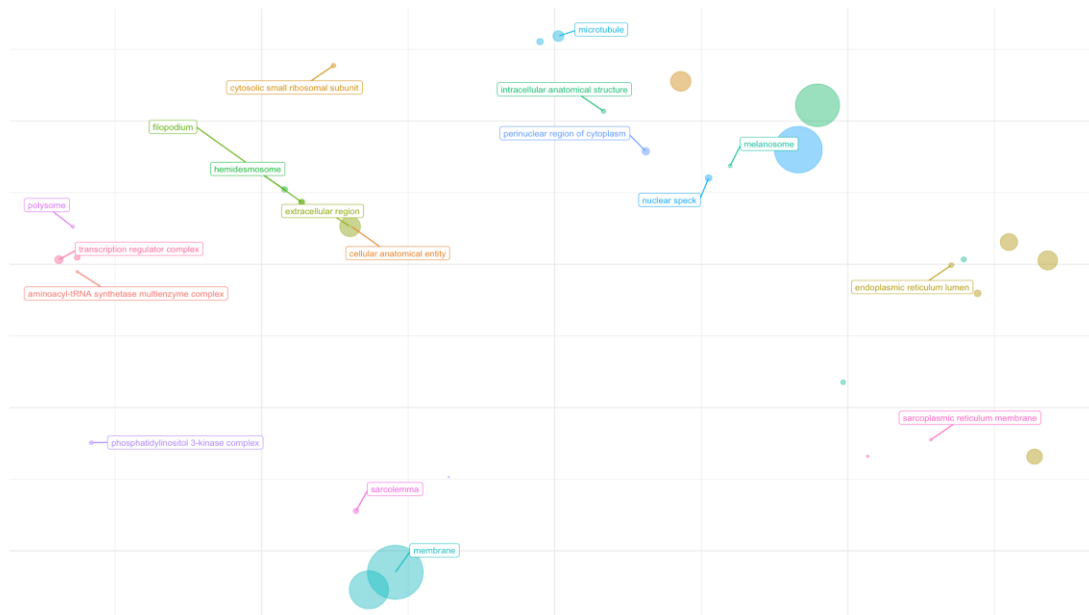


Figure 4.12 | Scatter plot of gene ontology terms of the cellular component domain for downregulated transcripts. An *in vitro* Acipenserid Herpesvirus 2 infection was performed on white sturgeon skin cells. Total RNA was collected at 10 days post-infection and sequencing was conducted. Reads were mapped to a reference genome and counts filtered and normalized. Differential gene expression analysis was performed, and the sequences for the differentially expressed genes were then subjected to blastx against the zebrafish (*Danio rerio*) annotated genome for subsequent gene ontology (GO) analysis. Parent GO terms of the cellular component (CC) domain for the downregulated transcripts obtained via the rrvgo package were plotted as scattered points. The distance between the points represents the similarity between the GO terms, while the size of the points represents the number of transcripts annotated with that GO term. Due to the amount of terms present, not all are plotted as labels (data available upon request).

The LGP2 protein is part of the RIG-I-like receptor family, an important family of receptors that detect the presence of RNA in the cytosol of cells. In response, these receptors induce the expression of genes involved in a type I interferon response, which is an important part of the antiviral response.⁴⁶ While herpesviruses are double-stranded DNA viruses, it has been demonstrated that various RNA molecules are either accumulated or mislocalized to the cytosol during infection, capable of triggering RIG-I-like receptors.⁴⁶ The LGP2 receptor in particular has had contradictory functions described in the past, most recently having been shown to have a regulatory role that shifts from positive to negative depending on the LGP2 or interferon expression levels in fish. If the expression levels are lower, the regulatory role is a positive one

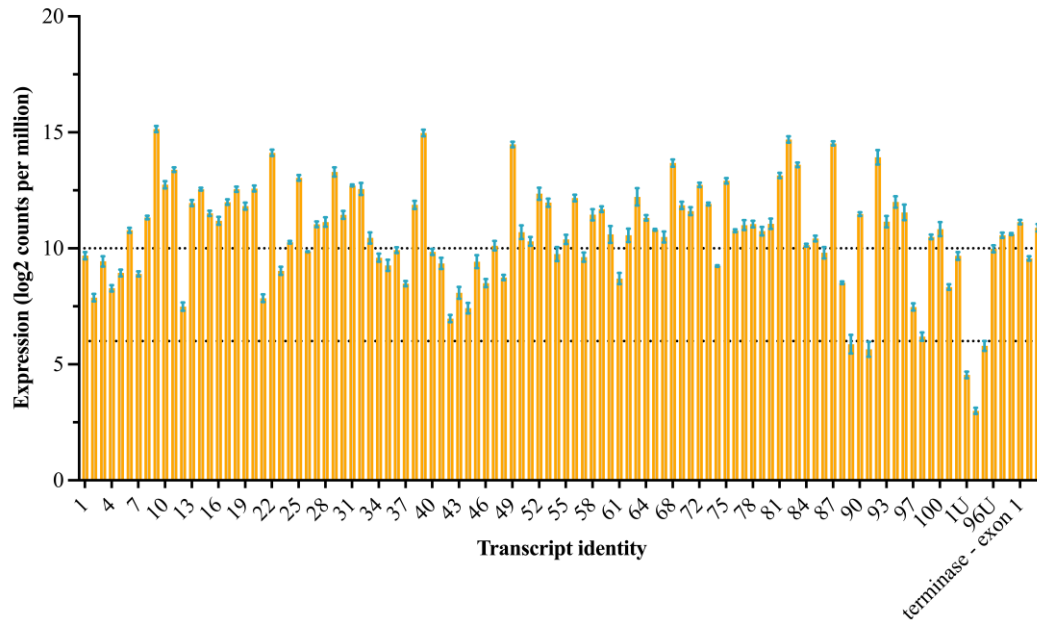


Figure 4.13 | Transcriptional profile of Acipenserid Herpesvirus 2 *in vitro*. An *in vitro* Acipenserid Herpesvirus 2 infection was performed on white sturgeon skin cells (WSSK-1 cells). Total RNA was collected at 10 days post-infection and sequencing was conducted. Reads were mapped to the UCD3-30 reference genome and counts filtered and normalized. The x axis contains open reading frame (ORF) identifiers as specified in chapter 2 of this thesis work. Not all labels are shown due to space constrains, but ORFs are listed from left to right as: 1-120, U-specific ORFs, DNA polymerase exons, and terminase exons. Horizontal lines indicate arbitrary zones of higher expression (above expression $\log_2(10)$ per million), medium expression (between expression $\log_2(6)$ - $\log_2(10)$ per million), and lower expression (below expression $\log_2(6)$ per million).

being an activator of type I interferon. If the expression levels are higher, the regulatory role is a negative one being a contributor to the downregulation of the type I interferon response.^{47,48} While it is expected that expression of LGP2 would be increased during viral infection, it is currently unknown what level of expression in the white sturgeon would constitute the threshold for the switch of LGP2 function in this host. More studies would be needed to evaluate this putative LGP2 transcript in terms of function and transcriptional patterns during AciHV-2 infection in white sturgeon.

The RAC-1 protein is a member of the Rho family of small guanosine triphosphatases (GTPases), which are a subfamily of the Ras-superfamily of GTPases, and has been shown to play

vital roles in a variety of cellular processes, including actin cytoskeletal remodeling.⁴² In the context of herpesviral infections, the ability of RAC-1 to modify the cell cytoskeleton is an important target for viral modulation in order to regulate vesicular trafficking and thus influence the viral lifecycle stages involving the cell surface.⁴⁹ This has been demonstrated in the Herpes simplex virus keratitis model, where inhibition of RAC-1 leads to a significant reduction in Herpes simplex virus 1 (HSV-1) replication *in vitro*. In contrast, overexpression of RAC-1 in human cells, by either HSV-1 infection or plasmid transfection, led to an increase in HSV-1 replication.⁵⁰ The upregulation of this putative RAC-1 transcript in the white sturgeon cells by AciHV-2 infection could be having profound effects on the ability of AciHV-2 to replicate. Further investigation into this transcript's function and transcriptional pattern during AciHV-2 infection is warranted. As seen in HSV-1 studies⁵⁰, RAC-1 inhibitors could represent a potential anti-viral therapy in AciHV-2-induced mortality events in white sturgeon.

The nucleosome is a histone octamer, composed of an H3-H4 tetramer associated with two H2A-H2B dimers, with a section of double-stranded DNA wrapped around it.⁵¹ While this function in the maintenance of chromatin structure is well described, studies have also demonstrated that histones have extrachromosomal functions capable of impacting various pathways. For example, the viral DNA of HSV-1 has been reported to be associated with H3 after entry into the nucleus.⁵¹ This association serves as a mechanism of gene transcription regulation during both lytic and latent infections.⁵² Histones have also been reported to play a role in the regulation of the type 1 interferon response. This regulatory function is of particular interest because both positive and negative regulation have been described. In human cells, H2B has been shown to be translocated to the cytoplasm where it is involved in double-stranded DNA-mediated signaling, inducing a type 1 interferon response upon detection of Human Papillomavirus (HPV) infection.⁵³ In contrast,

while H2A has also been shown to translocate to the cytoplasm in zebrafish cells and fathead minnow cells upon infection with Spring Viremia of Carp Virus (SVCV), it acts as a negative regulator of the type 1 interferon response by promoting the degradation of important players in the pathway such as interferon regulatory factor 3 (IRF3) and TANK-binding kinase 1 (TBK1).⁵⁴ Upregulation of a putative H2A transcript in this study could indicate a mechanism by AciHV-2 to regulate the antiviral immune response of the host cell in response to the infection. Additional studies are needed to elucidate the function of this transcript.

The immune-related downregulated transcript identified in this study (Table 4.2) is a homolog of a member of the tumor necrosis factor receptor superfamily (TNFRSF), member 21 to be precise (TNFRSF21). In humans, TNFRSF21 is an activator of nuclear factor kappa-B and mitogen-activated protein kinase 8, inducing cell apoptosis, and plays a role in T-helper cell activation.⁵⁵ While the TNF and TNFR superfamilies are significant players in the viral immune response and TNFRSF21 was described over 20 years ago, much remains unclear regarding the structure and function of this important protein.⁵⁵ Downregulation of TNFRSF21 in WSSK-1 cells during AciHV-2 infection may play a role in immune evasion by the virus, making this transcript a prime candidate for further studies that should include elucidation of the downregulation mechanism. While this mechanism was beyond the scope of this study, it has been described that herpesviruses, including a member of the *Alloherpesviridae* family (cyprinid herpesvirus 3, CyHV-3), target these superfamilies for regulation of the host's immune response by encoding homologs of their members.⁵⁶⁻⁵⁹ In fact, AciHV-2 was found to encode a putative TNFRSF14 homolog.³⁵ These viral TNFR molecules have been shown to have a variety of functions, including but not limited to binding to membrane-associated TNF for dampening of the immune response⁵⁶ and protection

from TNF-mediated killing⁶⁰, forming inhibitory complexes with soluble TNF for inhibition of cytolytic activities^{58,60}, and regulation of apoptosis for viral progeny dissemination⁵⁹.

This study also determined the transcriptional profile of AciHV-2 10 days after being inoculated onto WSSK-1 cells. At this time point, it was observed that all previously predicted ORFs³⁵ were transcriptionally present. While it is a common notion that herpesviruses have patterns of expression composed of immediate-early, early, and late genes^{61,62}, it has also been described that expression of all genes may be present at various degrees at specific time points.³⁰ Elucidation of the temporal transcriptional distribution of AciHV-2 ORFs will require a multi-time point transcriptional analysis. Finally, this study was able to confirm the predicted length of all ORFs previously described.³⁵

In summary, the results of this study provide a starting point for further investigations related to host-immune interactions of AciHV-2 and the white sturgeon, particularly as it pertains to the modulation of the host immune response. In addition, this study increases the accuracy of the whole genome of AciHV-2 previously elucidated³⁵ and provides information on highly expressed transcripts during active infection *in vitro* for further pathogenesis studies.

References:

1. Kelly J. White Sturgeon [Internet]. California Department of Fish and Wildlife. [cited 2022 Jan 20]. Available from: <https://wildlife.ca.gov/Conservation/Fishes/Sturgeon/White-Sturgeon>
2. Ethier V. Farmed Sturgeon [Internet]. Monterey Bay Aquarium Seafood Watch; 2014 [cited 2022 Jan 20]. Available from: <https://seafood.ocean.org/wp-content/uploads/2016/10/Sturgeon-Farmed-US.pdf>
3. Carocci F, Lagrange C, Levavasseur V, Yakimushkin A. Sturgeons (*Acipenseriformes*) [Internet]. Food and Agriculture Organization of the United Nations. Available from: <https://www.fao.org/3/Y5261E/y5261e06.htm>

4. Paul Zajicek, Keleher W. Seafood Security & Economic Development & A New Paradigm for Aquatic Animal Health in the US. In: 2023 Northeast Fish Culture Chiefs and Fish Health Committee Meeting. Burlington, VT; 2023.
5. Food and Agriculture Organization of the United Nations (FAO). The State of World Fisheries and Aquaculture | Towards Blue Transformation [Internet]. 2022. Available from: <https://doi.org/10.4060/cc0461en>
6. Cain K. The many challenges of disease management in aquaculture. *J World Aquac Soc.* 2022 Dec;53(6):1080–3.
7. Lepa A, Siwicki AK. Fish herpesvirus diseases: a short review of current knowledge. *Acta Vet Brno.* 2012;81(4):383–9.
8. Watson L, Yun S, Groff J, Hedrick R. Characteristics and pathogenicity of a novel herpesvirus isolated from adult and subadult white sturgeon *Acipenser transmontanus*. *Dis Aquat Organ.* 1995;22:199–210.
9. Mugetti D, Pastorino P, Menconi V, Pedron C, Prearo M. The Old and the New on Viral Diseases in Sturgeon. *Pathogens.* 2020 Feb 21;9(2):146.
10. Rinaldo CR. Immune suppression by herpesviruses. *Annu. Rev. Med.* 1990 41:331–38; 1990.
11. Alibek K, Baiken Y, Kakpenova A, Mussabekova A, Zhussupbekova S, Akan M, et al. Implication of human herpesviruses in oncogenesis through immune evasion and suppression. *Infect Agent Cancer.* 2014;9(1):3.
12. Crow MS, Lum KK, Sheng X, Song B, Cristea IM. Diverse mechanisms evolved by DNA viruses to inhibit early host defenses. *Crit Rev Biochem Mol Biol.* 2016 Nov;51(6):452–81.
13. Alcami A. Viral mimicry of cytokines, chemokines and their receptors. *Nat Rev Immunol.* 2003 Jan;3(1):36–50.
14. Gorshkova EA, Shilov ES. Possible mechanisms of acquisition of herpesvirus virokines. *Biochem Mosc.* 2016 Nov;81(11):1350–7.
15. Sehrawat S, Kumar D, Rouse BT. Herpesviruses: Harmonious Pathogens but Relevant Cofactors in Other Diseases? *Front Cell Infect Microbiol.* 2018 May 25;8:177.
16. Chang WLW, Baumgarth N, Yu D, Barry PA. Human Cytomegalovirus-Encoded Interleukin-10 Homolog Inhibits Maturation of Dendritic Cells and Alters Their Functionality. *J Virol.* 2004 Aug 15;78(16):8720–31.
17. Quijano Carde EM, Anenson K, Yun S, Heckman TI, Jungers H, Henderson EE, et al. Role of Acipenserid herpesvirus 2 infections on the Outcome of *Streptococcus iniae* Challenges in White Sturgeon (*Acipenser transmontanus*). In: Eastern Fish Health Workshop. 2023.

18. Doszpoly A, Kovács ER, Bovo G, LaPatra SE, Harrach B, Benkő M. Molecular confirmation of a new herpesvirus from catfish (*Ameiurus melas*) by testing the performance of a novel PCR method, designed to target the DNA polymerase gene of alloherpesviruses. *Arch Virol.* 2008 Nov;153(11):2123–7.
19. LaPatra SE. Section I: Diagnostic Procedures for Finfish and Shellfish Pathogens. In: *Fish Health Section Blue Book* [Internet]. 2020 Edition. AFS Fish Health Section; 2020. Available from: <https://units.fisheries.org/fhs/fish-health-section-blue-book-2020/>
20. Robinson MD, Oshlack A. A scaling normalization method for differential expression analysis of RNA-seq data. *Genome Biol.* 2010;11(3):R25.
21. Robinson MD, McCarthy DJ, Smyth GK. edgeR: a Bioconductor package for differential expression analysis of digital gene expression data. *Bioinformatics.* 2010 Jan 1;26(1):139–40.
22. Wickham H, Navarro D, Pedersen TL. *ggplot2: Elegant Graphics for Data Analysis*. Third edition. Springer International Publishing;
23. Ritchie ME, Phipson B, Wu D, Hu Y, Law CW, Shi W, et al. limma powers differential expression analyses for RNA-sequencing and microarray studies. *Nucleic Acids Res.* 2015 Apr 20;43(7):e47–e47.
24. Gotz S, Garcia-Gomez JM, Terol J, Williams TD, Nagaraj SH, Nueda MJ, et al. High-throughput functional annotation and data mining with the Blast2GO suite. *Nucleic Acids Res.* 2008 Apr 15;36(10):3420–35.
25. Costábile A, Castellano M, Aversa-Marnai M, Quartiani I, Conijeski D, Perretta A, et al. A different transcriptional landscape sheds light on Russian sturgeon (*Acipenser gueldenstaedtii*) mechanisms to cope with bacterial infection and chronic heat stress. *Fish Shellfish Immunol.* 2022 Sep;128:505–22.
26. Sayols S. rrvgo: a Bioconductor package for interpreting lists of Gene Ontology terms. *MicroPublication Biol.* 2023 Apr 18;
27. Sheng Q, Vickers K, Zhao S, Wang J, Samuels DC, Koues O, et al. Multi-perspective quality control of Illumina RNA sequencing data analysis. *Brief Funct Genomics.* 2016 Sep 29;elw035.
28. Conesa A, Madrigal P, Tarazona S, Gomez-Cabrero D, Cervera A, McPherson A, et al. A survey of best practices for RNA-seq data analysis. *Genome Biol.* 2016 Dec;17(1):13.
29. Kurissio JK, Araújo Júnior JP. Transcriptomic analysis of differential gene expression reveals an increase in COX2 levels during in vitro canine herpesvirus infection. *Ciênc Rural* [Internet]. 2018 Oct 25 [cited 2023 Nov 6];48(10). Available from: http://www.scielo.br/scielo.php?script=sci_arttext&pid=S0103-84782018001000451&lng=en&tlng=en

30. Harkness JM, Kader M, DeLuca NA. Transcription of the Herpes Simplex Virus 1 Genome during Productive and Quiescent Infection of Neuronal and Nonneuronal Cells. Longnecker RM, editor. *J Virol*. 2014 Jun 15;88(12):6847–61.
31. Mason GM, Poole E, Sissons JGP, Wills MR, Sinclair JH. Human cytomegalovirus latency alters the cellular secretome, inducing cluster of differentiation (CD)4⁺ T-cell migration and suppression of effector function. *Proc Natl Acad Sci*. 2012 Sep 4;109(36):14538–43.
32. Piazzon MC, Wentzel AS, Tijhaar EJ, Rakus KŁ, Vanderplasschen A, Wiegertjes GF, et al. Cyprinid Herpesvirus 3 I110 Inhibits Inflammatory Activities of Carp Macrophages and Promotes Proliferation of Igm⁺ B Cells and Memory T Cells in a Manner Similar to Carp I110. *J Immunol*. 2015 Oct 15;195(8):3694–704.
33. Doszpoly A, Somogyi V, LaPatra SE, Benkő M. Partial genome characterization of acipenserid herpesvirus 2: taxonomical proposal for the demarcation of three subfamilies in Alloherpesviridae. *Arch Virol*. 2011 Dec;156(12):2291–6.
34. Soto E, Richey C, Stevens B, Yun S, Kenelty K, Reichley S, et al. Co-infection of Acipenserid herpesvirus 2 (AcHV-2) and *Streptococcus iniae* in cultured white sturgeon *Acipenser transmontanus*. *Dis Aquat Organ*. 2017 Mar 30;124(1):11–20.
35. Quijano Carde EM. Whole-genome Sequencing of Acipenserid Herpesvirus 2 and Identification of Potential Host Homologs. In: American Fisheries Society | Fish Health Section: Fish Health Seminar Series. Virtual; 2022.
36. Du K, Stöck M, Kneitz S, Klopp C, Woltering JM, Adolphi MC, et al. The sterlet sturgeon genome sequence and the mechanisms of segmental rediploidization. *Nat Ecol Evol*. 2020 Jun;4(6):841–52.
37. Widziolak M, Janik K, Mojzesz M, Pooranachandran N, Adamek M, Pecio A, et al. Type I interferon-dependent response of zebrafish larvae during tilapia lake virus (TiLV) infection. *Dev Comp Immunol*. 2021 Mar;116:103936.
38. Johnson KE, Aurubin CA, Jondle CN, Lange PT, Tarakanova VL. Interferon Regulatory Factor 7 Attenuates Chronic Gammaherpesvirus Infection. Jung JU, editor. *J Virol*. 2020 Nov 23;94(24):e01554-20.
39. Matsumiya T, Stafforini DM. Function and Regulation of Retinoic Acid-Inducible Gene-I. *Crit Rev Immunol*. 2010;30(6):489–513.
40. Hu H, Yang H, Liu Y, Yan B. Pathogenesis of Anti-melanoma Differentiation-Associated Gene 5 Antibody-Positive Dermatomyositis: A Concise Review With an Emphasis on Type I Interferon System. *Front Med*. 2022 Jan 24;8:833114.
41. Cui M, Huang Y, Zhao Y, Zheng J. Transcription Factor FOXO3a Mediates Apoptosis in HIV-1-Infected Macrophages. *J Immunol*. 2008 Jan 15;180(2):898–906.

42. Bosco EE, Mulloy JC, Zheng Y. Rac1 GTPase: A “Rac” of All Trades. *Cell Mol Life Sci*. 2009 Feb;66(3):370–4.
43. Lees-Miller SP, Long MC, Kilvert MA, Lam V, Rice SA, Spencer CA. Attenuation of DNA-dependent protein kinase activity and its catalytic subunit by the herpes simplex virus type 1 transactivator ICP0. *J Virol*. 1996 Nov;70(11):7471–7.
44. Parkinson J, Lees-Miller SP, Everett RD. Herpes Simplex Virus Type 1 Immediate-Early Protein Vmw110 Induces the Proteasome-Dependent Degradation of the Catalytic Subunit of DNA-Dependent Protein Kinase. *J Virol*. 1999 Jan;73(1):650–7.
45. Shanaka KASN, Jung S, Madushani KP, Wijerathna HMSM, Neranjan Tharuka MD, Kim MJ, et al. Generation of viperin-knockout zebrafish by CRISPR/Cas9-mediated genome engineering and the effect of this mutation under VHSV infection. *Fish Shellfish Immunol*. 2022 Dec;131:672–81.
46. Rehwinkel J, Gack MU. RIG-I-like receptors: their regulation and roles in RNA sensing. *Nat Rev Immunol*. 2020 Sep;20(9):537–51.
47. Gong XY, Zhang QM, Zhao X, Li YL, Qu ZL, Li Z, et al. LGP2 is essential for zebrafish survival through dual regulation of IFN antiviral response. *iScience*. 2022 Aug;25(8):104821.
48. Gong XY, Qu ZL, Li YL, Sun HY, Zhao X, Dan C, et al. Function conservation and disparities of zebrafish and human LGP2 genes in fish and mammalian cells responsive to poly(I:C). *Front Immunol*. 2022 Aug 17;13:985792.
49. Zhang B, Ding J, Ma Z. ICP4-Associated Activation of Rap1b Facilitates Herpes Simplex Virus Type I (HSV-1) Infection in Human Corneal Epithelial Cells. *Viruses*. 2023 Jun 27;15(7):1457.
50. Zhang F, Liu Y, You Q, Yang E, Liu B, Wang H, et al. NSC23766 and Ehop016 Suppress Herpes Simplex Virus-1 Replication by Inhibiting Rac1 Activity. *Biol Pharm Bull*. 2021 Sep 1;44(9):1263–71.
51. Oh J, Fraser NW. Temporal Association of the Herpes Simplex Virus Genome with Histone Proteins during a Lytic Infection. *J Virol*. 2008 Apr;82(7):3530–7.
52. Coleman HM, Connor V, Cheng ZSC, Grey F, Preston CM, Efsthathiou S. Histone modifications associated with herpes simplex virus type 1 genomes during quiescence and following ICP0-mediated de-repression. *J Gen Virol*. 2008 Jan 1;89(1):68–77.
53. Kobiyama K, Takeshita F, Jounai N, Sakaue-Sawano A, Miyawaki A, Ishii KJ, et al. Extrachromosomal Histone H2B Mediates Innate Antiviral Immune Responses Induced by Intracellular Double-Stranded DNA. *J Virol*. 2010 Jan 15;84(2):822–32.

54. Wu XM, Fang H, Zhang J, Bi YH, Chang MX. Histone H2A Nuclear/Cytoplasmic Trafficking Is Essential for Negative Regulation of Antiviral Immune Response and Lysosomal Degradation of TBK1 and IRF3. *Front Immunol.* 2021 Nov 18;12:771277.
55. Ren X, Lin Z, Yuan W. A Structural and Functional Perspective of Death Receptor 6. *Front Pharmacol.* 2022 Mar 24;13:836614.
56. Al Rumaih Z, Tuazon Kels MaJ, Ng E, Pandey P, Pontejo SM, Alejo A, et al. Poxvirus-encoded TNF receptor homolog dampens inflammation and protects from uncontrolled lung pathology during respiratory infection. *Proc Natl Acad Sci.* 2020 Oct 27;117(43):26885–94.
57. Steinberg MW, Cheung TC, Ware CF. The signaling networks of the herpesvirus entry mediator (TNFRSF14) in immune regulation: HVEM networks in disease. *Immunol Rev.* 2011 Nov;244(1):169–87.
58. Schreiber M, Rajarathnam K, McFadden G. Myxoma Virus T2 Protein, a Tumor Necrosis Factor (TNF) Receptor Homolog, Is Secreted as a Monomer and Dimer That Each Bind Rabbit TNF α , but the Dimer Is a More Potent TNF Inhibitor. *J Biol Chem.* 1996 Jun;271(23):13333–41.
59. Zhou Y, Ouyang P, Tao Y, Yin L, Wang K, Geng Y, et al. Comparison the function of Cyprinid herpesvirus 3 encoded two viral tumor necrosis factor receptors. *Aquac Rep.* 2021 Nov;21:100878.
60. Reading PC, Khanna A, Smith GL. Vaccinia Virus CrmE Encodes a Soluble and Cell Surface Tumor Necrosis Factor Receptor That Contributes to Virus Virulence. *Virology.* 2002 Jan;292(2):285–98.
61. Huang S, Hanson LA. Temporal Gene Regulation of the Channel Catfish Virus (Ictalurid Herpesvirus 1). *J Virol.* 1998 Mar;72(3):1910–7.
62. Rozman B, Nachshon A, Levi Samia R, Lavi M, Schwartz M, Stern-Ginossar N. Temporal dynamics of HCMV gene expression in lytic and latent infections. *Cell Rep.* 2022 Apr;39(2):110653.

CONCLUSION

White sturgeon aquaculture is an important agricultural practice in the United States that has been affected by Acipenserid Herpesvirus 2 (AciHV-2) since its first report over 30 years ago. Throughout this time, research efforts have been focused on the initial characterization of AciHV-2 including its structure, replication in various tissues, detection in natural outbreaks, partial genome sequence, and phylogenetic positioning. To learn more about the pathogenesis of this disease, the host-microbe interactions during both acute and persistent/latent infections, and the effects of AciHV-2 on the response of the white sturgeon to heterologous infections, additional studies were needed. This thesis work focused on laying a foundation for further studies in the aforementioned topics and a concluding summary of the findings follows. The whole genome of AciHV-2 is approximately 134 Kb, with 102 shared open reading frames (ORFs) among the four studied isolates. Within the described ORFs, there are several host homologs that warrant additional studies. A diagnostic qPCR protocol is available for the detection of AciHV-2 in skin tissue during an active outbreak with 100% relative accuracy. A previous infection with AciHV-2 decreases survival during a subsequent *S. iniae* infection and alters the immune response of juvenile white sturgeon to the bacterium, including a decrease in the production of anti-*S. iniae* IgM. Finally, *in vitro* AciHV-2 infection in white sturgeon skin cells reveals differential transcript expression in putative immune-related transcripts that warrant further investigation. These conclusions support the ability of AciHV-2 to modulate the immune system of the host in an impactful manner not only in terms of the AciHV-2 outbreak itself but also in the ability of the host to combat subsequent heterologous infections. Further studies are needed to unveil the complex interactions between AciHV-2 and the white sturgeon, and careful consideration should be given to the consequences of these interactions when developing disease prevention strategies.